



VCU

Virginia Commonwealth University
VCU Scholars Compass

Theses and Dissertations


Graduate School

2017

The effects of the HIV-1 Tat protein and morphine on the structure and function of the hippocampal CA1 subfield

William D. Marks
SUNY College at Buffalo

Follow this and additional works at: <https://scholarscompass.vcu.edu/etd>

 Part of the [Molecular and Cellular Neuroscience Commons](#), [Pharmacology Commons](#), [Systems Neuroscience Commons](#), [Toxicology Commons](#), and the [Virology Commons](#)

© The Author

Downloaded from

<https://scholarscompass.vcu.edu/etd/5168>

This Dissertation is brought to you for free and open access by the Graduate School at VCU Scholars Compass. It has been accepted for inclusion in Theses and Dissertations by an authorized administrator of VCU Scholars Compass. For more information, please contact libcompass@vcu.edu.

**The effects of the HIV-1 Tat protein and morphine on the structure and function of
the hippocampal CA1 subfield**

A dissertation submitted in partial fulfillment of requirements for the degree of Doctor of
Philosophy at Virginia Commonwealth University

By
William D. Marks
Master of Arts, State University of New York College at Buffalo
Bachelor of Science, Franciscan University of Steubenville

Virginia Commonwealth University
Richmond, Virginia
December 2017

Acknowledgements

A great deal of gratitude is owed to a great many people who have been instrumental in this work and beyond. I would first like to thank my advisor, Dr. Kurt Hauser for his insight, energy, and his patience along the way. His enthusiasm and candor was most helpful, and, I feel, has given me valuable insight into life as a scientist beyond the lab bench. I am likewise grateful to Dr. Pamela Knapp, whose keen eye for experimental design and readiness to help made the setbacks I experienced (inevitable in any project) more manageable than they would have been otherwise. I also would like to thank Dr. Rory McQuiston and Dr. Thomas Reeves for their help, without which none of the electrophysiological studies presented here would have been possible. Also instrumental in getting this work done properly were Dr. Jason Paris, Dr. Virginia McLane, Mr. Aaron Barbour, and Ms. Jean Moon.

Thanks are due also to the two men who inspired and encouraged me from a very young age to pursue the natural sciences; my late grandfather, Mr. Arthur Marks, who went out of his way to make sure I had every chance to be exposed to the wonders of the natural world, and Dr. Norman Paolini Jr. who taught me to experiment with the things around me (much to my parents chagrin), for example, by growing fungi in petri dishes lightly coated with grape jelly (which I of course carried in my pockets for warmth).

A great many thanks are due to my closest friends, Ms. Eileen Bartolozzi, Ms. Maria Lang, Mr. Eric Smith, Dr. Michael Del Do, Mr. Zachary Curry, and Mr. Adam

DePriest. Your friendship over these past few years has been a constant source of inspiration, humor, and comfort.

To the members of the Hauser/Knapp collective past and present; I am incredibly glad to have met you all. You have made the -myriad- frustrations of graduate education more bearable. It's hard to imagine a more vibrant and enjoyable workplace, and I am seriously concerned that no place I go on from here will ever match y'all!

I would also like to thank the Catholic community of Richmond, especially the parishes at the Cathedral of the Sacred Heart, St. Benedict's and St. Mary's, and all the amazing people I've gotten to know through CatholicRVA. Finally, and most importantly, I give my thanks to God, who sustains and strengthens me -*Ad Majorem Dei Gloriam*-.

Table of Contents

Acknowledgements	ii
List of Figures.....	vii
List of Tables.....	ix
List of Abbreviations	x
Abstract.....	1
Chapter 1: Introduction.....	3
The human immunodeficiency virus.....	3
HIV-1 structure and viral proteins.....	4
HIV-1 Tat.....	5
Transmission and Epidemiology of HIV Infection.....	7
AIDS.....	7
Infection of the CNS.....	9
The HIV Associated Neurocognitive Disorders	10
Neuronal pathology.....	10
Astrocytic pathology and contribution to neuroAIDS.....	13
Microglial and MDM pathology and contribution to neuroAIDS.....	17
Oligodendrocytic and myelin pathology	20
Global effects of HIV on the central nervous system	21
The Hippocampus and HIV	24

Comorbidity of HIV infection and opioid abuse disorder	28
The opiate receptors, morphine, and the hippocampus	29
Morphine effects in the hippocampus	32
Interactions between HIV and opiate use.....	33
Hypotheses and Aims	36
Chapter 2: The effects of HIV Tat on CA1 interneuron microcircuitry and spatial memory	38
Introduction	38
Materials and methods.....	41
Results	47
Discussion.....	51
Chapter 3: The effects of Tat and Morphine on the structure and function of CA1	73
Introduction	73
Materials and Methods.....	75
Results	82
Discussion.....	90
Chapter 4: General Discussion and future directions	118
Future directions	133
Concluding remarks	141
References.....	146

Vita 184

List of Figures

Figure 2. 1: Barnes maze performance between Tat- and Tat+ mice	59
Figure 2. 2: Effects of Tat on novel object recognition task performance	61
Figure 2. 3: Tat effects on nNOS and NPY expressing CA1 interneurons	62
Figure 2. 4: nNOS and NPY subcellular localization	64
Figure 2. 5: Effects of Tat on PV and SST expressing CA1 interneurons	65
Figure 2. 6: PV and SST subcellular localization.....	67
Figure 2. 7: Tat does not affect amount of PV or SST+ neurites in CA1	69
Figure 2. 8: Interneurons affected by Tat are part of a memory microcircuit	70
Figure 3. 1: Effects of Tat and morphine on Barnes maze performance in mice	96
Figure 3. 2: Representative Barnes maze track traces.....	98
Figure 3. 3: Visual representation of planned comparisons design for electrophysiological analysis	99
Figure 3. 4: Firing frequency of CA1 pyramidal cells after exposure to Tat and/or morphine-treated mice (in vivo) in which morphine is present during electrophysiological recordings (ex vivo).....	100
Figure 3. 5: Membrane properties of CA1 pyramidal cells in Tat and/or morphine-treated mice (in vivo) in which morphine is present during electrophysiological recordings (ex vivo).....	101
Figure 3. 6: Firing frequency of CA1 pyramidal cells from Tat and/or morphine-treated mice (in vivo) in which morphine is withheld during electrophysiological recordings (ex vivo).....	103

Figure 3. 7: Membrane properties of CA1 pyramidal cells from Tat and/or morphine-treated mice (in vivo) in which morphine is withheld during electrophysiological recordings (ex vivo)	105
Figure 3. 8: Examples of a 3D-reconstructed biocytin-filled CA1 pyramidal cells	107
Figure 3. 9: Effects of Tat and morphine on the morphology of the portion of the pyramidal cell dendrite within the stratum oriens (SO)	108
Figure 3. 10: Effects of Tat and morphine on the morphology of the portion of the pyramidal cell dendrite within the stratum radiatum (SR)	110
Figure 3. 11: Effects of Tat and morphine on the morphology of the portion of the pyramidal cell dendrite within the stratum lacunosum-moleculare (SL-M).....	112
Figure 3. 12: Assessment of gephyrin puncta within the aspiny portion of pyramidal cell basilar and apical dendrites	114
Figure 4. 1: TdTomato x VIP expressing mice	143

List of Tables

Table 1. 1 Selected listing of regional effects of HIV/HIV proteins within the CNS	37
Table 2. 1: Raw exploration time and motor behavior among Tat- and Tat+ mice	72
Table 3. 1: Membrane properties of CA1 pyramidal cells after exposure to Tat and morphine	115
Table 3. 2: Membrane properties of CA1 pyramidal cells from Tat- and Tat+ animals in a withdrawal like state	116
Table 3. 3 Correlations between morphological and electrophysiological findings	117
Table 4. 1: Effects of Tat and morphine on hippocampal cytokine levels	144
Table 4. 2: Protein extracted from hippocampal samples	145

List of Abbreviations

AIDS- autoimmune deficiency syndrome

AEG- astrocyte elevated gene

CA- cornu ammonis

CNS- central nervous system

CSF- cerebrospinal fluid

DG- dentate gyrus

DOR- delta opiate receptor

EC- entorhinal cortex

EPSP- excitatory post synaptic potential

GABA- Gama-aminobutyric acid

GP120- glycoprotein 120

GUD- genital ulcer disease

HAND- HIV associated neurocognitive disorders

HIV- Human immunodeficiency virus

HIVE- HIV encephalopathy

IHC- immunohistochemistry/immunohistochemical

IDU- intravenous drug user

IPSP- inhibitory postsynaptic potential

IS1- interneuron specific interneuron type 1

IS3- interneuron specific interneuron type 3

IV- intravenous

KOR- kappa opiate receptor

LTP- long term potentiation

MOR- mu opiate receptor

MSM- Men who have sex with men

nNOS- neuronal nitric oxide synthase

NO- nitric oxide

NPY- neuropeptide Y

NR- nucleus reuniens

OLM- Oriens-lacunosum moleculare projecting cell

PFC- prefrontal cortex

P-TEFb- positive transcription elongation factor

PV- parvalbumin

ROS- reactive oxygen species

SIV- simian immunodeficiency virus

SL-M- Stratum lacunosum-moleculare

SO- stratum oriens

SP- stratum pyramidale

SR- stratum radiatum

SST- somatostatin

Syt2- synaptotagmin 2

Tat- transactivator of transcription

TAR- Transactivator response element

VIP- vasoactive intestinal peptide

Abstract

THE EFFECTS OF THE HIV-1 TAT PROTIEN AND MORPHINE ON THE STRUCTURE AND FUNCTION OF THE HIPPOCAMPAL CA1 SUBFIELD

By William D Marks, MA, Ph.D.c.

A dissertation submitted in partial fulfillment of the requirements for the degree of Doctor of Philosophy at Virginia Commonwealth University.

Virginia Commonwealth University, 2017.

Major Director: Kurt F. Hauser, Ph.D., Professor and Eminent Scholar,
Department of Pharmacology and Toxicology

HIV is capable of causing a set of neurological diseases collectively termed the HIV Associated Neurocognitive Disorders (HAND). Worsening pathology is observed in HIV+ individuals who use opioid drugs. Memory problems are often observed in HAND, implicating HIV pathology in the hippocampus, and are also known to be exacerbated by morphine use. HIV-1 Tat was demonstrated to reduce spatial memory performance in multiple tasks, and individual subsets of CA1 interneurons were found to be selectively vulnerable to the effects of Tat, notably nNOS+/NPY- interneurons of the pyramidal layer and stratum radiatum, PV+ neurons of the pyramidal layer, and SST+ neurons of stratum oriens. Each of these interneuron subsets are hypothesized to form part of a microcircuit involved in memory formation. Electrophysiological assessment of hippocampal pyramidal neurons with Tat and morphine together revealed that Tat caused a reduction in firing frequency, however, chronic morphine exposure did not have any effect. When morphine was removed after chronic exposure, non-interacting effects of Tat and morphine withholding on firing frequency were observed, suggesting that a homeostatic rebalancing of CA1 excitation/inhibition balance takes place in

response to chronic morphine exposure independently of any Tat effects. Additionally, differential morphological effects of Tat and morphine were observed in each of the three major dendritic compartments, with SR being less affected, suggesting complex circuit responses to these insults reflecting local change and potentially changes in inputs from other brain regions. Behaviorally, Tat and morphine interactions occur in spatial memory, with morphine potentially obviating Tat effects.

Chapter 1: Introduction

The human immunodeficiency virus

The Human Immunodeficiency virus (HIV)-1 is a Lentivirus, within the larger group of retroviruses, that was first isolated and identified as the cause of acquired immunodeficiency syndrome (AIDS) in 1983 following the initial identification of the disease in 1981 (Barre-Sinoussi et al, 1983; Gallo et al, 1983; Weiss, 1993; Sharp & Hahn, 2011). A second species, HIV-2, was identified in 1986 (Clavel et al, 1986). Although cases of AIDS and AIDS-related illnesses became common in the 1980s, evidence of HIV infection can be seen as far back as 1959 (Weiss, 1993; Zhu et al, 1998; Worobey et al, 2008). The two major forms of the virus (HIV-1 and HIV-2) are believed to have diverged relatively recently from the simian immunodeficiency virus (SIV), with some studies suggesting the divergences occurred between 1880 and 1970 depending on the specific viral group (e.g. HIV-1 M or HIV-2 B), with 1940 being the favored date for development of HIV-1 group M, the pandemic form of the virus. These events are attributed to a number of interacting factors favorable to the transition and initial spread of HIV, including low rates of circumcision, high rates of genital ulcer disease (GUD), and unsafe injection practices (Chitnis et al, 2000; Marx et al, 2001; Sharp et al, 2001; de Sousa et al, 2010; Sharp & Hahn, 2011). The transfer of SIV/HIV to humans is believed to be due to a number of cross-species events, in which SIV strains infecting various subgroups of apes were able to make the leap to humans, with

the animal vector differing between the origin of HIV-1 and HIV-2 (Marx et al, 2001; Sharp & Hahn, 2011).

HIV-1 and HIV-2 are related, but distinct viruses, with disparate evolutionary origin and differing virulence and transmission rates. Specifically, HIV-1 is more virulent, and more transmissible than HIV-2. As a result, HIV-1 is the major cause of HIV infection and AIDS worldwide, with HIV-2 infections being found only in West Africa (Sharp et al, 2001; Reeves & Doms, 2002; Gilbert et al, 2003; Sharp & Hahn, 2011). The rest of this work will focus on the details of HIV-1 and HIV-1 infections. HIV-1 can be further divided into four distinct groups; M, N, O, and P. HIV-1 group M represents the majority of HIV-1 infections worldwide, and is considered the pandemic form of the virus. Groups N and O each make up less than 1% of total HIV-1 infections. HIV-1 group P is newly discovered, and has infected only a handful of individuals (Sharp & Hahn, 2011). Group M can be further divided into 9 major groups, termed clades, (A, B, C, D, F, G, H, J, and K) as well as a number of circulating recombinant forms (Taylor et al, 2008; Sharp & Hahn, 2011).

HIV-1 structure and viral proteins

HIV has a single stranded RNA genome consisting of three main genomic elements; gag, pol, and env. These regions produce a number of different proteins from a relatively short genomic strand utilizing a combination of overlapping open reading frames, differential splicing, and post-translational modifications. The structure of the genomic RNA is also known to play a role in multiple facets of viral function, through use of binding sites and superstructures (King, 1994; Paillart et al, 2002; Kuiken et al, 2010). The genomic RNA is packaged within the lipid membrane-covered capsid which

is comprised of several proteins (p24/CA-capsid, p17/MA-matrix, p7/NC-nucleocapsid, and p6) which are cleavage products of p55, the product of the Gag gene. These proteins form specific functions in the formation of the capsid structure, binding of the genome, interaction with viral and host proteins as well as binding of the membrane envelope, which the virus takes upon budding from its cellular host (King, 1994; Kuiken et al, 2010). The product of the Env gene is broken down to gp41 and gp120, which insert into the viral membrane and play a critical role in binding to and infecting cells (Kuiken et al, 2010). The Pol gene product is the proenzyme for several components necessary for viral integration and replication; Protease, Reverse Transcriptase, RNase H, and Integrase (King, 1994; Kuiken et al, 2010). The remaining proteins are encoded by individual genes; Rev, Vif, Vpr, Vpu, Nef, Tef, and finally Tat, which is the main focus of the work to be presented this document (Kuiken et al, 2010).

HIV-1 Tat

The HIV-1 transactivator of transcription (Tat) protein is critical for viral replication. Tat will interact with host positive transcription elongation factor b (P-TEFb) during the initiation of viral replication, and bind to the viral TAR genomic element. Formation of this complex causes the phosphorylation and subsequent activation of Abbreviation, and RNA Polymerase II, allowing for whole-genome transcription of the virus to occur (Kim & Sharp, 2001; Sobhian et al, 2010; Debaisieux et al, 2012). Low level production of Tat is achieved by reverse transcriptase production following infection of a cell. This small initial amount of Tat allows for viral replication to occur more rapidly (Kim & Sharp, 2001). The length of the Tat protein is variable depending on specific viral strain, ranging from 80-103 residues (Walker & Burton, 2008;

Debaisieux et al, 2012). There are several highly conserved residues and domains within the various Tat protein sequences. Notable domains include a Zn²⁺ binding domain, a highly basic domain, and the N-terminal domain which is strongly acidic (Bayer et al, 1995; Debaisieux et al, 2012). Internal interactions within the Tat protein are fluid, and influenced by a number of extrinsic factors, and as such the secondary structure of the Tat protein is highly variable, with the basic domain usually being available for binding interactions. Binding via the basic domain stabilizes the Tat protein, and Tat binding interactions tend to be very tight (Zhang et al, 2000; Pantano et al, 2002; Pantano et al, 2004; Rayne et al, 2010; Debaisieux et al, 2012). In addition to its role in binding, the basic domain of the Tat protein serves as a targeting sequence which facilitates passage through plasma membranes. Tat can also be actively secreted via vesicular transport, meaning that cellular lysis is not necessary to release Tat into the extracellular space. (Frankel & Pabo, 1988; Green & Loewenstein, 1988; Rayne et al, 2010; Debaisieux et al, 2012). Additionally, truncated Tat fragments can pass through the membrane to interact with intracellular components (Soulas et al, 2009). The flexibility in structure and lack of spatial restriction give Tat the ability to interact with a wide variety of molecules outside of the Transactivation response (TAR) element, including various cell surface receptors, conferring on Tat the ability to induce a number of pathological states associated with AIDS and NeuroAIDS even in the absence of active viral replication. The unique properties of Tat make it highly pathogenic, as well as a candidate for re-engineering to deliver targeted therapeutics to otherwise difficult-to-reach targets (Bayer et al, 1995; Nath et al, 1996; Debaisieux et al, 2012; Cohen-Avrahami et al, 2014).

Transmission and Epidemiology of HIV Infection

HIV is spread by blood and sexual fluids, specifically, seminal, vaginal, and rectal fluids. Early on in the AIDS crisis, several high-risk groups emerged; men who have sex with men (MSMs), those receiving blood transfusions, and intravenous (IV) drug users. Sexual transmission, however, is not limited to MSMs. Any sexual contact involving sexual fluids coming in contact with a mucous membrane can transmit HIV (van der Graaf & Diepersloot, 1986; CDC, 2016). Several other conditions of infection were also noted; healthcare workers may become infected due to needlestick events, and HIV can be transmitted mother-to-child in several ways; perinatally due to bodily fluid contact events during the birthing process, and rarely across the placenta or by breastmilk (van der Graaf & Diepersloot, 1986). Casual contact does not spread HIV, and while viral particles have been found in other bodily fluids, transmission is uncommon unless blood is present in the fluids, and fluid-to-blood contact occurs (van der Graaf & Diepersloot, 1986; CDC, 1987; CDC, 2016). Cerebrospinal fluid (CSF) can contain measurable levels of HIV viral particles, however, the likelihood of actual transmission by CSF contact is low outside of occupational exposure (CDC, 1987; Bell et al, 1998; Nath, 2015). Recent estimates by the World Health Organization (WHO) suggest 36.7 million people worldwide are living with HIV infection, with 18.2 million HIV+ individuals on antiretroviral therapy (WHO, 2016).

AIDS

The disease caused by HIV infection is called Autoimmune Deficiency Syndrome (AIDS). When sufficient contact between the blood or sexual fluids of the infected individual and the new host occurs, the virus will infect the CD4+ T cells and CD4/CD8+

macrophages of the peripheral immune system via interactions with CCR5 or CXCR4, depending on viral tropism (Berger et al, 1998; Coakley et al, 2005; Zhou & Saksena, 2013). Shortly after infection, an initial drop in CD4+ cells will occur as the immune system is attacked by the virus. Symptoms during this phase appear similar to a flu-like viral infection; fever, lethargy, etc., although the overt symptoms of viral infection may not present in all patients (WHO, 2017). This phase soon resolves as the immune system produces antibodies to the virus and suppresses the infection, restoring the CD4+ cell count to near pre-infection levels. At this point, the patient enters a relatively symptom free period of latency (Shah et al, 2010; Elliot et al, 2012). The latency period of the HIV virus lasts an average of 8 years, and since the viral genome is integrated into the host genome, the virus continues to be actively replicated within infected cells (Harris & Bolus, 2008; Elliot et al, 2012; CDC, 2017). Over this 8 year period, the patients CD4+ cell count will steadily decline. A patient's status changes from being HIV positive to having AIDS when their CD4+ cell count drops below 200 (Crum-Cianflone et al, 2009), with the number of CD4+ cells remaining being negatively correlated with post-AIDS seroconversion survival (Jacobson et al, 1993). At this point, the patients' immune system is compromised, and they become susceptible to a wide variety of opportunistic infections that healthy individuals are generally able to handle, and infections that are typically mild can become terminal (Gilmore et al, 1983). In addition, the immune response to naturally occurring aberrations in cell growth is also affected. As such, many patients develop a specific type of tumor known as Kaposi's sarcoma (Gilmore et al, 1983; Bohlius et al, 2014). There are also neurological complications to HIV infection. Early on in the initial HIV epidemic period, the neurological effects,

although sometimes quite severe, were less of a concern, as patients who contracted HIV and developed AIDS died rapidly from various infections. However, as the lifespan of HIV patients was extended by the use of antiretroviral therapies and the immunological disease became more manageable, the treatment and study of the neurological disease became more practical (Gelman et al, 2013).

Infection of the CNS

HIV enters into the brain and establishes a reservoir quickly after infection (Masliah et al, 2000). The infection of the CNS is thought to occur via the “Trojan horse model”, in which infected CD8+ monocytes cross over the blood brain barrier, allowing the virus access to an area where it would typically be unable to cross on its own (Peluso et al, 1985; Haase, 1986; Meltzer et al, 1990; Zhou & Saksena, 2013). While the evidence most strongly supports the Trojan horse model, other less likely alternative methods for viral entry have been proposed (Harouse et al, 1989; Kaul et al, 2001; Zhou et al, 2008; Zhou & Saksena, 2013). Alternative theories include transcytosis, in which viral particles in the blood are taken up into vacuoles by endothelial cells, and then released into the brain (Kaul et al, 2001; Liu et al, 2002; Bobardt et al, 2004), and primary infection of the choroid plexus which then spreads to the rest of the CNS via the cerebrospinal fluid, or CSF (Harouse et al, 1989; Chen et al, 2000). Regardless of the viral entry mechanism, once introduced, HIV will infect microglia, the resident immune cells of the brain, as well as astrocytes. Neurons, however, are not infected by HIV (Soulas et al, 2009).

The HIV Associated Neurocognitive Disorders

Soon after the discovery of AIDS, it was realized that severe neurological impairments could accompany the disease (Snider et al, 1983; Levy et al). Presently, there are three broad classifications of HIV-associated neurocognitive disorders (HAND); asymptomatic neurocognitive impairment (ANI), Mild neurocognitive disorder (MND), and HIV associated dementia (HAD), in order of increasing severity (Antinori et al, 2007; McArthur et al, 2010), with some of the most severe cases exhibiting HIV encephalopathy (HIVE) (Everall et al, 2009). Greater understanding leading to treatment of HAND, especially the more severe varieties, is crucial, as it is not prevented entirely by combined antiretroviral therapy (cART) (Sacktor et al, 2002; Tozzi et al, 2005). In fact, as longevity of AIDS patients is increasing, the number of AIDS patients living with HAND is increasing, although there are declines in the prevalence of HAD as well as HIVE (McArthur, 2004; Ellis et al, 2007; Everall et al, 2009; Heaton et al, 2011). Neuroinflammation is considered to be the main cause for development of HAND (Glass et al, 1995; Persidsky & Gendelman, 2003; Everall et al, 2009; Levine et al, 2016). The presentation of HAND differs among patients, but tends to involve some common symptomatology, which include deficits in various types of memory, learning and attention, verbal function, mood disorders, generalized processing speed deficits, motor dysfunction, and difficulties in processing visual information or performing spatial manipulations (Antinori et al, 2007; Dawes et al, 2008; Levine et al, 2016). The severity of HAND sometimes progresses to the point of inability to care for oneself or function in society (Antinori et al, 2007).

Neuronal pathology

Excitotoxicity is one of the main neuronal pathologies caused by HIV infection, and also commonly presents in other neurodegenerative diseases, seizure disorders, and traumatic brain injuries (Haughey et al, 2001; Avignone et al, 2005; Mattson et al, 2005; Li et al, 2008; Mehta et al, 2013). Excitotoxicity occurs when a neuron becomes overactivated by glutamate signaling, which can be due to excessive glutamate release, lack of glutamate clearance, or improper inhibitory feedback. Excitotoxicity is not a single process, but rather an umbrella term used to describe the general effects which can be driven by many pathological states, and have subtle differences in cellular and systems presentation. (Bouilleret et al, 2000; Mehta et al, 2013). While excitotoxic damage does not appear to be immediately deadly in neurons in vivo, a long-term buildup of damage over time can lead to a loss of function and eventually death by the activation of caspases, but not wholesale sudden necrosis. This sustained cumulative damage is believed to explain why neurological symptoms take so long to appear after the onset of AIDS (Coleman et al, 2004). An example of this can be seen in the loss of dendritic spines in hippocampal neurons of transgenic mice with an active Tat transgene without evidence of decreased neuronal number, or significant increase in evidence of cell death (Fitting et al, 2013). Interestingly, some components of Tat-induced excitotoxic injury appear to be reversible (Kim et al, 2008). The HIV proteins Tat and gp120 can induce excitotoxicity (Haughey & Mattson, 2002). Tat binding to the LRP receptor on neurons, which is associated with the NMDA receptor, causes an abnormal association of PSD-95 and nNOS to the NMDA/LRP complex. Interestingly, this can lead to apoptotic events in neurons that lack NMDA receptors as well as due to increased nitric oxide (NO) production (Eugenin et al, 2007; King et al, 2010). This

complex plays a role in the phosphorylation of several sites on the NMDA receptor subunit 2A through the activation of Src kinase, the most important being Y1325.

Gp120 can also potentiate excitotoxicity; exposure potentiates calcium signaling of NMDA receptors, with a greater effect driven by interactions with subunit 2B (King et al, 2010; Krogh et al, 2014; Zhou et al, 2016). Tat can also directly bind the receptor itself and act as an agonist, causing further toxicity (Li et al, 2008). The calcium dysregulation that comes with excitotoxic injury will also cause mitochondrial dysfunction, which may explain the shortening and loss of complexity seen in neurites after HIV infection or exposure to HIV proteins (Iskander et al, 2004). Additionally, Tat can act directly as a COX inhibitor, but only after it permeabilizes the mitochondrial membrane, which will further contribute to mitochondrial failure. (Iskander et al, 2004; Lecoecur et al, 2012). The HIV viral proteins Vpr and Tat may also have an effect on neurons by altering miRNA expression. A study by Mukerjee et al (2011) showed that Vpr is taken up by cultured neurons, leading to disturbances in calcium levels, increased oxidative stress, synaptic dysfunction and damage to the mitochondria. The group found an increase in miRNAs against several critical mRNAs, a number of which (CACNB1, STIM1, IRIBT) are involved in calcium control within neurons. Others are involved in synaptic plasticity (SIRT-1), general cellular processes and maintenance (CREB) and maintaining structural integrity of processes (NEFM). Most of these mRNAs were decreased compared to control in neurons exposed to Vpr. In Tat-treated cells, the group found upregulation of miRNAs against many of the same mRNAs that are targeted in the case of Vpr exposure. The data on miRNAs are presently contested, however, due to questions of reproducibility (Chang et al, 2011; Mukerjee et al, 2011;

Witwer, 2014). In addition to the direct effects of HIV on neurons there are also bystander effects that cause neuronal injury which can be due to the direct effect of HIV proteins on glia, the natural immune response, or other pathological processes (González-Scarano & Martín-García, 2005; Fitting et al, 2010b; Ton & Xiong, 2013; Zhou & Saksena, 2013). Some of these effects will be discussed in the subsequent sections, which deal with HIV effects on glial cells.

Astrocytic pathology and contribution to neuroAIDS

Astrocytes perform a number of key roles in the brain including trophic support, clearance of the synaptic cleft, and formation of the blood brain barrier. It is not surprising that once these cells are infected, they play a significant role in the progression of neurological disease. The onset of astrocytosis occurs rapidly once HIV has entered the brain (An et al, 1999), and can be induced by direct infection of astrocytes, or by independent extracellular action of viral proteins. This condition leads to the production of pro-inflammatory cytokines and other neurotoxic factors (Ton & Xiong, 2013; Zhou & Saksena, 2013).

There are many cytokines known to be released by astrocytes in HIV infection, for example IL-1 β , IL-6, IL-8 and TNF- α . A significant portion of these secreted products are also produced by microglia (González-Scarano & Martín-García, 2005; Ton & Xiong, 2013). To go into detail for each one of them would require its own review and so this section will cover some of the more current research on astrocyte cytokine production and effects in response to HIV infection and other general insults. The basic profile of astrocyte cytokine production in the absence of an insult was recently profiled in cultured human cells. The basic expression profile includes G-CSF, GM-CSF, GRO α ,

IL-6, IL-8, MCP-1, MIF, and Serpin E1. The cultured astrocytes were then subjected to insult via IL-1 β and TNF- α . These cytokines caused expression of six other cytokines by activation of an NF- κ B pathway; IL-1 β , TNF- α , RANTES, MIP-1 α , IP-10, and IL-1ra, along with other factors traditionally involved in cell adhesion, chemotaxis, and immunity. Additionally, the basally-expressed cytokines G-CSF, GM-CSF, GRO α , and IL-6 were increased relative to their control levels while MCP-1 and MIF were decreased. The authors believe that there are still more astrocyte derived cytokines involved in neuroinflammation than what they found in their study (Choi et al, 2014). It is important to note that the basal production of cytokines by astrocytes in different brain regions will vary. In a 2010 study by Fitting *et al*, cultured astrocytes taken from mouse cortex, cerebellum and spinal cord were probed for basal levels of cytokine production, and then challenged with combinations of Tat, gp120, and with morphine (Fitting et al, 2010b). This study noted several more cytokines produced by resting astrocytes than the previously-discussed study; KC, eotaxin, IL-9, MIP-1 α , MIP-1 β , and IFN- γ , although this may be a species difference (Fitting et al, 2010b; Choi et al, 2014). Basal cortical production of most cytokines was much lower than that observed in cerebellum or spinal cord. The secretory response of activated astrocytes to HIV proteins independent of morphine also varies by region and specific HIV protein. Only IL-1 β production was independent of brain region. Exposure to Tat elevated most cytokine production in all assayed brain regions, but the cerebellar astrocytes had a much weaker response than astrocytes of the cortex or spinal cord. In contrast gp120 did not significantly affect cytokine release despite causing an increase in intracellular calcium levels (Fitting et al,

2010b). CXCL8/IL-8 is also found to be upregulated in astrocytes following HIV infection (Mamik & Ghorpade, 2012).

Aside from direct damage to neurons, HIV proteins along with cytokines can cause astroglia to produce other toxic compounds. For example, gp-120 induced production of arachidonic acid (Samikkannu et al, 2011). The oncogene AEG (astrocyte elevated gene)-1 has been found to play a role in cytokine cascades that lead to neuronal injury. It is found to be upregulated in astrocytes which are exposed to Tat and complete HIV-1 virions, along with pro-inflammatory cytokines commonly observed in neuroAIDS TNF- α , and IL-1 β . Not only do these insults increase expression of AEG-1, they cause it to translocate from the cytoplasm to the nucleus where it interacts with NF- κ B, leading to the downregulation of EAAT2, a glutamate transporter, and upregulated YY1, which acts to repress EAAT2. Constitutive overexpression of AEG-1 causes the same effects, but the process is exacerbated when IL-1 β is introduced, presumably because it precipitates nuclear translocation. Altogether, this novel pathway which culminates in decreased glutamate clearance highlights one of the ways in which released cytokines can cause indirect excitotoxic injury to neurons (Vartak-Sharma et al, 2014).

Disruption of the blood brain barrier is also a contributing factor in the progression of HAND. Astrocytic cytokines play a role in facilitating the passage of infected immune cells across the BBB. In addition to having direct neurotoxic effects, the increased expression of CXCL10 in HIV has been shown to have a chemotactic effect on peripheral blood mononuclear cells (Mehla et al, 2012). CX₃CL1/fractalkine has been shown, with leukotrienes, to facilitate contact of HIV infected monocytes and

brain macrophages and transfer of infection. This process itself does not induce disruption of the blood brain barrier (Bertin et al, 2014). Additionally, IL-6 has also been shown to act as a chemoattractant to circulating lymphocytes (Almolda et al, 2014). This may be an important process for establishing the reservoir in the brain after initial infection and exacerbating inflammatory damage as the creation of a more permissive barrier due to decreases seen in expression of tight junction proteins, increased matrix metalloproteinase-9 activity in brain endothelial cells, and endothelial cell apoptosis is coupled with the increased attraction of immune cells from the blood stream (Andras et al, 2003; Kim et al, 2003; Xu et al, 2012; Zhou & Saksena, 2013; Rao et al, 2014; Leibbrand et al, 2017; Patel et al, 2017).

Finally, the overall health of the astrocytes can contribute to neuronal pathology, as astrocytes play a key role in supporting neuronal health. Astrocytes form the first line of defense against aberrant ROS production in the brain (Desagher et al, 1996; Masanetz & Lehmann, 2011; Ferrucci et al, 2013). Exposure of astrocytes to HIV-1 VPR causes an increase in oxidative stress along with increased cytokine production. VPR also causes decreases in ATP and glutathione levels, which would normally help to alleviate oxidative stress. It was also found that there was a decrease in GAPDH expression and therefore decreased glycolytic activity after VPR exposure, resulting in neuronal apoptosis. Astrocytes normally secrete glutathione which is taken up by neurons. Neurons exposed to conditioned medium taken from VPR-treated astrocytes showed increased apoptosis compared to neurons exposed to control astrocyte conditioned medium. This is likely due to the neurons' inability to reduce oxidative stress due to the lack of secreted glutathione (Desagher et al, 1996; Ferrucci et al, 2013). The

HIV-1 protein Nef, which is expressed in infected astrocytes also decreases fitness. Under normal circumstances, immune cells put out reactive oxygen species in addition to inflammatory cytokines, and astrocytes play a strong role in protecting neurons from damage due to ROS production acting as a buffer and providing glutathione. Astrocytes transfected with Nef and exposed to a medium containing 10 μ M hydrogen peroxide were much more likely to die in a four hour incubation than astrocytes not transfected. This effect may be due to the loss of glutathione production (Desagher et al, 1996; Masanetz & Lehmann, 2011; Ferrucci et al, 2013).

Microglial and MDM pathology and contribution to neuroAIDS

Microglia and monocyte-derived macrophages (MDMs) also contribute to the progression of neuroAIDS. Microglia are the resident immune cells of the brain, and are known to produce cytokines, ROS, and other soluble factors against potential insults. Many of the pro-inflammatory cytokines that are produced by astrocytes are also produced by microglia and MDMs, with microglia representing the main source of pro-inflammatory cytokines (Rock et al, 2004; Ghorpade et al, 2005; González-Scarano & Martín-García, 2005; Almolda et al, 2014; Rao et al, 2014). Microglia respond rapidly to HIV infection. Infection of cultured microglia with HIV causes the production of pro-IL-1 β and other inflammatory products as early as four hours after exposure to the virus (Walsh et al, 2014). It is important to note that the production of inflammatory molecules is only one of the reasons that the increased attraction of immune cells across the BBB and activation of microglia play such a significant role in the progression of neuroAIDS pathology (Andras et al, 2003; Kim et al, 2003; González-Scarano & Martín-García, 2005; Xu et al, 2012; Almolda et al, 2014; Rao et al, 2014). It is also important to note

that in HIV patients receiving antiretroviral therapy, microglia remain activated and continue to produce inflammatory molecules. This phenomenon correlates with mild neurocognitive decline in otherwise asymptomatic patients (Garvey et al, 2014).

Much like astrocytes, microglia also have different characteristics and responses depending on where in the brain they are located. In a comparison of microglia collected from a patient with HAD against seronegative patients, tissue samples were collected from multiple brain regions (cortex, basal ganglia, striatum, cerebellum, brain stem, and hippocampus). Microglia in all the regions observed were activated in the HIV patient, and increased microglial numbers were seen in the cortical white matter, basal ganglia, cerebellum and brain stem. In all areas, immunohistochemical (IHC) tissue analysis showed that there were microglia (identified by CD68 and vimentin IHC reactivity) positive for HIV-1 p24, indicating infection, although the number of cells varied region to region and correlated with presence of microglial nodules and immune activation. Microglia also formed multinucleated giant cells post-infection. Comparison of the amount of viable glial cells showed no significant differences. In all brain regions surveyed, microglia in the HIV+ patient showed less production of TNF- α both basally and induced, indicating a decreased immune reaction rather than a die-off of microglia (Ghorpade et al, 2005). In addition to a decreased immune response, increases in production of IL-8 (CXCL8) by astrocytes and microglia can contribute to increasing viral genome integration rates and replication rates within infected microglia and macrophages. The replication rates increase with longer exposure to the factors involved and infection of new cells, leading to a downward spiral effect (Huang et al, 2011; Mamik & Ghorpade, 2012; Mamik & Ghorpade, 2014).

These cells also play a role in exacerbating neuronal excitotoxicity. Microglia infected by HIV produce an increased amount of glutamate due to an increased expression of microglial glutaminase in culture. This effect is also found in patients suffering from HAD (Huang et al, 2011). Additionally, the production of TNF- α and IL-1 β by microglia and MDMs causes upregulation of glutaminase in human neuronal cultures (Ye et al, 2013). Other microglial/monocyte produced compounds can strengthen the effect. For example, activated microglia and monocytes produce quinolinic acid, a metabolite of tryptophan that acts as an NMDA agonist at the glutamate binding site. This agonism has been shown to enhance excitotoxicity. The production of quinolinic acid is more robust in MDMs (Kerr et al, 1998; Guillemin et al, 2005). Another MDM secreted factor that promotes excitotoxicity is Platelet activating factor (PAF), which can also be secreted by astrocytes (Gelbard et al, 1994).

Microglia can also play a more direct role in neural damage than simply secreting toxic factors. In mice injected intracranially with Tat, microscopy on tissue slices indicated that activated microglia produce filopodia, and form contacts with dendritic spines, presynaptic terminals, and extend into excitatory and inhibitory synaptic clefts, which may disrupt the synapses in a process called synaptic stripping. The filopodia had phagosomes which contained parts of the synaptic structures, and the surrounding area showed evidence of proteolytic degradation, indicating that microglia may be actively breaking down synapses in response to HIV proteins (Tremblay et al, 2013). This could be a potential mechanism contributing to the loss of dendritic spines observed in neurons when combined with the problem of failing metabolic support which

leads to loss of dendritic length and arborization (Iskander et al, 2004; Vander Jagt et al, 2008; Tremblay et al, 2013).

Oligodendrocytic and myelin pathology

While oligodendrocytes are not believed to be infected by HIV (Zhou & Saksena, 2013), they do have receptors for many of the inflammatory cytokines released by astrocytes, MDMs, and microglia, making them susceptible to damage by the pathological processes that occur in neuroAIDS (González-Scarano & Martín-García, 2005). In individuals infected with HIV, a condition called vacuolar myelopathy (VM) can arise in white matter. A post-mortem assessment of AIDS patients revealed that in white matter tracts of the spinal cord, there was significant vacuolation, demyelination, and increased presence of macrophages, and there was no correlation with astrocyte activation (Gyorkey et al, 1987; Tran et al, 1995). In some regions of the brain, but not all, myelin thickness around axons has been observed to decrease, as has the volume of the anterior corpus callosum from loss of both nerve fibers and myelin (Wohlschlaeger et al, 2009). There is a significant reduction in oligodendrocyte process length observed in an in vivo Tat injection model, and losses in oligodendrocyte membrane area in the HIV-1 Tat transgenic mouse model (Hauser et al, 2009; Zou et al, 2015). Additionally, oligodendrocytes exposed to Tat alone show an upregulation in caspase production, but no increase in apoptosis rate (Hauser et al, 2009). This is likely related to increases in Ca^{2+} influx into the oligodendrocytes mediated the interaction of Tat with the AMPA and NMDA receptors (Zou et al, 2015).

MRI often shows “white matter pallor”, which might indicate demyelination or an area of edema, perhaps due to increased leak through the blood brain barrier in HIV

patients. In a 2001 study using MRI diffusion tensor imaging, an MRI method for white matter, microstructural abnormalities were seen in early stage HIV positive patients in the frontal cortex and the internal capsule, however newer data suggest other disturbances can occur in any CNS white matter tract (Pomara et al, 2001; Xuan et al, 2013). The altered myelination may lead to decreased conduction velocity along white matter tracts as is the case in the HIV infected peripheral nervous system (Kokotis et al, 2007), and such changes would undoubtedly contribute to aspects of HAND.

One of the pathological conditions that arises in oligodendrocytes/white matter is the production of self-antibodies against myelin proteins as seen in multiple sclerosis (Maimone et al, 2009; Lackner et al, 2010). In a comparison of HIV patients, MS patients, and control subjects, myelin basic protein antibodies were found in the CSF of HIV patients at higher levels than MS patients while none were found in control subjects. Patients who had both HIV and MS had equivalent antibody levels to MS free HIV patients (Maimone et al, 2009). Antibodies against myelin oligodendrocyte glycoprotein (MOG) were found in the CSF of AIDS patients, but not of patients suffering from other neurological conditions. Furthermore, the antibodies of HAND patients were more specific than those in asymptomatic patients. Additionally the antibodies against MOG were found before and after effective antiretroviral therapy (Lackner et al, 2010).

Global effects of HIV on the central nervous system

Throughout the brain, there appears to be a decrease in volume across multiple regions. This atrophy is observed in adults and in children, and correlates with decreases in CD4+ cell count and cognitive decline, but not with duration of infection

(Johann-Liang et al, 1998; Thompson et al, 2006; Chiang et al, 2007; Andronikou et al, 2014). Concurrent with brain atrophy is an expansion of ventricular volume by an average of 2.18 times the observed volume in control patients as detected by MRI. The expansion is not uniformly distributed within the ventricles, with the occipital and frontal horns expanding more than the temporal horn (Thompson et al, 2006). These effects are persistent even with effective ART, as is the progression of neurocognitive impairment (Gongvatana et al, 2013; Hua et al, 2013). Elevated quinolinic acid in the CSF is linked to the atrophy observed in the brain, specifically in those regions that are susceptible to excitotoxic injury (Heyes et al, 2001). Histologically, it has been observed that in patients with HAD, the spatial distribution of astrocytes changes as the disease progresses. Astrocytes cluster near interneurons, and away from large pyramidal cells, with the level of clustering correlating to the severity of the disease. The clustering was determined by identifying specific cell types in slices and measuring the closeness to the interneurons by applying concentric rings of a known distance and observing the number of cells present within these rings (Roberts et al, 2013). Additionally, there is deposition of amyloid- β plaques as in Alzheimer's disease, with higher levels of amyloid- β in cases of HIVE, and a correlation between amyloid- β deposition and age. While amyloid- β deposition is not necessarily causative of HAND symptoms, it can serve as a marker of disruption in protein clearance (Esiri et al, 1998; Achim et al, 2009; Soontornniyomkij et al, 2012).

While there are global changes, a wide variety of pathologies are observed in most brain subregions, giving rise to the various behavioral facets of NeuroAIDS (Table 1) (Nath, 2015). These differences in pathology are due to numerous factors both

anatomical and cellular which influence the nature of HIV-host interactions. A variety of genes, with the most notable being MAP2 and synaptophysin (SYP), have been identified as being correlated with HAND severity and increased HIV RNA levels across multiple brain regions (Masliah et al, 1997; Moore et al, 2006; Levine et al, 2016). Due to the complex interplay between genes in individuals, the response to HIV-induced neuroinflammation may vary from patient to patient, in part explaining the differential presentation of HAND in individual cases (Lojek & Bornstein, 2005; Dawes et al, 2008; Fazeli et al, 2014; Levine et al, 2016). Anatomically, the relative closeness of a structure to the ventricles is suspected to be a factor, as viral particles, produced toxins like quinolinic acid, and pro-inflammatory factors are found to be elevated in the CSF (Kerr et al, 1998; Petito et al, 1999; Heyes et al, 2001; Thompson et al, 2006; Tate et al, 2011; Ances et al, 2012; Andronikou et al, 2014; Choi et al, 2014). At the cellular level, HIV Tat has been shown to have disparate effects on the astrocytes of different regions (Fitting et al, 2010b). There have been observations of regional heterogeneity in astrocytic and microglial subpopulations genetically and functionally (Hochstim et al, 2008; Chaboub & Deneen, 2012; Martin et al, 2015; Covelo & Araque, 2016; Grabert et al, 2016). This is in addition to the wide array of neuronal phenotypes found in the structures of the CNS (Klausberger & Somogyi, 2008; Bikoff et al, 2016), So it should come as no surprise that the great variety in CNS cell subtypes within discrete brain regions would create unique responses to HIV infection and its sequelae (Fitting et al, 2010b; Nath, 2015).

The Hippocampus and HIV

The region of interest in the studies to be discussed is the hippocampus. This structure can be found in each hemisphere of the brain, and is folded up beneath the edge of the cortex. While the neocortex has six layers, the hippocampus has 3-4 depending on the subfield of interest. The hippocampal formation is defined as the hippocampus proper (the Dentate gyrus and cornu ammonis regions) and several associated structures, usually referring to the subiculum, entorhinal cortex, and fimbria of the hippocampus. The two main regions of the hippocampus proper can be further divided into anatomically and functionally distinct domains. The dentate gyrus can be divided by layers, the principal cell layer, or granule cell layer forms a chevron-like structure opening onto the end of cornu ammonis (CA). The layer within the chevron is called the hilus. This layer contains axonal projections to the CA. On the outer edge of the dentate gyrus is the molecular layer, which borders the interior edge of the CA/subiculum border. The CA structure is divided into three main regions, CA3, CA2, and CA1 (Ranson, 1932; Amaral & Lavenex, 2007). The CA3 region can be divided into 4 layers; in order from the outside border with the alveus; the SO, stratum pyramidale or pyramidal layer, stratum lucidum, and the stratum lacunosum-moleculare (SL-M). The stratum lucidum is unique to CA3. Outside of this difference, the layered structure of CA2 and CA1 is very similar to CA3. The overall flow of information in the hippocampus follows a defined path from the entorhinal cortex to the dentate gyrus via axons known as the perforant path. The dentate gyrus projections to CA3 are termed the mossy fibers, and the projections from CA3 to CA1/2 are referred to as the Schaffer collaterals. CA1 pyramidal neurons primarily project to the entorhinal cortex, completing the

processing loop through the hippocampus. In addition to this main loop, several back-and-co-projections occur, allowing for more complex processing (Amaral & Lavenex, 2007). Most notably, some perforant path axons also project directly to CA3 and CA1 (Deng et al, 2010). Within the hippocampal subfields, a wide variety of cell types interact to build defined regional microcircuits that allow for complex processing of information to occur (Amaral & Lavenex, 2007; Klausberger & Somogyi, 2008; Deng et al, 2010; Muller & Remy, 2014). Originally thought to simply be a high-order olfactory processing center (Ranson, 1932), this region of the brain is responsible for a number of functions, including spatial and social memory (Okuyama et al, 2016), as well as having some involvement in emotional processes.

The hippocampus has been shown to be vulnerable to the effects of HIV and HIV proteins. Learning, memory and spatial awareness, which are among the deficits observed in neuroAIDS, are mediated in part by the hippocampus (Castelo et al, 2006). A 2013 study by Fitting *et al* showed that in Tat transgenic mice, a loss of dendritic spines and inhibitory synaptic proteins within pyramidal layer of the CA1, indicating the loss of a specific subset of GABAergic interneurons, correlated with reduced hippocampal LTP and a reduction of both spatial learning and contextual fear conditioning. Another study also showed increased evidence of autophagy in hippocampal astrocytes (Vander Jagt et al, 2008). Similarly, Vpr also causes memory impairment. Vpr transfected astrocytes injected into the hippocampus of rats caused a decrease in long-term memory formation and an increase of neurons undergoing chromatolysis in CA1 and CA3 (Torres & Noel, 2014). These memory deficits exist in human patients as well. In a study consisting of only women, three different measures

of memory were found to be impaired; verbal episodic memory, visual memory, and working memory both in short and long term. Neuroimaging of the hippocampi in these subjects showed a lesser response during the encoding process, and a heightened response when attempting to recall after a delay in stimulus presentation (Maki et al, 2009). An earlier study also showed that regions of the hippocampus exhibit a reduced response during encoding, but increased activity was observed in the frontal and parietal cortices (Castelo et al, 2006). Hippocampal tissue is also susceptible to the accelerated aging processes associated with HIV infection and experiences a decrease in volume (Ances et al, 2012; Pfefferbaum et al, 2014), It likewise sees increased deposition of α -synuclein and β -amyloid (Kallianpur et al, 2012). In addition to its contribution to memory, dysfunction in the hippocampus also contributes to the depressive disorders seen in HIV patients resulting from the activation of indoleamine 2,3 dioxygenase (IDO) via p38 MAPK in response to inflammatory cytokine secretion (Fu et al, 2011).

The excitotoxic effects of HIV proteins are evident in the hippocampus. Synaptosome preparations of hippocampal neurons from Tat transgenic mice demonstrate an increased K⁺ evoked glutamate release but no change in GABA release (Zucchini et al, 2013), suggesting that Tat effects on GABAergic transmission within the hippocampus involve more than simply altered release mechanisms (Marks et al, 2016). In culture, hippocampal neurons have been demonstrated to lose synaptic terminals as a result of Tat-induced excitotoxicity, as indicated by a decrease in synaptophysin levels (Shin & Thayer, 2013). In addition to this, the remaining synaptic terminals are also affected. Neurons treated with Tat are more likely to generate

inhibitory synapses than excitatory synapses (Hargus & Thayer, 2013). These effects on synaptic integrity and formation are also based on excitotoxicity, and mediated by the binding of Tat to LRP, and formation of the LRP-PSD95-NMDA-nNOS complex rather than the apoptotic processes of excitotoxicity (Eugenin et al, 2007; King et al, 2010; Hargus & Thayer; Shin & Thayer, 2013). This may appear to conflict with the results from Fitting et al (2013) which show a decrease in inhibitory synaptic formation in CA1, however with the wide variety of hippocampal neuronal types, it is likely that there is a differential effect on a specific subset in that specific region (Klausberger & Somogyi, 2008; Fitting et al, 2013). This effect can be seen in an earlier study on the differential neuronal toxicity of Tat and gp120 in the hippocampus by Fitting *et al.* in 2008 (Fitting et al, 2008). Tat or gp120 were injected bilaterally into the hippocampi of newborn rats to assess long term toxicity. Neuron numbers were found to be decreased by Tat in CA 2/3, dentate gyrus, and subiculum, while gp120 only reduced neuron number in CA2/3, suggesting differential sensitivity of neuron subsets in those regions. Differential effects were also noted in glia, with astrocyte number being increased in the dentate gyrus and subiculum by Tat, and oligodendrocyte numbers being increased only in the dentate gyrus (Fitting et al, 2008). In addition, the hippocampus has been shown to have a reduced capacity to respond to oxidative stress in an HIV-transgenic rat model via the 2,2'-azino-bis(3-ethylbenzothiazoline-6-sulphonic acid; ABTS) assay (Pang et al, 2013).

The hippocampus is different from other regions, in that research indicates that it has a greater likelihood of recovery following injury resulting in loss of neurons. The hippocampus is one of the few regions in which neurogenesis continues into

adulthood. This neurogenesis is inhibited by HIV (Lee et al, 2011; Avraham et al, 2015), however, in a gp120 transgenic model, treating with an SSRI can rescue adult neurogenesis (Lee et al, 2011). In animals with a deletion of the gene encoding FAAH, the enzyme responsible for breakdown of endocannabinoids, neurogenesis in adult mice was not affected by gp120 (Avraham et al, 2015), raising hope for potential development of treatments. In fact, the damage caused to the hippocampus might not be irreversible. Within CA1, the chromatolysis induced by HIV proteins does not necessarily lead to neuronal death (Torres & Noel, 2014). The cellular deficits observed in CA1 do not appear to include loss of neuronal cells, but simply their impairment (Fitting et al, 2008; Fitting et al, 2013; Zucchini et al, 2013) . A 2008 paper by Kim *et al.*(Kim et al, 2008) also showed that in hippocampal cultures, synaptic loss via excitotoxicity is due to the LRP-PSD95-NMDA-nNOS complex rather than the apoptotic events of excitotoxicity (Eugenin et al, 2007; Kim et al, 2008; King et al, 2010; Hargus & Thayer, 2013; Shin & Thayer, 2013). It additionally showed that the process is reversible by treatment with receptor associated protein (RAP), which is an LRP blocker, after Tat treatment, while NMDA antagonists did not reverse the effect after Tat administration. The authors of this paper suggest that this reversible loss of synaptic structures is a compensatory mechanism meant to mitigate the effects of the excitotoxic state (Kim et al, 2008).

Comorbidity of HIV infection and opioid abuse disorder

A growing problem worldwide is the coincidence of HIV infection with opioid abuse disorder (Bruce & Altice, 2007). HIV infection can occur through the sharing of needles between injection drug users (IDUs), resulting in the transfer of small amounts

of blood between individuals and allowing the chance of HIV infection (van der Graaf & Diepersloot, 1986). The sharing of needles between users is a significant contributor to infections in individuals not engaging in risky sexual contact (Friedland, 1985; van der Graaf & Diepersloot, 1986; NIDA, 2017), and there is a significant overlap in the populations of individuals that are IDUs and those that engage in risky sexual behaviors (Bruce & Altice, 2007). Between 40 and 45% of IDUs are also HIV positive (Francis, 2003), and while opiates are not the only drugs injected intravenously, they do make up a large proportion of total injection drug use (Bruce & Altice, 2007). Even in the absence of injection drug use and the risk of increased infection, there is still a risk posed by the abuse of prescription opioids, which may or may not be prescribed to an HIV infected individual. Around 8% of HIV-Infected patients may be on long term, physician-prescribed courses of opiates. In an analysis of individuals whose tissue had been donated to a national brain tissue bank, over half of the HIV positive patients that were prescribed opiates were determined to exhibit improper use, however the lack of longitudinal data on these individuals leaves this value open to interpretation (Robinson-Papp et al, 2012; Silverberg et al, 2012).

The opiate receptors, morphine, and the hippocampus

There are three main classes of opiate receptor; mu (MOR), kappa (KOR), delta (DOR), with a fourth, the nociceptin opioid receptor (NOP), having close sequence homology, but little functional overlap with the other three. All of these receptors are G-protein coupled receptors that respond to a group of peptide neurotransmitters collectively known as the endogenous opioids, including enkephalins and endorphins (Butour et al, 1997; Gutstein & Akil, 2006; Bodnar, 2012). The three main receptors

have distinct functions and ligand affinities, with differential cell signaling cascades and behavioral outcomes associated with the activation of each receptor (Gutstein & Akil, 2006; Bodnar, 2012; Beckman, 2014). Activation of the opioid receptor system in general is associated with analgesia, however, other effects beyond analgesia occur (Gutstein & Akil, 2006; Lutz & Kieffer, 2013; Stein, 2016). Activation of the MOR causes the activation of reward pathways, and underlies the abuse liability of many opiate drugs. At the same time, MOR activation can cause depressive effects (Lutz & Kieffer, 2013; Stein, 2016). DOR acts in many ways as a mirror to MOR activity, with its activation effecting reward pathways, however, its role is modulatory and does not independently establish reward/dependence processes. As a result, many DOR agonists do not have the same abuse liability as MOR agonists. DOR activation also has been shown to have a mood elevating effect, and to be neuroprotective against excitotoxic damage (Gutstein & Akil, 2006; Kawalec et al, 2011; Lutz & Kieffer, 2013). Activation of the KOR runs counter to MOR/DOR activity, having dysphoric properties and having an anti-reward effect. KOR is involved in, and potentiated by stress processes (Lutz & Kieffer, 2013). Morphine, the prototypical opiate drug, and a drug of abuse, has the strongest affinity for the MOR, with off-target interactions at both the DOR and KOR (Gutstein & Akil, 2006; Hauser et al, 2012; Lutz & Kieffer, 2013; Beckman, 2014). In addition to the neurological effects of morphine, activation of the opioid receptors in immune cells has been shown to modulate inflammatory processes, and therefore can affect neuroinflammation (Stein et al, 2003; Gutstein & Akil, 2006).

As is common with most drugs of abuse, chronic use of opioid drugs leads toward development of tolerance and dependence. Anytime a drug is used over time in

a receptor system, the natural function of the system is supplanted by over- or under-activation, hence giving the desired effect. Sometimes, these systems will either adjust to the new levels of receptor activation by increasing or decreasing the available receptors or ligands in an attempt to return to a homeostatic baseline, resulting in more and more need for (dependence on) the drug, as the amount of drug or neurotransmitter needed to obtain the desired effect increases (tolerance). Morphine has been shown to cause tolerance and dependence in patients with chronic or repeated use (Gutstein & Akil, 2006). Interestingly, tolerance to the various effects of morphine develop at differential rates, with tolerance to analgesia developing rapidly, but tolerance to motor effects having a more complex progression depending on dosage regimen rates (Vasko & Domino, 1978; Ling et al, 1989). This effect may be tied to differential development of tolerance by the different receptor groups (MOR vs DOR/KOR) or MOR subtypes (Ling et al, 1989; Angelopoulos et al, 1995). The development of tolerance has been attributed to reductions in the available receptor at the cell surface, reduced availability of the endogenous opioid peptides, or a shift in agonist efficacy (Wimpey et al, 1989). While multiple mechanisms exist, the one described here is of particular interest due to the strong potential for overlap with HIV-induced excitotoxicity (King et al, 2010). In healthy neurons, the activation of the MOR by morphine activates Akt/PKB, which in turn activates nNOS. nNOS signaling leads to activation of PKC, which activates Src, resulting in phosphorylation of the NMDA NR2A subunit at Y1325, and increased calcium influx. This calcium influx triggers a feedback mechanism to reduce Akt and nNOS activity to reduce phosphorylation of NR2A. This process also leads to phosphorylation of MOR over time, resulting in receptor internalization and the

development of morphine tolerance (Wimpey et al, 1989; Sanchez-Blazquez et al, 2010). The inhibition of NOS has been demonstrated to reduce the development of tolerance due to MOR activation, but not KOR (Kolesnikov et al, 1993; Lue et al, 1999). The specific agonist studied is important, as some drugs but not others precipitate receptor internalization despite having similar activity at the receptor, making it an important consideration in drug replacement therapies used to treat opioid dependence (Kolesnikov et al, 1993; Fitting et al, 2015b) and in experimental paradigms.

Morphine effects in the hippocampus

Morphine is known to be neurotoxic on its own in cases of chronic and repeated exposure (Hauser et al, 2012; Liu et al, 2013; Razavi et al, 2014), and is especially detrimental to development of hippocampal neurons in pre- and postnatal development (Traudt et al, 2012; Bajic et al, 2013; Ghafari & Golalipour, 2014). Morphine's effects on behavioral processes linked to the hippocampus are largely on development of conditioned place preference in relation to morphine cues, and are also involved in modulation of contextual fear conditioning (Razavi et al, 2014; Tan et al, 2015), but can also cause deleterious effects on spatial memory performance (Kitanaka et al, 2015). This is linked to the effects of morphine on synaptic plasticity within the hippocampus (Heidari et al, 2013; Portugal et al, 2014; Sadegh & Fathollahi, 2014; Tan et al, 2015), and notable alterations to the normal pattern of activity in the ability of the endogenous opioid system to modulate inputs and outputs (Wimpey et al, 1989; Harrison et al, 2002; Erbs et al, 2016). Morphine has demonstrated effects on hippocampal glutamatergic and GABAergic neurotransmission that may interact synergistically to enhance

excitotoxicity. Levels of glutamate were found to be increased after morphine sensitization, but decreased prior to the establishment of sensitization, and GABA levels were found to be initially decreased in the sensitization process, but then later become elevated following repeated exposure to morphine (Bodzon-Kulakowska et al, 2010; Farahmandfar et al, 2011a; Farahmandfar et al, 2011b; Zucchini et al, 2013). The increase of glutamate levels does not necessarily relate to the amount of glutamate synthetase, but rather to its biochemical activity, which is an important point to keep in mind when considering the levels of expression of other enzymes (Bodzon-Kulakowska et al, 2010). Even with the increase in glutamatergic activity, and the tendency toward excitotoxic states with long term opiate exposure in the hippocampus, altering the levels of activation between the three receptor groups can offset the damaging effects of morphine (Kawalec et al, 2011; Fitting et al, 2015b). The effects of morphine in the hippocampus are largely discussed in terms of broad outputs. However, from a modulatory standpoint it is important to recognize that the endogenous opioid system in the hippocampus is largely involved with regulation of the Inhibitory interneuron network, with differential expression of opioid receptors occurring on different subsets of interneurons, and notable overlap between signaling modalities found in CA1 (eg somatostatin) and opioid receptor activity (Hatzoglou et al, 1995; Drake & Milner, 2002; Pfeiffer et al, 2002; Rácz & Halasy, 2002; McQuiston, 2008; Jorand et al, 2016).

Interactions between HIV and opiate use

The effects of HIV on brain function and immunosuppression in both the periphery and CNS can be exacerbated by the use of opiates (Bell et al, 1998; Anthony et al, 2008; Byrd et al, 2012; Hauser et al, 2012; Meyer et al, 2013; Edelman et al,

2017). Increased severity of cognitive deficits has been linked to interaction of HIV and drug abuse (Bell et al, 1998), and HIV encephalitis has been found more frequently in drug-abusing patients infected with HIV than in HIV-infected non-abusers (Byrd et al, 2012). This is linked with increased inflammatory markers (Meyer et al, 2013), and coincides with increases in the viral load both in AIDS patients and in infected animal models (Anthony et al, 2008; Byrd et al, 2012; Hauser et al, 2012; McLane et al, 2014). The interaction between HIV and opiates can increase the severity of neuroAIDS, with increases in markers of disease severity such as multinucleated giant cells and HIV-1 p2-positive microglia (Anthony et al, 2008; Hauser et al, 2012). In addition to increased severity, HIV will emerge from latency earlier in opiate-abusing individuals (Anthony et al, 2008; Hauser et al, 2012). In the HIV-1 Tat transgenic mouse model (Bruce-Keller et al, 2008), morphine has been demonstrated to exacerbate excitotoxic effects in cultured neurons from the striatum and from the enteric nervous system (Hauser et al, 2012; Fitting et al, 2014). The development of neuronal excitotoxicity after Tat exposure is likely due to multiple interactive pathways with multiple points of convergence. For example, exposure to Tat results in phosphorylation of site Y1325 on the NR2A subunit of NMDA (King et al, 2010). This site is also a target of phosphorylation in the cascade triggered by activation of the μ -opioid receptor (MOR) (Sanchez-Blazquez et al, 2010; Garzon et al, 2011). The influx of Ca^{2+} through open NMDA channels into the dendrites of neurons after combined HIV-1 Tat and morphine exposure contributes to excitotoxic injury (Fitting et al, 2014). The activation of GSK3 β is another point of convergence for HIV pathology and opiate pathology. Inhibition of GSK3 β can block both HIV-induced neurotoxicity in cultured cells as well as the synergistic effects of morphine exposure

(Masvekar et al, 2015). There is some evidence, however, that the use of opiates does not always result in a synergistic worsening of HIV induced neurotoxicity, and can in fact be mildly neuroprotective. When buprenorphine, a common replacement therapy used to treat opiate addiction is used instead of morphine at high doses in neuronal culture, interactive neurotoxicity occurs. In contrast, at low doses, a mild neuroprotective effect is noted (Fitting et al, 2015b). This could be due to multiple factors. Tat has been shown to alter expression of the mu opiate receptor and certain endogenous opioids in the striatum and hippocampus while leaving kappa- and delta-opioid receptor expression unchanged. Similarly, MOR association with downstream signaling components has been demonstrated to be altered by morphine in the striatum and amygdala (Fitting et al, 2010a; Hahn et al, 2016). The activity of buprenorphine at these other receptors is likely to have played a role in the mild neuroprotection observed (Ammon-Treiber et al, 2007; Fitting et al, 2010a; Fitting et al, 2015b). In fact, there is some evidence suggesting that under the right circumstances, even morphine itself can be mildly neuroprotective due to its off-target effects if the dosage and receptor type spread within a region is right, despite its normal pro-apoptotic effects (Ammon-Treiber et al, 2007; Kawalec et al, 2011; Razavi et al, 2014). The extent to which this is true is likely to vary by brain region just as vulnerability to HIV pathologic processes vary, and to be affected by the degree to which different drugs affect internalization of the different opioid receptors (Ammon-Treiber et al, 2007; Fitting et al, 2010b; Gelman et al, 2012; Nath, 2015; Hahn et al, 2016). Additionally, HIV-1 Tat has been shown to increase the level of tolerance mice develop to chronic morphine exposure, while decreasing the

physical symptoms of withdrawal, perhaps through a series of compensatory mechanisms (Fitting et al, 2012; Fitting et al, 2016; Hahn et al, 2016).

Hypotheses and Aims

Although a number of studies have focused on the comorbidity of HIV-1 infection and opiates in the brain, few of these studies have assessed these comorbid interactions within the hippocampus. Moreover, while the response of the hippocampus to opioid drugs is fairly well defined from a functional standpoint (Valentino & Dingledine, 1982; Bao et al, 2007; Saboory et al, 2007; McQuiston, 2008), the functional response to Tat in the hippocampus is not as well characterized, with few studies examining the functional effects of the protein within the area (Carey et al, 2012; Fitting et al, 2013; Kesby et al, 2016). At present, no studies focus specifically on the functional circuit outcomes of HIV-1 Tat and morphine interactions within the hippocampus. The studies laid out here are aimed at first addressing in greater detail the effects of Tat on the hippocampal formation. This facilitated a more robust comparison between its effects and the effects of morphine during the later phases of these studies, which are aimed at understanding the potential interactions between Tat and morphine on hippocampal structure and function.

CNS Region	Effect
Striatum	Atrophy (Johann-Liang et al, 1998; Chiang et al, 2007; Andronikou et al, 2014) Calcification in juveniles (Andronikou et al, 2014)
	Decreased expression of DAT, VMAT2 (Midde et al, 2012; Theodore et al, 2012) MAO expression altered (Acharjee et al, 2014; Meulendyke et al, 2014) Decreased synaptogenesis (Gelman et al, 2012; Yuferov et al, 2013) Decreased dopamine levels (Kumar et al, 2011)
SN	Decreased dopamine levels (Kumar et al, 2011)
	Selective loss of dopaminergic/TH+ neurons (Agrawal et al, 2010)
Frontal Cortex	Regional atrophy (Thompson et al, 2005; Chiang et al, 2007; Hua et al, 2013) Accelerated aging (Khanlou et al, 2009; Pfefferbaum et al, 2014) Loss of synchronous firing in frontal eye field (Wilson et al, 2013) Increased ROS sensitivity (Zhang et al, 2012; Pang et al, 2013) Increased glutamate neurotransmission (Zucchini et al, 2013) Decreased GABA neurotransmission (Zucchini et al, 2013)
	Loss of dendritic spines (Fitting et al, 2013) Increased chromatolysis (Torres & Noel, 2014)
	Decreased activity during encoding tasks (Maki et al, 2009) Increased glutamate neurotransmission (Zucchini et al, 2013) Increased ROS sensitivity (Pang et al, 2013) Impaired adult neurogenesis (Lee et al, 2011; Avraham et al, 2015)
Corpus callosum	Regional atrophy (Johann-Liang et al, 1998; Thompson et al, 2006; Chiang et al, 2007; Tate et al, 2011; Ances et al, 2012; Hua et al, 2013; Andronikou et al, 2014)
	White matter pallor and volumetric disturbances (Gongvatana et al, 2009; Pfefferbaum et al, 2009; Muller-Oehring et al, 2010; Tate et al, 2011; Zou et al, 2015)
	Axonal damage (Gongvatana et al, 2009; Pfefferbaum et al, 2009; Muller-Oehring et al, 2010; Tate et al, 2011; Zou et al, 2015)
Amygdala	Variable volumetric disturbance (Ances et al, 2012)
Cingulate gyrus	Atrophy (Heyes et al, 2001)
	Decreased synaptogenesis (Yuferov et al, 2013) Beta oscillations diminished (Becker et al, 2013)
Cerebellum	Regional atrophy (Abe et al, 1996)
	Increased neuronal glutamate toxicity (Savio & Levi, 1993) Increased pH (Patton et al, 2001)
	Decreased neuronal kinase activity (Everall & Barnes, 1999)
Retina	Activation of Müller glia (Krishnan & Chatterjee, 2014)
	Decreased neural and glial cell viability (Chatterjee et al, 2011; Krishnan & Chatterjee, 2014) Decreased thickness of RNFL (Plummer et al, 2001; Cheng et al, 2011)
	Abnormal pattern evoked firing patterns (Iragui et al, 1996)
Optic nerve	Demyelination/vacuolar myelopathy (Sadun et al, 1995)
	Axonal degeneration (Sadun et al, 1995)
	Abnormalities in Visually evoked potentials (Iragui et al, 1996; Mwanza et al, 2004; Mahadevan et al, 2006)

Table 1. 1 Selected listing of regional effects of HIV/HIV proteins within the CNS

Chapter 2: The effects of HIV Tat on CA1 interneuron microcircuitry and spatial memory

Parts of this chapter appear in the Journal of Neurovirology, and are reproduced with permission of Springer (License #4205710527260):

J. Neurovirol. HIV-1 Tat causes cognitive deficits and selective loss of parvalbumin, somatostatin, and neuronal nitric oxide synthase expressing hippocampal CA1 interneuron subpopulations 22(6). 2016, 747-762, Marks WD, Paris JJ, Schier CJ, Denton MD, Fitting S, McQuiston AR, Knapp PE, Hauser KF. © Journal of NeuroVirology, Inc. 2016, with permission of Springer.
PMID: 27178324

Clarification of contributions: Novel object recognition testing was performed by Dr. Jason Paris

Introduction

Following the discovery of human immunodeficiency virus type 1 (HIV-1) and acquired immunodeficiency syndrome (AIDS), a profile of progressive neurological symptoms came to be associated with HIV-1 infection (Snider et al, 1983; Levy et al, 1985), now collectively referred to as HIV-associated neurocognitive disorders (HAND) (Antinori et al, 2007; McArthur et al, 2010). Although there is variation among patients, common symptoms include deficits in attention, learning, memory, and impaired motor function. The neurocognitive aspects of HAND can be severe enough to interfere with independent living (Antinori et al, 2007). Notably, combined antiretroviral therapy (cART) does not fully ameliorate these symptoms (Sacktor et al, 2002; McArthur, 2004; Tozzi et al, 2005; Ellis et al, 2007).

HIV may contribute to the progressive neurocognitive impairment in combination antiretroviral therapy (cART)-controlled patients through the continued production of

neurotoxic HIV-1 proteins from cellular reservoirs within the central nervous system (CNS) (Johnson et al, 2013). Shortly after infection, HIV-1 can enter the brain and establish central reservoirs (Lane et al, 1996; An et al, 1999), infecting microglia or astrocytes, but not neurons (He et al, 1997; Brack-Werner, 1999; Kramer-Hammerle et al, 2005; Churchill et al, 2009; Li et al, 2011). Uninfected cells can be damaged by viral proteins, as well as by the host neuroinflammatory response to virions and free viral proteins (Nath et al, 1996; Kruman et al, 1998; Nath et al, 1999; Aksenov et al, 2001; Soulas et al, 2009; Zhou & Saksena, 2013; Nath & Steiner, 2014). Among these neurotoxic factors, the HIV-1 transactivator of transcription (Tat) protein is critical for HIV replication (Zhou & Saksena, 2013; Nath & Steiner, 2014) and can be secreted by infected cells (Ensoli et al, 1990; Thomas et al, 1994; Rayne et al, 2010; Debaisieux et al, 2012) even in the presence of cART (Johnson et al, 2013). Furthermore, Tat can bind to a large number of extracellular receptors due to its highly basic domain (Philippon et al, 1994; Zhou & Saksena, 2013), penetrate and traverse the plasma membrane, and interact with a number of intracellular factors (Debaisieux et al, 2012).

Despite regional differences in CNS vulnerability to HIV-1 (Nath, 2015), few studies have examined why some brain regions and neuronal types are preferentially susceptible to the virus. A number of behavioral deficits, including attenuation of spatial learning and memory, which are common features of HAND, can be recapitulated by Tat exposure and may be attributed to cellular and functional deficits in the hippocampus (Li et al, 2004; Fitting et al, 2006; Fitting et al, 2013). Long-term potentiation (LTP) is lost when Tat is injected intrahippocampally or expressed endogenously (Behnisch et al, 2004; Li et al, 2004; Fitting et al, 2013). Despite the

pronounced loss of LTP and deficits in behavior, CA1 pyramidal cells showed only a modest decrease in the density of apical dendritic spines, but no loss in dendrite length or synaptic integrity at the ultrastructural level, and no alterations in the level of proteins involved in excitatory glutamatergic pre- and post-synaptic function (Li et al, 2004; Fitting et al, 2013). By contrast, there were selective alterations in proteins involved in inhibitory γ -aminobutyric acid-ergic (GABAergic) synaptic function, including a significant decline in synaptotagmin 2 (Syt2) expression (only within SR) and marked increases in the expression of gephyrin throughout CA1 (Fitting et al, 2013). These findings concur with human gene array data which show a high degree of correlation between the expression of genes associated with inhibitory GABAergic synaptic transmission, including *GAD1* and *GABAR1*, and the severity of HAND, but showed less robust correlations with genes associated with glutamatergic neurotransmission (Gelman et al, 2012).

GABAergic interneurons are a diverse population of specialized cells responsible for much of the processing that occurs in the hippocampus. With estimates of at least 21 distinct interneuron subtypes in CA1, there are numerous potential targets for the development of hippocampal pathology (McBain & Fisahn, 2001; Klausberger & Somogyi, 2008; Lovett-Barron & Losonczy, 2014). While numerous studies have examined the effects of HIV-1 on glutamatergic transmission in the hippocampus, few studies have assessed whether GABAergic synapses are altered. Pathology within specific GABAergic interneuron subpopulations, and the hippocampal interneuron network as a whole, has been demonstrated in a number of neurological disorders (Korotkova et al, 2010; Toth et al, 2010; Hazra et al, 2013; Levenga et al, 2013), some

of which produce behavioral deficits similar to those observed in experimental models of neuro-acquired immunodeficiency syndrome (neuroAIDS) (Carey et al, 2012; Fitting et al, 2013). In HIV models, reductions in the number of hippocampal neurons expressing parvalbumin (PV) in CA3 and somatostatin (SST) in CA1 have been observed (Masliah et al, 1992; Fox et al, 1997); however, since multiple neuron types in CA1 and CA3 express these markers, the identities of the affected interneuron subtypes remain unclear.

Based on the collective findings above, we hypothesized that specific interneuron subpopulation(s) might be preferentially vulnerable to HIV-1 Tat and that deficits in one or more interneuron subtypes following Tat exposure would coincide with impaired cognitive performance on hippocampus-dependent behavioral tasks. Our data show that HIV-1 Tat exposure was accompanied by memory impairment in mice and resulted in a selective decrease in the proportion of nNOS positive (nNOS+), neuropeptide Y negative (NPY-) neurons in both the stratum pyramidale and SR, as well as decreases in somatostatin-positive (SST+) neurons in the SO and parvalbumin positive (PV+) neurons in the stratum pyramidale.

Materials and methods

Animals and treatments

Male mice were used exclusively throughout these studies. Inducible, glial fibrillary acidic protein-driven transgenic Tat mice (aged 60–80 days) were used to identify the effects of HIV-1 Tat1–86 on hippocampal interneuron subpopulations and associated behavior (Bruce-Keller et al, 2008). In order to induce Tat expression, mice

expressing the *tat* and *rtTA* transgenes (Tat+) were fed doxycycline-containing chow (DOX; 6 mg/g, Harlan, Indianapolis, IN) for 12–14 days depending on the experiment. Control mice lacking the *tat* transgene, but expressing the *rtTA* gene (Tat–), were given the same DOX treatment. Animal procedures were approved by the Virginia Commonwealth University Institutional Animal Care and Use Committee and are in accordance with Association for Assessment and Accreditation of Laboratory Animal Care guidelines.

Barnes maze

Tat– ($n = 13$) and Tat+ ($n = 8$) mice were assessed for spatial learning and motor function in a Barnes maze test (Barnes, 1979). Mice consumed DOX chow for 7–8 days prior to 1 day of prehabitation, followed by 4 days of testing and 1 day of probe trials. For prehabitation, mice were placed in the escape hole (positioned in a randomly assigned location) for 2 min, then were placed in the brightly lit center of a Barnes maze (91 cm diameter, 90 cm height, with 20 holes each 5 cm diameter; Stoelting Co., Wood Dale, IL), and guided to the assigned escape hole where they remained for 2 min, then were placed under a glass cylinder next to the escape hole, and allowed up to 3 min to volitionally enter (mice that did not enter the hole were guided in and remained for 2 min). On testing days (four trials per day over 4 days), mice were placed in the brightly lit center of the Barnes maze and were allowed up to 3 min to enter the escape hole. Mice that did not enter the hole were gently guided to the hole and allowed to remain for 2 min. Shorter latencies to find the escape hole, a greater proportion of time spent in the correct quadrant of the maze, and fewer errors were considered indices of greater

learning (Camara et al, 2013). On day 5, a reversal probe trial was conducted wherein the maze was turned 180° such that the correct goal box was on the opposite end of the Barnes maze table, and the proportion of time spent in the new target quadrant, latency to find the new escape hole, and number of errors made were assessed. Distances and velocities traveled were used as an index of motor behavior.

Novel object recognition

Tat- ($n = 14$) and Tat+ ($n = 14$) mice were assessed for neurocognitive function in a novel object recognition test (Ennaceur & Delacour, 1988; Dere et al, 2007) after 14 days on DOX. Briefly, mice were habituated to a testing room, placed in an open field (35 × 40 × 40 cm; Stoelting Co., Wood Dale, IL), and allowed to explore two identical round objects (plastic toys in the shape of kiwis, oranges, potatoes, or tomatoes; each ~6 × 3 cm) for a 10-min training trial. After a 4-h inter-trial interval, one of the previously explored objects was replaced with a novel cone-shaped object of similar size (a plastic toy in the shape of a half ear of corn or a half-pickle), which mice were allowed to explore for a 10-min retention trial. Across subjects, replacement of the familiar object on the left vs. right side of the apparatus was counterbalanced to control for potential side-preferences. For each trial, the time spent investigating the object in the novel position, as a function of the entire time spent investigating, was calculated: [(novel object time – familiar object time)/(novel object time + familiar object time)]. To assess motor behavior, the overall distance traveled, as well as the time and frequency spent rearing were recorded.

Vision testing

Tat⁻ ($n=6$) and Tat⁺ ($n=6$) mice were assessed for visual function based on prior methods (Wersinger et al, 2002) prior to DOX exposure, and at 7 and 14 days following DOX exposure. In brief, mice were suspended approximately 12 in. above a vertical ring-stand and were gently lowered with the ring-stand approximately 2 in. from the left or right visual field (close enough to allow visual, but not whisker, contact with the ring-stand). The left and right visual fields were assessed consecutively for each mouse. Visual responding was considered positive when mice reached with the forepaws for the rod when presented to both the left and right side (a response to only one visual field would have been considered a negative response). Two observers rated visual responses.

Immunohistochemistry

Brains were fixed in 4 % paraformaldehyde using transcardial perfusion, removed, halved, and embedded in Tissue-Tek O.C.T. compound (Sakura Finetek, Torrance, CA). Hemisected brains were sectioned in the sagittal plain at a thickness of 16 μm for analysis of interneuron populations or in the coronal plane at a thickness of 40 μm to determine the reference volume using stereology. A Leica CM1850 cryostat was used to cut the sections (Leica Biosystems, Buffalo Grove, IL). Sections were mounted on slides and then stored at $-80\text{ }^{\circ}\text{C}$ until use. Tissue sections for interneuron analyses were blocked, then incubated with individual primary antibodies (anti-PV,

Synaptic Systems, Cat. No. 195 004, guinea pig polyclonal, 1:1200; anti-nNOS, Abcam, ab1376, goat polyclonal, 1:5000; anti-NPY, Abcam, ab30914, rabbit polyclonal, 1:100; anti-SST, Santa Cruz Biotechnology, sc-13099, rabbit polyclonal, 1:50; anti-NeuN, Chemicon, MAB377, mouse monoclonal, 1:500) for 18 h at 4 °C, and rinsed in phosphate-buffered saline (PBS). Solutions containing appropriate, fluorescently labeled secondary antibodies (goat anti-guinea pig IgG-Cy3, Abcam ab6965-100, 1:500; Abcam ab102370, 1:500; donkey anti-goat IgG-Alexa Fluor® 488, Invitrogen, A11055, 1:500; goat anti-rabbit IgG-Alexa Fluor® 647, Invitrogen A21244, 1:500; donkey anti-mouse IgG-Alexa Fluor® 594, Invitrogen, A21203, 1:500; goat antimouse IgG-488 Oregon green, Molecular Probes, 0-6380, 1:500) were placed onto tissue sections for 2 h at room temperature. Slices were then rinsed 3 × 10 min in PBS. All tissue sections were incubated in PBS/Hoechst solution (0.5 µg/ml, Invitrogen, H3570) for 5–10 min, repeatedly rinsed in PBS, and mounted in ProLong Gold Antifade reagent (Invitrogen, P36930).

Reference volume analysis

Hoechst-stained 40-µm serial sections were sampled through the entire hippocampus. From a random starting position, sections at evenly spaced intervals were sampled to obtain an unbiased stereological assessment of hippocampal volume (Gundersen et al, 1988). In short, sections from halved brains were taken from Tat⁻ ($n = 6$) and Tat⁺ ($n = 5$) mice and imaged using a Zeiss Axio-Observer Z1 microscope, MRm digital camera, and a 10× objective (Zeiss, Oberkochen, Germany). Montages of the entire left hemisphere of the brain (5 × 6) were obtained utilizing a motorized stage

encoder (Zeiss) and a computerized tile reconstruction method (Zeiss, Axio-Vision software). Hippocampal volume was then estimated by overlaying a standardized grid over the image of the brain and performing a point count analysis (Gundersen et al, 1988; Mouton, 2002).

Imaging

Hippocampi were imaged using a Zeiss LSM 700 microscope at 20× magnification (Zeiss, Oberkochen, Germany). Neurons, as noted by the presence of NeuN immunoreactivity within the nucleus, were counted in SO, stratum pyramidale, SR, and SL-M of CA1. Immunoreactivity for each protein was noted independently, and the markings were overlaid to confirm co-expression of proteins without bias. From 4 to 10 sections (typically 7 to 8) were analyzed and averaged per animal, and 6 mice per experimental group were used for all experiments. All cell count data are presented as a percent of the total NeuN+ population in each layer. To examine the potential effects of the Tat transgene on the neuritic processes, densitometric analysis of PV+ dendrites and SST + axons was performed using ImageJ (NIH, Bethesda, MD). In addition, dendritic varicosities of PV+ interneurons were quantified on the five most pronounced dendrite segments from each image within SR from 2 to 3 sections per animal. Dendrites not reaching at least 50 μm in length or discontinuous dendrites were not analyzed.

Statistical analyses

Behavioral endpoints were recorded and digitally encoded by an ANY-maze animal tracking system (Stoelting Co., Wood Dale, IL) and assessed via repeated-measures analyses of variance (ANOVA) with novel object recognition trial (training trial or retention trial) or Barnes maze testing day (days 1–5) and mouse genotype (Tat⁻ or Tat⁺) as the respective within-, and between-, subjects factors. Tukey's honestly significant difference post hoc tests were used to assess group differences following main effects. Interactions were delineated via simple main effects and main effect contrasts with alpha corrected for multiple comparisons. Immunohistochemical endpoints were assessed with one-tailed Student's *t* tests. Effects were considered significant when $p < 0.05$.

Results

HIV-1 Tat expression impairs mnemonic performance

Inducing HIV-1 Tat expression in the CNS of mice significantly impaired spatial learning in the Barnes maze test. Compared to Tat⁻ controls, Tat⁺ mice demonstrated significantly longer latencies to find the escape hole [$F(1,76)=9.39$, $p < 0.05$] and spent a significantly lower proportion of time [$F(1,76)=8.17$, $p < 0.05$] in the correct quadrant of the Barnes maze (Fig. 1). Irrespective of genotype, all mice took significantly longer to find the escape hole following a 180° swap of the escape location on the probe trial day [$F(4,76)=3.42$, $p < 0.05$] compared to any previous day's performance ($p = 0.0001$ – 0.01 ; Fig. 1). No differences were observed in the number of errors made or the distance traveled between Tat⁻ and Tat⁺ mice (Fig. 1); however, a difference in velocity was observed between Tat⁻ and Tat⁺ mice [$F(1,76)=5.35$, $p < 0.05$] with a significant

reduction observed in the reversal probe trial [$F(4,76)=8.45$, $p<0.05$], compared to day 1 performance ($p < 0.0001$). All mice demonstrated significantly decreased maze exploration (indicated by distance traveled) [$F(4,76)=12.86$, $p<0.05$] and made fewer errors [$F(4, 76) = 11.37$, $p < 0.05$] compared to day 1 ($p = 0.0001-0.02$; Fig. 1).

Similarly, HIV-1 Tat expression significantly impaired cognitive performance in a novel object recognition task [$F(1, 26) = 5.67$, $p < 0.05$]. Compared to performance in the training trial, Tat- control mice spent a significantly greater proportion of time with a novel object in the retention trial ($p = 0.0007$; Fig. 2) indicating intact mnemonic performance. However, Tat+ mice demonstrated impaired object recognition during the retention phase (Fig. 2), spending significantly less time investigating the novel object compared to Tat- controls ($p = 0.04$). No significant differences were observed between Tat- or Tat+ mice on the total amount of time spent investigating objects nor on any motor measure investigated (Table 1).

Given that a visual component is present in the Barnes maze and novel object recognition tasks, vision was assessed in a separate group of mice. All Tat- and Tat+ mice responded positively to a stimulus presented to the left and right fields of vision prior to DOX exposure and at 7 and 14 days following DOX exposure.

Hippocampal volume is unchanged following Tat exposure

Point count analysis of hippocampal volume revealed no difference between Tat- (16.71 ± 0.39 mm³) and Tat+ (17.62 ± 0.47 mm³) mice. Additionally, the volume of the CA1 subfield was unchanged between Tat- (9.97 ± 0.19 mm³) and Tat+ (10.74 ± 0.69

mm3) mice indicating that there was no difference in the volume of the hippocampus or in hippocampal area CA1 following 12–14 days of Tat induction.

HIV-1 Tat expression is associated with reductions in specific CA1 nNOS-expressing interneuron subpopulations

We investigated Tat effects on a subset of nNOS+/NPY+ cells known as ivy cells. These cells are found primarily in the stratum pyramidale as well as the SR of CA1 (Fuatealba et al, 2008). To assess the vulnerability of nNOS+/NPY+ cells to HIV-1 Tat, hippocampal sections were immunolabeled for nNOS, NPY, and NeuN (Figs. 3 and 4). The distribution of nNOS and NPY immunoreactivity within CA1 was consistent with previous research (Morris, 1989; Jinno et al, 1999; Fuatealba et al, 2008). Significant reductions in the percentage of nNOS-expressing cells were observed in the stratum pyramidale [$t(8) = 2.25, p < 0.05$] and SR [$t(8) = 2.43, p < 0.05$] of Tat+ mice compared to Tat- mice (Fig. 3). Importantly, the reduction in nNOS+ interneurons was specifically restricted to the subpopulation of interneurons that did not possess NPY antigenicity in both the stratum pyramidale [$t(8) = 2.36, p < 0.05$] and SR [$t(8) = 1.92, p < 0.05$] after Tat exposure, indicating ivy cells were not selectively vulnerable. No significant differences were observed for NPY+ interneurons lacking nNOS in any layer of CA1. Tat induction did not significantly alter the percentage of NPY+ interneurons or interneurons coexpressing nNOS and NPY in any layer of the hippocampus (Fig. 3).

The proportion of SST+ and PV+ neurons is reduced by HIV-1 Tat expression

To assess the vulnerability of PV+ and SST+ interneurons, hippocampal sections were immunolabeled for PV, SST, and NeuN (Figs. 5 and 6). PV immunoreactivity was nearly exclusive to stratum pyramidale and SO, consistent with previous research (Kosaka et al, 1987). Observations of SST immunoreactivity in SO, stratum pyramidale, and SR also agree with previous findings (Oliva et al, 2000); however, SST+ neurons occurring in the SR were not quantified as part of this study (Fig. 5). The percentage of PV+ neurons were significantly diminished in the stratum pyramidale of Tat+ mice compared to Tat- mice [$t(10) = 1.839$, $p < 0.05$]. While no significant effect of Tat was observed in PV+/SST- interneurons, there was a trend toward significance in PV+/SST+ interneurons in the stratum pyramidale [$t(10) = 1.711$, $p = 0.059$]. No effect of Tat was observed in PV+ interneuron groups in the SO. In contrast, the proportion of SST+ interneurons was reduced in the SO [$t(10) = 2.664$, $p < 0.05$], but not in the stratum pyramidale of Tat+ mice. While there were no significant differences in SO to suggest that subpopulations of SST+ neurons were reduced in the layer, there was a trend toward significant decreases in the proportion of PV-/SST+ [$t(10) = 1.673$, $p = 0.063$]. These data indicate subregion-specific declines in interneuron populations, supporting the idea of selective vulnerability among hippocampal neuron subpopulations.

PV+ and SST+ processes in CA1 appear unaffected by Tat

ImageJ analysis of PV expression in the SR and SST expression in the SL-M showed no differences in fiber density between Tat+ and Tat- mice. There were also no differences in dendritic varicosity number or size in PV+ neurons (Fig. 7).

Discussion

Given the great diversity in function, morphology, and localization of hippocampal interneurons, the highly localized reduction of Syt2+ fibers described by Fitting et al (Fitting et al, 2013) suggests selective vulnerability of distinct subpopulations of interneurons to HIV-1 Tat. We thus hypothesized that a subpopulation of hippocampal interneurons would be selectively vulnerable to HIV-1 Tat and used an immunohistochemical/morphological approach to identify neurodegenerative changes in cells within defined regions of CA1. We found that Tat+ animals exhibited aberrant learning behavior in both the Barnes maze and novel object recognition tests. Tat expression reduced the population of nNOS+/NPY- interneurons in both the SR and stratum pyramidale, SST+ cells in the SO, and PV + cells in the stratum pyramidale. nNOS+/NPY+ or nNOS-/NPY+ neurons remained unchanged.

The pathology of specific interneuron subpopulations, and the hippocampal interneuron network as a whole, have been demonstrated in a number of neurological disorders (Korotkova et al, 2010; Toth et al, 2010; Antonucci et al, 2012; Fitting et al, 2013; Levenga et al, 2013), some of which produce behavioral deficits in learning similar to the findings of Fitting et al (Fitting et al, 2013). Due to neuronal heterogeneity in the hippocampus (Bouilleret et al, 2000; Moga et al, 2002; Avignone et al, 2005), differential responses to Tat-induced excitotoxicity and neuroinflammation may be expected. In a kainate-induced model of excitotoxicity, a loss of GAT-1, a GABA reuptake protein, was greater in the stratum pyramidale than in the SO and the SR, suggesting regional variability in selective vulnerability of hippocampal interneurons

(Boulleret et al, 2000). In HIV models, reductions in the number of cells expressing PV in CA3, and SST in CA1 were observed, although identification of the affected subtypes was incomplete (Masliah et al, 1992; Fox et al, 1997). The results of the present study indicate that there is at least one subtype of nNOS+ interneuron within CA1 that is selectively vulnerable to HIV-1 Tat. nNOS+ interneurons appear in all layers of the hippocampus, a majority of which are subpopulations of neurogliaform cells (NGFCs; nNOS+/NPY-) (Jinno et al, 1999; Tricoire et al, 2010). In addition to NGFCs, there are ivy (nNOS+/NPY+) and interneuron-specific interneuron type III (IS3; nNOS+/NPY-) cells. Ivy cells exist primarily in the stratum pyramidale, as well as the SR (Fuatealba et al, 2008; Lapray et al, 2012). nNOS+/NPY- cells have been found in the stratum pyramidale (IS3s) and SR (NGFCs) (Acsady et al, 1996a; Acsady et al, 1996b; Porter et al, 1998; Jinno et al, 1999; Jinno & Kosaka, 2002; Jinno & Kosaka, 2004; Tricoire et al, 2010; Armstrong et al, 2012; Somogyi et al, 2012).

Our findings suggest that the ivy cells (i.e., nNOS+/NPY+ neurons residing in the stratum pyramidale) are not vulnerable to HIV-1 Tat as previously hypothesized (Fuatealba et al, 2008). Rather, a significant decline was observed in the number of nNOS+/NPY- interneurons in both the stratum pyramidale and SR. In the stratum pyramidale, these vulnerable neurons are thought to be IS3s (given the lack of NPY). Additionally, these neurons are positive for vasoactive intestinal polypeptide (VIP), and calretinin (CR) (Acsady et al, 1996a; Acsady et al, 1996b; Porter et al, 1998; Jinno et al, 1999; Jinno & Kosaka, 2002; Tricoire et al, 2010) and the expression of nNOS differentiates them as IS3s versus an IS1 subtype (Tricoire et al, 2010). Functionally, IS3s support feedback inhibition within CA1 (Gulyas et al, 1996; Chamberland et al,

2010; Chamberland & Topolnik, 2012; Tyan et al, 2014). Of particular interest, the selective vulnerability of multiple subsets of CR + cells in the hippocampus may occur in a temporal-lobe epilepsy model, a good predictor of neuronal vulnerability to excitotoxicity. Those cells that remain exhibit pathologic dendritic varicosities and a loss of dendritic complexity and synapses, as a result of excitotoxic injury (Toth et al, 2010; Toth & Magloczky, 2014). Patients with epilepsy can have fewer nNOS+ interneurons within CA1 (Leite et al, 2002).

The population of nNOS+/NPY- cells affected by Tat in SR likely consists of multiple nNOS+ interneuron subtypes, including IS3s (Acsady et al, 1996a; Acsady et al, 1996b; Porter et al, 1998; Jinno et al, 1999; Jinno & Kosaka, 2002; Tricoire et al, 2010) and NGFCs (Tricoire et al, 2010; Armstrong et al, 2012; Somogyi et al, 2012; Tricoire & Vitalis, 2012). Since IS3s represent a small proportion of nNOS+ cells in the SR, it is probable that NGFCs constitute a majority of nNOS+/NPY- cells lost (Jinno et al, 1999; Jinno & Kosaka, 2002; Tricoire et al, 2010; Armstrong et al, 2012). The presence or absence of CR, which is expressed in IS3s, but not NGFCs, might be used to further differentiate these interneuron subtypes in the future (Jinno & Kosaka, 2002; Armstrong et al, 2012; Somogyi et al, 2012). Considering the lack of cell death in the hippocampus observed at early time points following Tat induction (Fitting et al, 2013), we speculate that the affected interneuron subtypes are downregulating nNOS in response to excitotoxic injury in order to restore homeostasis (Hu et al, 2008; Di et al, 2012).

nNOS is required for the normal functioning of the hippocampal interneuron network and maintenance of related behavioral endpoints. In complete nNOS knockout

mice, there is an attenuation of contextual fear conditioning and spatial memory formation similar to what is observed in Tat transgenic mice (Kirchner et al, 2004; Weitzdoerfer et al, 2004; Kelley et al, 2009; Fitting et al, 2013). While nNOS is important for normal hippocampal function (Kirchner et al, 2004; Zanelli et al, 2009), research indicates that nNOS-induced neuronal damage occurs in pathological states (Cui et al, 2007; Eugenin et al, 2007; Steinert et al, 2010; Wang et al, 2010; Drury et al, 2014; Hsu et al, 2014; Wu et al, 2014b). The role of nNOS in excitotoxicity, including HIV-1 Tat excitotoxicity, is reportedly linked to its activation of PSD-95 and NMDA receptor complexes (Christopherson et al, 1999; Eugenin et al, 2007; Fan et al, 2010; King et al, 2010; Steinert et al, 2010). Exposure to excitotoxic levels of glutamate causes temporal dysregulation of nNOS activation-inactivation processes (Rameau et al, 2007). Thus, Tat-induced increases in the activation of nNOS may enhance NMDA receptor phosphorylation, the recruitment of additional AMPA receptors, and the generation of peroxynitrite resulting in greater susceptibility to excitotoxic damage in nNOS-expressing interneurons (Yu et al, 1997; Grima et al, 2001; Rameau et al, 2007; Hossain et al, 2012). Lastly, we speculate that the proposed compensatory downregulation of nNOS may be absent or may be less prevalent in nNOS+/NPY+ neurons due to the neuroprotective effects of NPY, which can regulate neuronal excitability via paracrine/ autocrine signaling (Xapelli et al, 2006; Smialowska et al, 2009).

The present findings stand in contrast to prior studies that did not demonstrate a loss of PV+ interneurons in CA1 of HIV-infected patients or rodent models (Masliah et al, 1992; Guo et al, 2012). Herein, we differentiate the percentages of CA1 PV

expressing cells by CA1 layer and by SST co-expression, allowing for delineation of CA1 cell types (PV+ interneurons including bistratified and oriens-lacunosum-moleculare (O-LM) cells) (Kosaka et al, 1987; Masliah et al, 1992; Buhl et al, 1994; Freund & Buzsáki, 1998; Jinno & Kosaka, 2000; Jinno & Kosaka, 2002; Klausberger et al, 2004; Klausberger & Somogyi, 2008; Muller & Remy, 2014; Yamada & Jinno, 2015). Bistratified cells were discerned from O-LM interneurons via the relative intensity of PV (high in bistratified) and SST (minimal in bistratified) immunoreactivity. In contrast, O-LMs exert an opposing PV/SST profile, with a subset of O-LMs being entirely PV- (Chittajallu et al, 2013; Muller & Remy, 2014). Our data show a modest effect of Tat on the total PV+ population of the stratum pyramidale; however, this was not restricted to a particular PV+ cell type. Although we believe Tat may be selectively affecting bistratified cells based on a trend toward reduced PV+/SST+ interneuron numbers, additional information is needed for confirmation. Interestingly, while the loss of PV+ cells in CA1 is not reported in patients with neuroAIDS, many of the PV+ interneurons were reportedly unhealthy with damaged neurites being the chief descriptor (Masliah et al, 1992). Despite limitations in generalizing findings from Tat transgenic mice to HIV-infected individuals, the collective findings suggest PV+ interneuron subsets are selectively vulnerable to HIV—perhaps through synaptodendritic injury and pruning.

Reductions in SST gene expression in the brains of HIV patients are linked to the development of depression (Everall et al, 2006). Fox et al. (Fox et al, 1997) showed a reduction in SST+ interneurons in HIV patients, but did not differentiate between the layers of CA1. We observed a strong net reduction of SST+ interneurons in the SO, but not in the stratum pyramidale. The SR was not quantified due to the relative rarity of

SST+ cells in this region. Interestingly, there was a trend toward reductions in SST+/PV- interneurons in the SO following Tat induction. The loss of SST has been shown to have profound effects on LTP within CA1, with differential effects in the apical and basilar dendrites of pyramidal cells based on receptor subtypes and response to specific oscillation patterns (Fan & Fu, 2014). Considering the decline in SST+ neurons observed in this study and previous findings of reduced SST expression in HIV patients (Everall et al, 2006), it will be important to examine whether region-specific SST losses contribute to impairments in LTP and related behavior following Tat-exposure (Behnisch et al, 2004; Fitting et al, 2013). In support of this notion, ablating SST+ interneurons, focal to distal apical dendrites of pyramidal cells in SL-M (likely O-LMs), causes a loss of cue-based fear learning, while removal of PV+ neurons, focal to basal dendrites and proximal portions of apical dendrites in the SR, does not result in loss of fear learning. (Leão et al, 2012; Lovett-Barron et al, 2014; Lovett-Barron & Losonczy, 2014; Muller & Remy, 2014)} While it is not possible to say with certainty which SST+ population is affected in the present study, the net loss in SST in the SO is most likely due to O-LM cell vulnerability.

We and others have found that HIV-1 Tat can impair learning and memory, and the present study begins to advance our understanding of the limbic neuronal types that may underlie such effects. In the present study, Tat+ mice exhibited deficient performance on two hippocampally dependent tasks, the Barnes maze and novel object recognition tests, compared to their Tat- counterparts. Consistent with these results, stereotaxic injections of Tat directly to dorsal hippocampus have recently been demonstrated to increase the latency to find a hidden platform in a Morris water maze

and to impair novel object recognition among Sprague-Dawley rats (Harricharan et al, 2015). Similar intracerebroventricular injections of Tat impaired radial arm maze performance concurrent with disrupted LTP in the hippocampus of C57BL/6J mice (Li et al, 2004). Additionally, similar impairment of Barnes maze performance and object recognition has been observed in a separate GFAP driven Tat-inducible mouse model (Carey et al, 2012). Considering that behavioral deficits similar to those seen in neuroAIDS can be traced back to the dysfunction of one or more of the interneuron types discussed here, it is reasonable to assume that imbalance in this complex circuit may contribute to the attenuation of spatial memory observed in HAND (Masliah et al, 1992; Buhl et al, 1994; Acsady et al, 1996a; Fox et al, 1997; Sik et al, 1997; Ali et al, 1998; Kirchner et al, 2004; Klausberger et al, 2004; Weitzdoerfer et al, 2004; Carey et al, 2012; Leão et al, 2012; Fitting et al, 2013; Lovett-Barron et al, 2014; Muller & Remy, 2014; Sun et al, 2014; Tyan et al, 2014).

Hippocampal interneurons interact as part of a functional network and it is clear that the removal of even one cell type from the network can have drastic effects on information processing, pyramidal cell excitation, and consequent behavioral outcomes (Moga et al, 2002; Dugladze et al, 2007; Goldin et al, 2007; Toth et al, 2010; Peng et al, 2013; Long et al, 2014; Lovett-Barron et al, 2014; Lovett-Barron & Losonczy, 2014; Toth & Magloczky, 2014; Orban-Kis et al, 2015). Importantly, the susceptible nNOS+/NPY- interneurons of the stratum pyramidale and the SR, PV+ cells of the stratum pyramidale, and SST+ interneurons of the SO form a microcircuit known to be involved in a complex feedback loop/input gating mechanism that regulates network synchronization within CA1 (Fig. 8) (Buhl et al, 1994; Acsady et al, 1996a; Sik et al, 1997; Ali et al, 1998;

Klausberger et al, 2004; Chamberland et al, 2010; Chamberland & Topolnik, 2012; Leão et al, 2012; Muller & Remy, 2014; Sun et al, 2014; Tyan et al, 2014; Milstein et al, 2015). Herein, we propose this microcircuit to be selectively vulnerable to HIV-1 Tat. Given clinical observations that implicate HAND- and psychostimulant-related neurocognitive deficits to be associated with interneuron losses in other brain regions (Chana et al, 2006), the present findings suggest that a proportionally small, interconnected ensemble of hippocampal CA1 interneurons may contribute to key functional and neurobehavioral deficits observed in HAND.

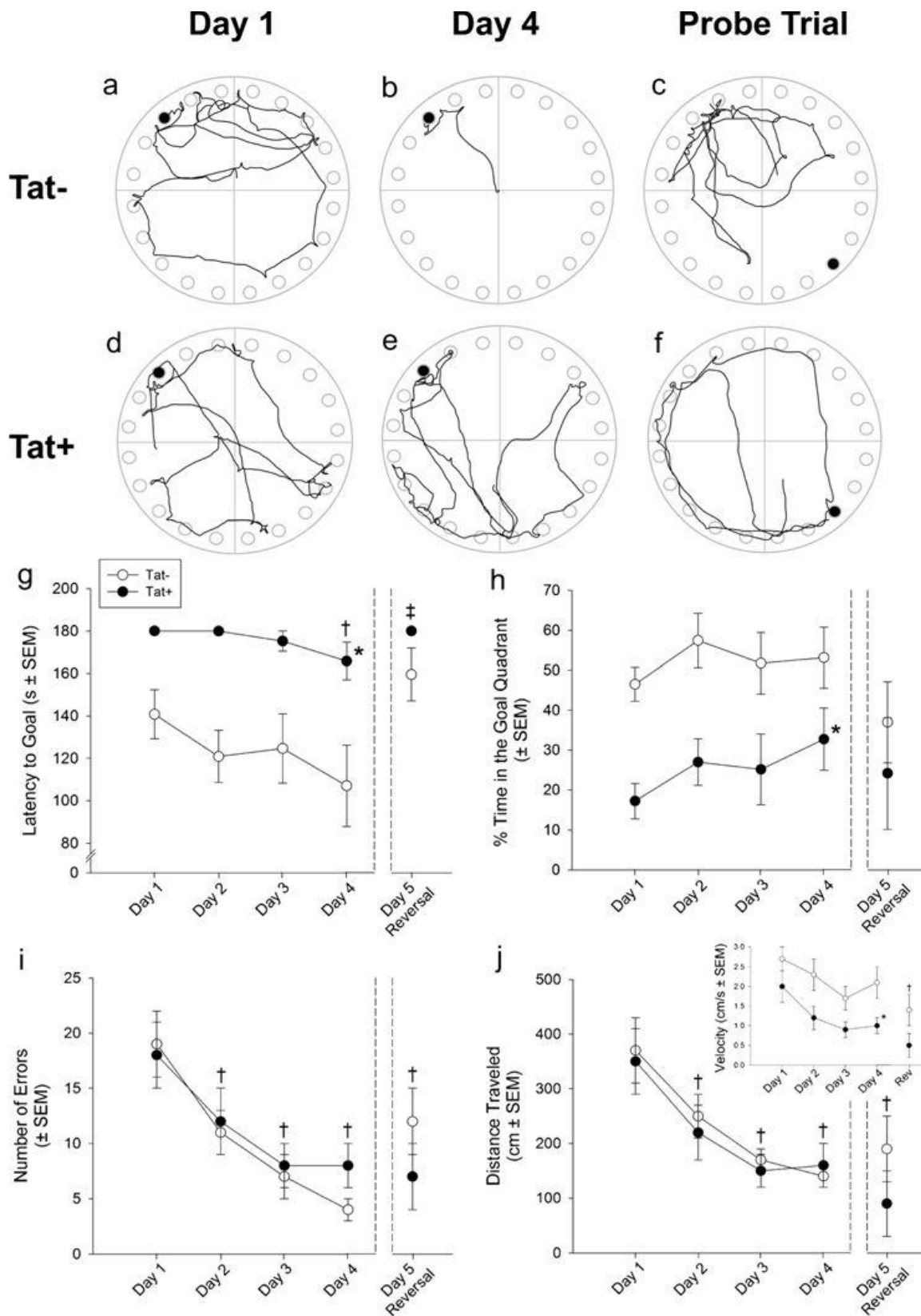
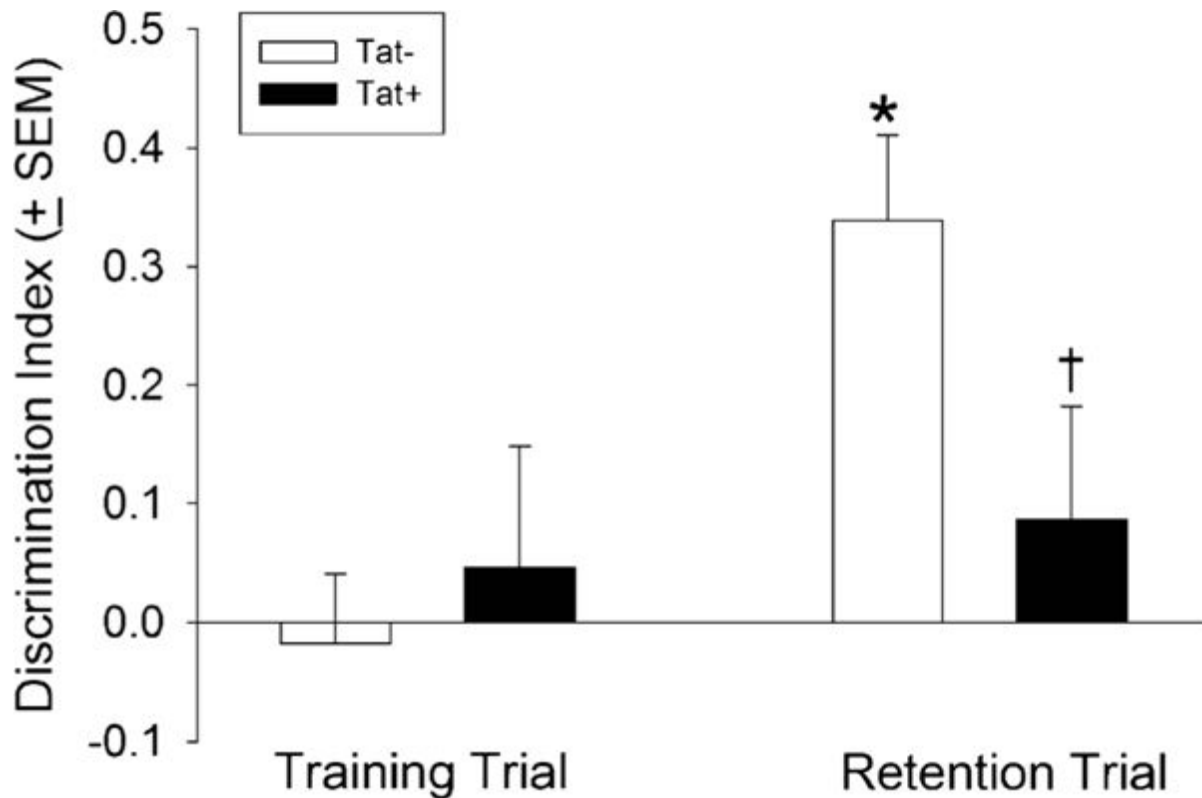


Figure 2. 1: Barnes maze performance between Tat- and Tat+ mice

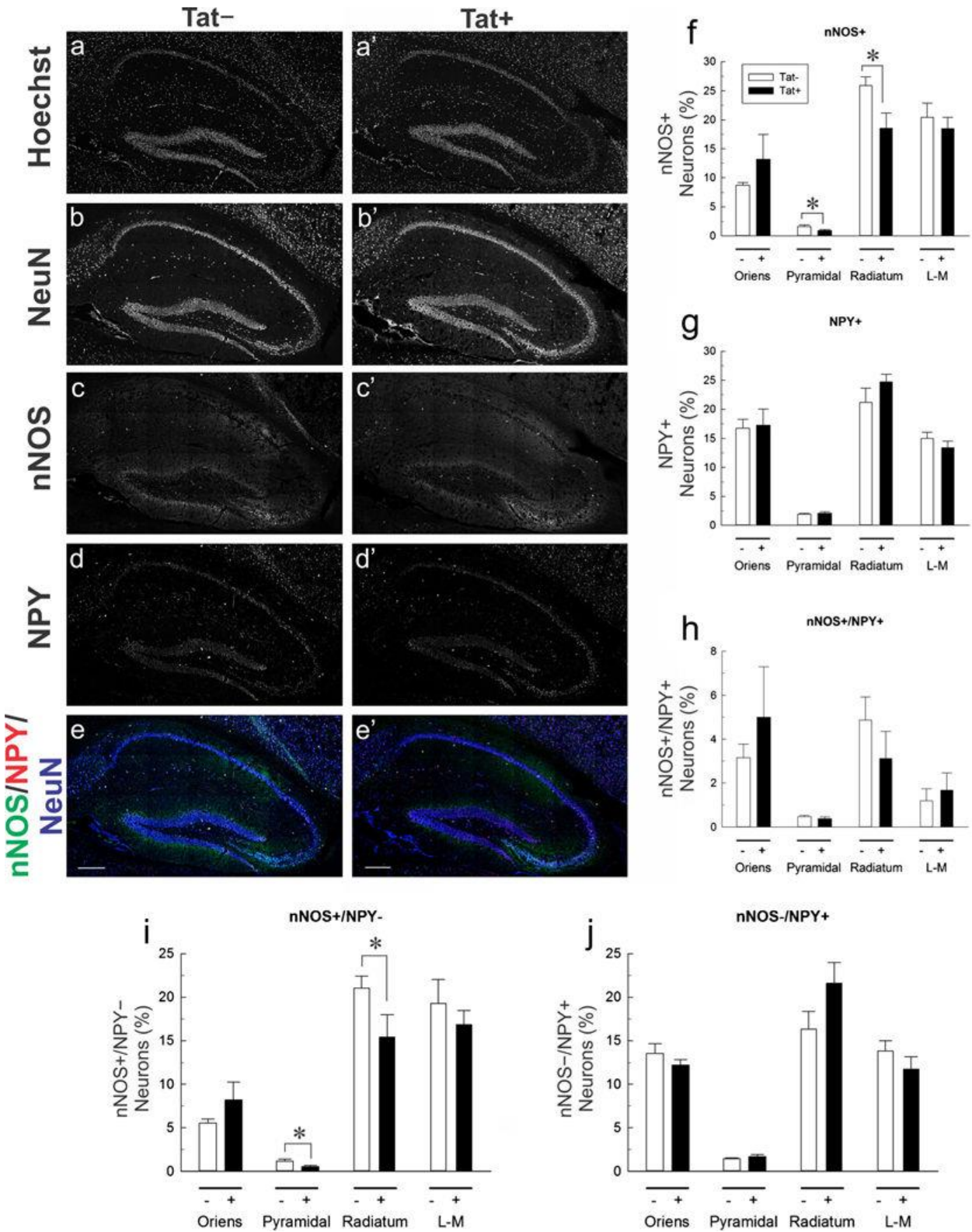
Representative traces of the movements of Tat- (a-c) and Tat+, (d-f) mice exploring a Barnes maze on testing days 1 (a, d) and 4 (b, e), as well as the reversal probe trial [escape hole reversed 180° (c, f)]. Escape hole is noted as the *black circle* in each figure. Tat+ mice ($n = 8$) demonstrate significantly longer latencies to find the escape hole (g) and (h) spend a significantly lower proportion of time in the correct quadrant of the Barnes maze test, indicating impaired learning compared to Tat- control mice ($n = 13$). Neither the number of errors made (i) nor the distance traveled (j) differs between Tat- and Tat+ mice, but decreases among all animals from day 1 performance. Tat+ mice have a reduced velocity compared to Tat- mice, and all mice show reduced velocity in the reversal probe trail compared to day 1 performance (j, *inset*). The *asterisk* indicates a main effect for Tat- and Tat+ mice to significantly differ. The *dagger sign* indicates performance significantly differs from day 1 performance. The *double dagger* sign indicates reversal probe trial performance significantly differs from all other testing days, except day 1 (main effects, repeated measures ANOVA, $p < 0.05$)

Figure 2. 2: Effects of Tat on novel object recognition task performance



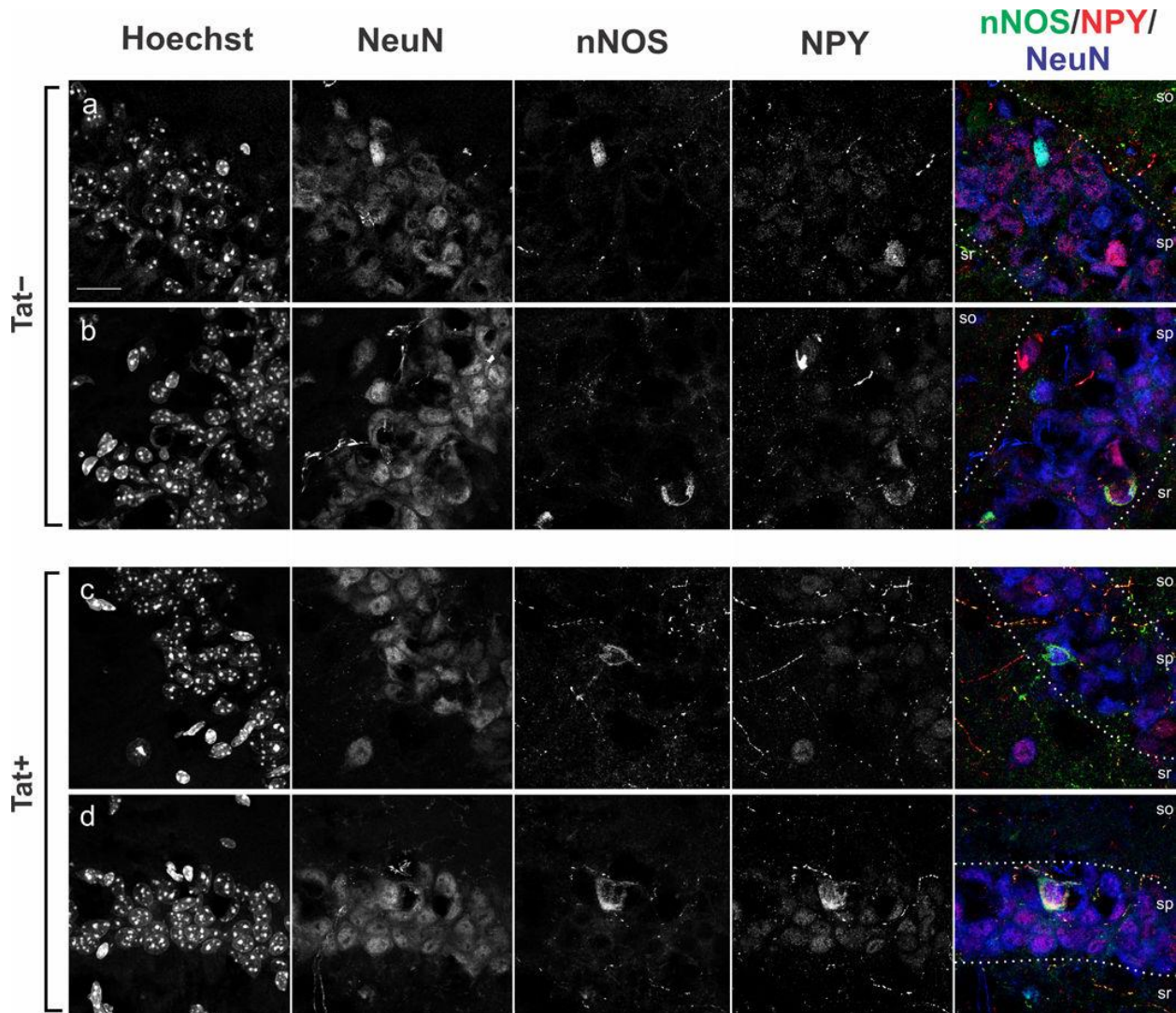
Tat+ mice ($n = 14$) spend a significantly lower proportion of time investigating a novel (vs. familiar) object in a novel object recognition test, indicating impaired cognitive performance compared to Tat- control mice ($n = 14$). The *asterisk* indicates a significant difference from the respective training trial exploration. The *dagger sign* indicates a significant difference between Tat- and Tat+ mice in the retention trial (interaction, repeated measures ANOVA, $p < 0.05$)

Figure 2. 3: Tat effects on nNOS and NPY expressing CA1 interneurons



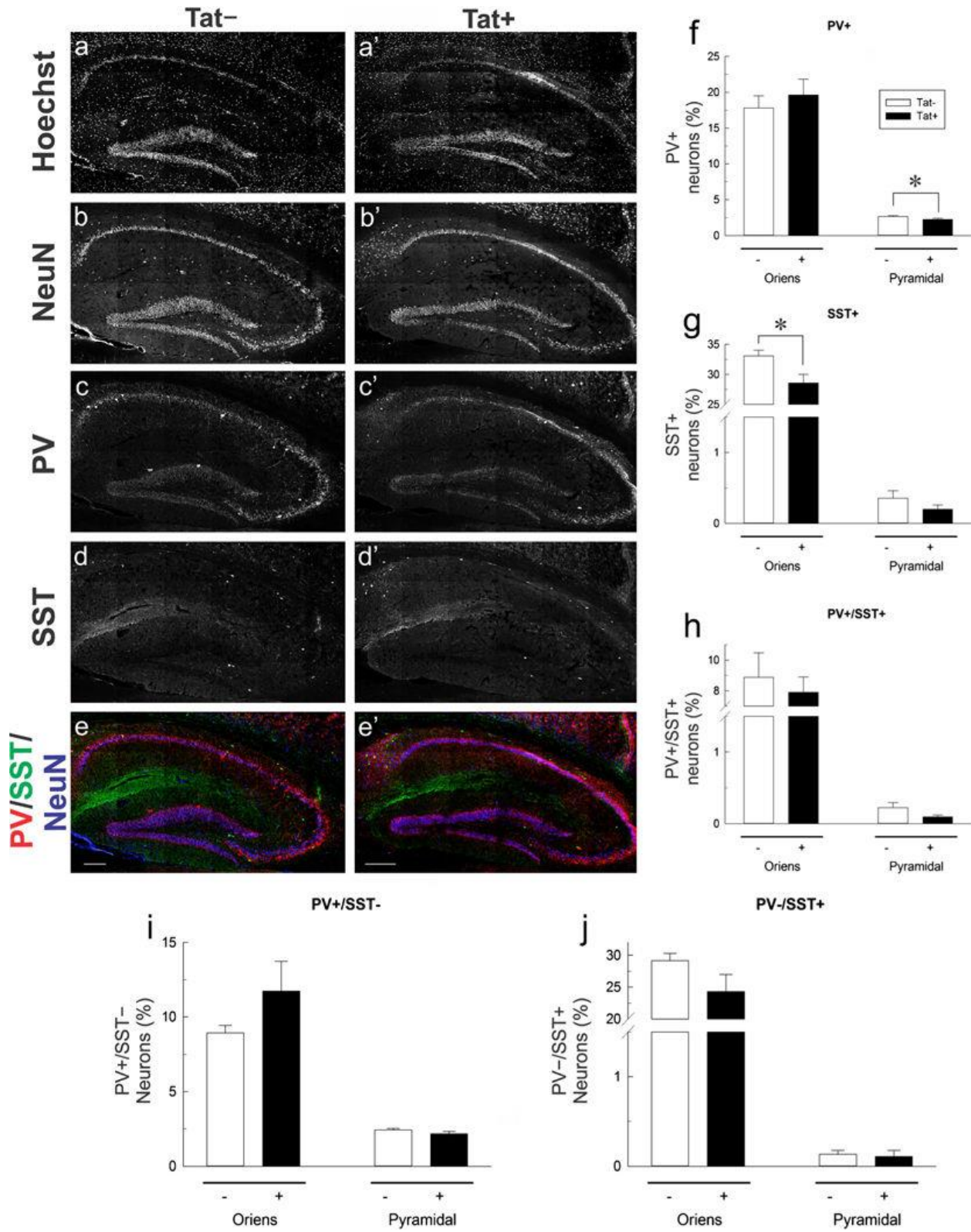
Effects of HIV-1 Tat induction on neuronal nitric oxide synthase (nNOS) and neuropeptide Y (NPY) immunoreactive interneuron subpopulations in hippocampal area CA1. **a–e** Immunoreactivity for nNOS (**c, c'**), NPY (**d, d'**), and the neuronal marker, NeuN (**b, b'**), was co-localized in sections from Tat⁺ and Tat⁻ mice counterstained using Hoechst dye (**a, a'**). **e, e'** NeuN (*blue*), nNOS (*green*), and NPY (*red*) merged. **f–j** The percentage of labeled neurons in hippocampal area CA1 by layer and marker. The proportion of nNOS⁺ neurons in stratum pyramidale (Pyramidal) and stratum radiatum (Radiatum) is significantly decreased in Tat⁺ compared to Tat⁻ mice ($*p < 0.05$, one tailed *t* test) (**f**), while the percentage of NPY⁺ neurons or neurons co-expressing nNOS and NPY in any layer is unaffected by Tat (**g, h**). The percentage of cells expressing nNOS in the absence of NPY is significantly reduced in stratum pyramidale and in stratum radiatum ($*p < 0.05$, one tailed *t* test) (**i**), while the proportion of NPY cells that lack nNOS was unaffected by Tat (**j**). Stratum oriens (Oriens), stratum lacunosum-moleculare (L–M). *Scale bar = 200 μm*

Figure 2. 4: nNOS and NPY subcellular localization



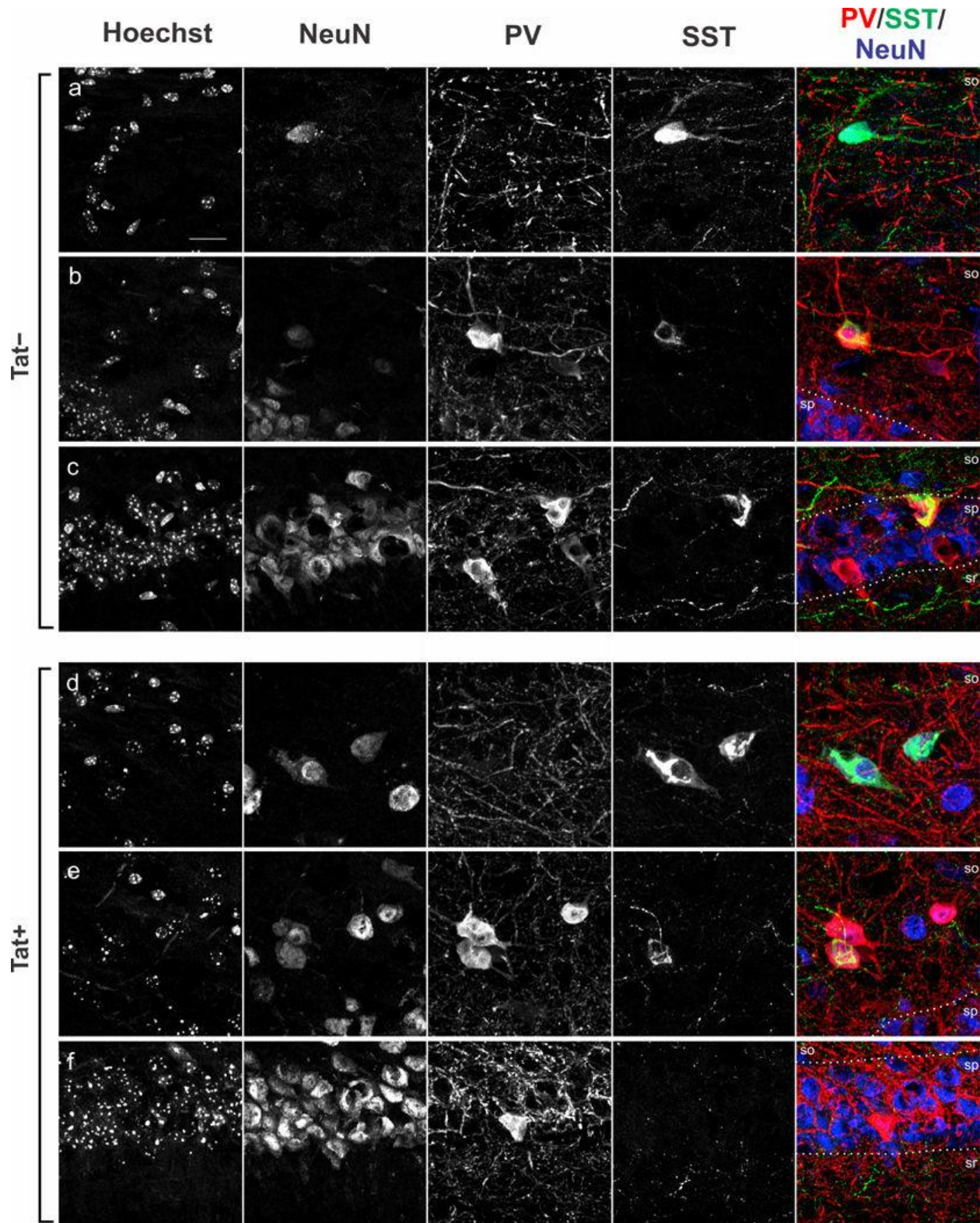
Subcellular localization of neuronal nitric oxide synthase (nNOS) and neuropeptide Y (NPY) immunoreactivity in interneurons in hippocampal area CA1 of Tat+ and Tat- mice. **a–d** Immunoreactivity for nNOS (*green*), NPY (*red*), and the neuronal marker, NeuN (*blue*), was co-localized in sections from Tat+ and Tat- mice counterstained using Hoechst dye (nuclei). **a, c** nNOS+/NPY- interneurons located in stratum pyramidale (sp). **b, d** nNOS+ and NPY+ interneurons of stratum pyramidale. Stratum oriens (so), stratum radiatum (sr). *Scale bar* = 10 μ m

Figure 2. 5: Effects of Tat on PV and SST expressing CA1 interneurons



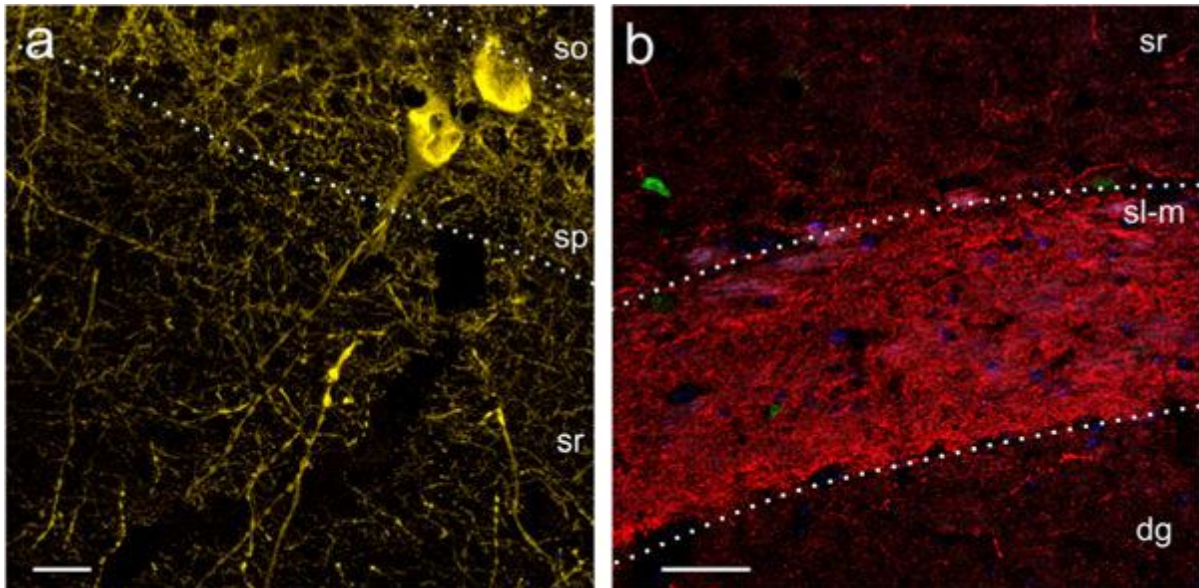
Effects of HIV-1 Tat induction on parvalbumin (PV) and somatostatin (SST) immunoreactivity in interneurons within hippocampal area CA1. **a–d** Low-magnification images of PV, SST, and NeuN immunoreactivity in sections from Tat+ and Tat– mice additionally counterstained with Hoechst dye. **a–e** Hippocampal sections from Tat+ and Tat–mice treated with DOX, probed with Hoechst (**a, a'**), NeuN (**b, b'**), PV (**c, c'**), and SST (**d, d'**). **e, e'** NeuN (*blue*), PV (*green*), and SST (*red*) merged. **f–j** The percentage of labeled neurons in hippocampal area CA1 by layer and marker. A decrease in the percent of PV+ neurons is seen in stratum pyramidale (Pyramidal) (**f**), and a decrease in the percent of SST+ neurons is observed in stratum oriens (Oriens) (**g**). No significant decrease is observed for neurons expressing both PV and SST or for neurons that express either marker in the absence of the other (**h–j**). The *asterisk* denotes a significant reduction from Tat– control population percentage (one tailed *t* test, $p < 0.05$). *Scale bar* = 200 μm

Figure 2. 6: PV and SST subcellular localization



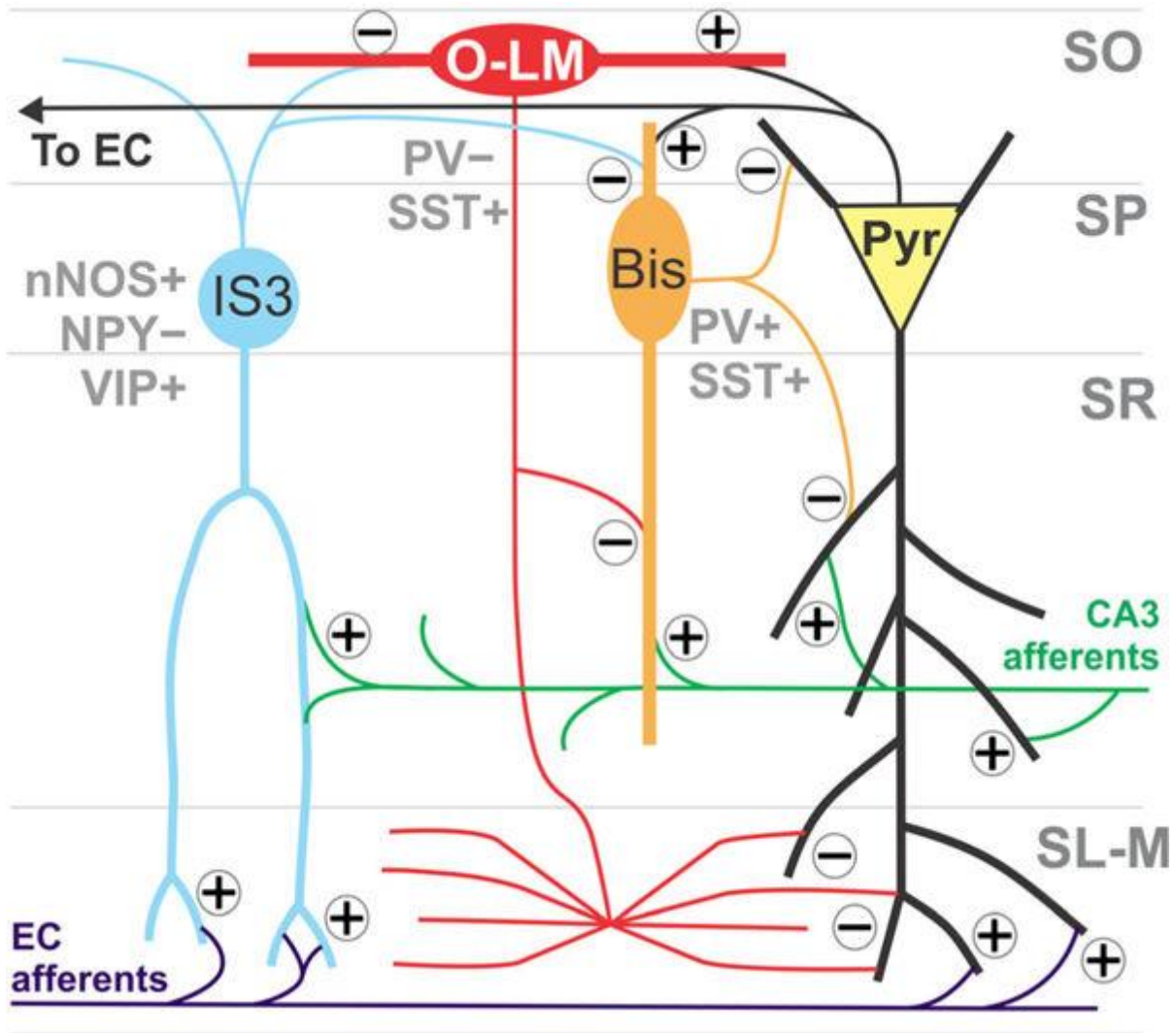
Subcellular localization of parvalbumin (PV) and somatostatin (SST) immunoreactivity in interneurons in hippocampal area CA1 of Tat⁺ and Tat⁻ mice. **a-d** High-magnification images of PV (*red*), SST (*green*), and NeuN (*blue*) immunoreactivity in sections from Tat⁺ and Tat⁻ mice additionally counterstained with Hoechst dye (**a-f**). **a, d** PV⁺/SST⁻ interneurons located in stratum oriens (so). **b, e** PV⁺ and SST⁺ interneurons of the stratum oriens. **c, f** PV⁺ neurons of stratum pyramidale (sp). Stratum radiatum (sr). *Scale bar* = 10 μ m

Figure 2. 7: Tat does not affect amount of PV or SST+ neurites in CA1



No evidence of changes to parvalbumin-immunoreactive (PV+) dendrites or somatostatin immunoreactive (SST+) axons is observed following Tat induction. **a** PV+ neurons and neurites in Tat⁻ mice. No differences in the density of PV+ fibers or increases in the number of dendritic varicosities was seen in the stratum radiatum (sr). *Scale bar* = 20 μ m. **b** Tat⁻ SST+ axons in stratum lacunosum-moleculare (sl-m). No difference in fiber density of SST+ axons in the SL-M was observed. Stratum oriens (so), stratum pyramidale (sp), dentate gyrus (dg). *Scale bar* = 50 μ m

Figure 2. 8: Interneurons affected by Tat are part of a memory microcircuit



The interneurons affected by Tat form a microcircuit within the CA1 area of the hippocampus. CA1 pyramidal cells receive inputs from both hippocampal area CA3 and the entorhinal cortex. Oriens-lacunosum-moleculare (O-LM) cells gate inputs from the entorhinal cortex onto pyramidal cell distal apical dendrites. CA3 inputs are disinhibited by bistratified cells and Shaffer collateral-associated interneurons in the stratum radiatum (Sik et al, 1997; Klausberger et al, 2004; Leão et al, 2012). O-LMs receive excitatory inputs from CA1 pyramidal cells and the septum, and inhibitory innervation

from interneuron-specific interneuron type 3 (IS3) cells (Acsady et al, 1996a; Muller & Remy, 2014; Sun et al, 2014; Tyan et al, 2014). Bistratified cells receive excitatory input from Shaffer collaterals, CA1 pyramidal cells, and the septum (Ali et al, 1998; Klausberger et al, 2004; Muller & Remy, 2014) and innervate pyramidal cells (Buhl et al, 1994; Sik et al, 1997; Klausberger et al, 2004). In addition to being inhibited by O-LMs, bistratified cells receive GABAergic inputs from the neuronal nitric oxide (nNOS)+/neuropeptide Y (NPY)- IS3s (Leão et al, 2012; Tyan et al, 2014). IS3s innervate O-LMs preferentially, as well as bistratified cells, in the stratum oriens (Acsady et al, 1996a; Tyan et al, 2014). Disruption of this circuit by Tat may disrupt the gating of inputs from CA3 and the entorhinal cortex and therefore produce aberrant pyramidal cell outputs, which could account for the behavioral phenotype observed following Tat exposure (Sik et al, 1997; Klausberger et al, 2004; Leão et al, 2012). CA1 pyramidal cell (*yellow*), bistratified cell (Bis, *orange*), O-LM (red), IS3 (light *blue*), Shaffer collateral input from CA3 (*green*), perforant path input from the entorhinal cortex (EC, *purple*). Glutamatergic synapses are noted with a *plus* (+) and GABAergic synapses are noted with a *minus* (-).

	Tat- n= 14	Tat+ n= 14
Familiar Object Exploration (s)	12 ± 2	15 ± 2
Novel Object Exploration (s)	24 ± 3	20 ± 3
Total Distance Traveled (m)	13 ± 1	11 ± 1
Frequency of Rearing	51 ± 8	44 ± 8
Total Time Rearing (s)	43 ± 7	35 ± 6

Table 2. 1: Raw exploration time and motor behavior among Tat- and Tat+ mice

Raw exploration time and motor behavior among Tat- and Tat+ mice ($n = 14/\text{group}$) that were assessed in a novel object recognition task (mean \pm SEM). No significant differences were observed between Tat- and Tat+ mice.

Chapter 3: The effects of Tat and Morphine on the structure and function of CA1

Parts of this chapter will be submitted for publication in the Journal of Neuroscience

Clarification of contributions: Dr. Virginia McLane, Aaron Barbour, and Jean Moon assisted with morphological analyses

Introduction

Infection of the CNS by the human immunodeficiency virus (HIV) results in a series of neurological impairments collectively termed the HIV associated neurocognitive disorders (HAND). The neurological effects of HIV have also been shown to be exacerbated by using opiates (Hauser et al, 2012). Diminished spatial memory, frequently associated with hippocampal dysfunction, is a hallmark of HAND and aggravated by opiate abuse (Maki et al, 2009; Keutmann et al, 2017). Despite this, the mechanisms underlying the pathological effects of HIV and morphine alone or in combination within the hippocampus are incompletely understood.

Both Tat (Kesby et al, 2016; Marks et al, 2016), and morphine (Zhu et al, 2011; Kitanaka et al, 2015) have been demonstrated to impair spatial memory in mice. Previous work identified HIV-1 Tat-induced reductions of long term potentiation (LTP) in CA1, which coincides with deficits spatial memory formation in HIV transgenic mice (Fitting et al, 2013). However, reductions in LTP were accompanied by only modest reductions in the density of dendritic spines in CA1 pyramidal cells and no change in the levels of excitatory synaptic proteins. In contrast, Tat markedly reduced expression of synaptotagmin 2, while triggering presumably compensatory increases in gephyrin

postsynaptically, reflecting a disruption in inhibitory GABAergic transmission within CA1. Further investigation of the GABAergic cells within CA1 revealed that several distinct subgroups of GABAergic interneurons were preferentially vulnerable to Tat, while others were unaffected (Fitting et al, 2013; Marks et al, 2016). Many of the interneurons affected by Tat are known to be part of a microcircuit within CA1 that is involved in feedback regulation and input gating of pyramidal cells (Buhl et al, 1994; Sik et al, 1997; Klausberger et al, 2004; Leão et al, 2012; Muller & Remy, 2014; Tyan et al, 2014; Marks et al, 2016), making it likely that Tat will cause notable effects on the physiological activity of these targets as a consequence of disruptions in the supporting microcircuitry, even beyond any direct Tat effects on pyramidal cells themselves. Morphine generally decreases neuronal excitability (Liao et al, 2005; McQuiston, 2008; Xu et al, 2013; Fitting et al, 2015a; Fitting et al, 2016). However, because morphine disinhibits GABAergic interneuron inputs onto pyramidal cells, this may exacerbate Tat-induced excitotoxicity in pyramidal cells. This is all dependent on neuron type and opiate receptor distribution (Drake & Milner, 2002; Liao et al, 2005; McQuiston, 2007; McQuiston, 2008; Xu et al, 2013). Interestingly, Tat and morphine can exert effects in pathways which have converging processes (Sanchez-Blazquez et al, 2010; Garzon et al, 2011). Tat can also cause morphine to have differential effects on sodium channel activity in cultured neurons. Depending on morphine concentration, combined Tat and morphine can profoundly disrupt physiologic processes (Fitting et al, 2015a).

With observed deficits in the GABAergic network of the hippocampus, accompanied by only slight morphological disturbances in the pyramidal cells, we hypothesized that the functional output of CA1 might be disrupted by HIV-1 Tat. We

also set out to examine whether the observation of reduced synaptotagmin 2 in SR results in loss of synaptic contacts on pyramidal cells. Additionally, the evidence that morphine exacerbates HIV effects in human patients as well as our Tat transgenic mouse model led us to hypothesize that the deleterious effects of Tat would be exacerbated by the presence of morphine, especially in the morphologic domain, considering the very modest effects previously observed. To test these hypotheses, we used whole cell patch clamp to examine the firing frequency and other electrophysiological properties of CA1 pyramidal cells, as they represent the focal point of inhibitory and excitatory processed in the region before projecting out toward the entorhinal cortex, and perform morphological analyses on the cells recorded from afterward. Additionally, we sought to identify behavioral deficits in spatial memory formation, closely associated with the hippocampus associated with the combined effects of HIV-1 Tat and morphine exposure.

Materials and Methods

The use of mice in these studies was pre-approved by the Institutional Animal Care and Use Committee at Virginia Commonwealth University and the experiments were conducted in accordance with ethical guidelines defined by the National Institutes of Health (NIH Publication No. 85-23).

Subjects and housing

Male mice between 8 and 12 weeks of age with or without the presence the HIV-1 *tat* transgene (HIV-1 T Tat₁₋₈₆) under the control of a doxycycline activated Tet-on expression system driven by glial fibrillary acidic protein (GFAP) were used in these

studies (Bruce-Keller et al, 2008). Doxycycline (Dox) was administered in a specially formulated diet (Dox Diet #2018, 6 g/kg, Harlan Laboratories, Madison, WI) to the mice for 10-11 days. On the last day, animals were sacrificed for electrophysiological experiments or tissue harvesting. All mice were housed 4-5/cage and maintained in a temperature- and humidity-controlled room on a 12:12 h light/dark cycle (lights off at 18:00 h) with food and water available *ad-libitum*. On day 5 following Dox administration, animals had a morphine pellet (25 mg morphine sulfate, NIH) or placebo pellet implanted in beneath the skin in the subscapular region.

Tissue preparation for electrophysiological experiments

Following 10-11 days of Dox exposure, adult male mice were transcardially perfused with sucrose cutting media (in mM; 3 KCl, 4.12 MgSO₄, 1.2 NaH₂PO₄, 206 sucrose, 25 NaHCO₃, 25 glucose) chilled to around 1-3°C and bubbled with a 5% CO₂ balanced oxygen mix. Brains were extracted and halved along the sagittal sulcus, then cut horizontally in 350 µm sections from the ventral surface using a Leica VT1200 S vibratome (Leica Biosystems, Buffalo Grove, IL). Slices were cut in oxygenated sucrose cutting media held at 1-3°C by an external cooling apparatus (Huber, Offenburg, Germany). Following the cutting procedure, slices were transferred onto a nylon mesh submerged in oxygenated extracellular recording solution (in mM; 3 KCl, 1.2 CaCl₂, 1.2 MgSO₄, 1.2 NaH₂PO₄, 125 NaCl, 25 NaHCO₃, 25 glucose) maintained at 36.5°C for 30 minutes. The beaker was then returned to room temperature and the slices allowed to rest for 30 minutes prior to recording. In some cases, both the cutting solution and extracellular solution were supplemented with 500nM morphine sulfate.

Electrophysiological recording

Slices were continuously perfused with extracellular recording solution warmed to 30-34°C with an external heating apparatus (Warner instruments, TC-344B, Hamden, CT). The CA1 subfield of the hippocampus was visualized using a 4x magnification objective on a Zeiss Axio Examiner A1 microscope (Zeiss, Oberkochen, Germany). Magnification was switched to a 63x fluid-immersion objective to identify putative pyramidal neurons in the CA1 pyramidal layer. Pipettes for whole cell patch clamp were pulled (Narishige PC-10 pipette puller; Narishige, Tokyo, Japan) from borosilicate glass pipettes (WPI #1B1505-4) to a resistance of 2-6 MΩ. Pipettes were filled with an intracellular solution containing (in mM) 135 KMeSO₄, 10 HEPES, 2 MgATP, 0.1 MgGTP, 8 NaCl, 0.1 BAPTAK4, Biocytin 0.2% (pH 7.25). Membrane potentials were recorded using a MultiClamp 700B amplifier (Molecular Devices, Sunnyvale, CA), processed using a Digidata 1550A digitizer, and analyzed using Clampex 10.4 software (Molecular Devices, Sunnyvale, CA) on a Windows-based computer. Membrane potentials were observed in response to step-wise, 25 pA current increases from -100 pA to 400 pA.

Histology: Upon termination of whole cell patch clamp configuration, slices containing biocytin-filled cells were moved into a 24-well plate and fixed with 4% paraformaldehyde in 1x phosphate buffered saline (PBS) for 4-7 days at 4°C. Following fixation, slices were rinsed in PBS 6 times for 10 min each on a rocking platform at 4°C. Slices were permeabilized for 30 min in a solution of 50% ethanol in 1x PBS, containing 0.02% Triton X100, then transferred into a similar solution containing 70% ethanol for 30 min, and returned to 50% ethanol for 30 min. Slices were rinsed as described earlier, and then blocked in PBS containing 2% chicken serum, 0.02% bovine serum albumin, and

0.02% Triton X100 for 30 min. Primary antibodies against gephyrin (goat polyclonal, 1:1000, Santa Cruz, Sc-6411), and synaptotagmin 2 (Syt2; Rabbit polyclonal, 1:1000, Synaptic Systems, Goettingen, Germany; Cat. No. 105 123) were applied, and slices were incubated for 48 h on a rocking platform at 4°C. The slices were rinsed as before, and incubated in secondary antibodies (donkey anti-goat IgG-Alexa Fluor® 488 1:500, Invitrogen A-1055; goat anti-rabbit IgG-Alexa Fluor® 647 1:500, Invitrogen A-21244), as well as an Alexa Fluor® 594 Conjugated streptavidin probe (1:100, Invitrogen, S-32356) for 48 h, and then rinsed in PBS. Slices were incubated in Hoechst (0.5 µg/ml in PBS, Invitrogen, H3570) for 10 min, rinsed in PBS, and mounted on slides using ProLong Gold Antifade reagent (Invitrogen, P36930).

Imaging and morphological analysis:

Z-stack imaging of neurons was performed using a Zeiss LSM 700 (0.55 NA) at 20x (Plan-Apochromat 20x/0.8 NA, M27) and 63x (Plan-Apochromat 63x/1.40 NA Oil immersion DIC, M27) magnification (Zeiss, Oberkochen, Germany). Hoechst was visualized using a 405 nm laser with an SP 490 nm Filter, Alexa 488 using a 488 nm laser and a BP 490-555nm filter, and Alexa 594 using a 555nm laser with a BP 505-600 nm filter. Z-Stack data was reconstructed into a 3-D image using Imaris Bitplane 7.6.4 (Zurich, Switzerland). Primary dendrites were determined as dendrites that protrude from the cell body and dendritic order increased with every branching point. Dendritic spine analysis was performed with Imaris Bitplane 7.6.4 and regions selected for analysis were 20-30 µm in length and were selected at a 5-10 µm distance from the previous branch point and at least 5 µm from the next branch point. Dendritic spine densities are reported as the average number of spines per 10 µm length of dendrite.

Spine morphology was analyzed using uncompressed Z-stacks. Spines were counted along 20-30 μm long dendrite segments laying parallel to the plane of view. Three categories of spine morphology were quantified: thin, stubby, and mushroom (Harris et al, 1992; Ochs et al, 2015). Each spine type was counted and expressed as a percentage of total spines. Analysis of the co-localization of inhibitory puncta within neurite segments was performed using the co-localization module of Imaris Bitplane [version 9.0]. Briefly, background signal was filtered out of from the 488 channel (gephyrin), and the signal from the 594 channel (streptavidin tagged pyramidal cells) was used as a mask to create a co-localization channel for gephyrin puncta occurring within spaces occupied by filled pyramidal cells. The number of puncta within a measured length of approximately 10 μm along the identified neurite segment was then counted. Data is expressed as number of gephyrin puncta per micrometer. Analysis of inhibitory contacts took place on the aspiny portions of the apical and basilar dendrites immediately adjacent to the cell body, as well as the spiny portions at the distal ends of dendrites terminating in SL-M, as these dendritic compartments are have the highest percentage of inhibitory contacts in the average CA1 pyramidal cell (Megías et al, 2001).

Barnes maze

Tat⁻ and Tat⁺ mice were implanted with either morphine (n = 15 Tat⁻, 15 Tat⁺) or placebo pellets (n = 17 Tat⁻, 18 Tat⁺) and assessed for spatial learning and motor function using a Barnes maze test (Barnes, 1979). Mice consumed DOX chow for 6 days prior to 1 day of prehabitation (1 day following subscapular pellet implantation), followed by 4 days of testing. In the prehabitation phase, mice were placed in a

randomly positioned escape hole for 2 min, then were placed in the brightly lit center of the Barnes maze (91 cm diameter, 90 cm height, with 20 holes each 5 cm diameter; Stoelting Co., Wood Dale, IL). Mice were then guided to the same assigned escape hole where they remained for 2 min. Finally, the mice then were placed under a glass cylinder next to the escape hole, and allowed up to 3 min to voluntarily enter (mice that did not enter the hole were guided in and remained for 2 min). On testing days (two trials per day over 4 days), mice were placed in the brightly lit center of the Barnes maze and were allowed up to 3 min to enter the escape hole. Mice that did not enter the hole were gently guided to the hole and allowed to remain for 2 min. Shorter latencies to find the escape hole, a greater proportion of time spent in the correct quadrant of the maze, and fewer errors were considered indices of greater learning (Camara et al, 2013). On the final day, following the completion of training trials, a reversal probe trial was conducted in which the maze was rotated 180° from its original position such that the correct goal box was on the opposite end of the Barnes maze table. The proportion of time spent in the new target quadrant, latency to find the new escape hole, and number of errors made were assessed. Distances and velocities traveled were used as an index of motor behavior. Behavioral data were recorded and digitally encoded using the ANY-maze animal tracking system (Stoelting Co., Wood Dale, IL).

Vision testing

All mice were tested for visual function following conclusion of the Barnes maze test (Wersinger et al, 2002; Marks et al, 2016). Briefly, mice were suspended approximately 12 in. above a vertical ring-stand and were lowered with the ring-stand approximately 2 in. from the left or right visual field (close enough to allow visual, but not

whisker, contact with the ring-stand). The left and right visual fields were assessed for each mouse, with the starting side selected randomly. Visual responding was considered positive when mice reached with the forepaws for the rod when presented to both the left and right side. A response to only one visual field is considered a negative response. One male animal (Tat+/morphine) failed vision testing and was excluded from analysis.

Statistical analysis

Behavioral data were assessed via repeated-measures analyses of variance (ANOVA) with Barnes maze testing trial (days 1–4 and reversal probe) as the within subjects factor, and both mouse genotype (Tat– or Tat+) and drug treatment (morphine or placebo) as the between subjects factors. Fishers PLSD post hoc tests were used to assess group differences following main effects. Interactions were delineated via simple main effects and main effect contrasts with alpha corrected for multiple comparisons. All electrophysiological data was collected and analyzed using a planned comparisons paradigm. Tat– and Tat+ animals treated with placebo pellets were compared against Tat– and Tat+ animals treated with morphine pellets and maintained in morphine containing solutions. As a separate comparison, Tat– and Tat+ animals treated with morphine pellets and maintained in morphine-containing solutions were compared against Tat– and Tat+ animals treated with morphine pellets and maintained in morphine-free solutions. Firing frequency was analyzed using a repeated measures ANOVA with current step as the within-subjects factor, and Tat genotype and drug treatment combination as the between-subjects factors. Intrinsic firing properties were performed with a standard two-way ANOVA. In all cases, the threshold for

significance was considered $p < 0.05$, and post-Hoc testing was performed using Fisher's PLSD except where the requirements of planned comparisons testing necessitated more stringent application of Bonferroni corrections for multiple comparisons.

Results

Barnes maze

A main drug effect was noted in latency to escape [$F(1,61) = 15.708, p < 0.05$], with morphine treated animals taking longer to escape in all trials than placebo treated animals, regardless of genotype [$p = 0.0002$] (Fig. 3.1A). A significant interaction was observed for the factors of time, genotype, and drug in a repeated measures ANOVA [$F(1,61) = 2.704, p < 0.05$] for the percentage of time animals spent in the correct quadrant. Tat⁻, placebo-treated animals outperformed Tat⁺, placebo-treated animals after four days of training trials. Morphine-treated animals were unaffected by genotype status ($p = 0.0402$), obviating the Tat effect (Fig 3.1B, 3.2) While no significant effects were noted in the number of errors made between groups, an overall effect of time was observed, in which all groups made fewer errors as testing progressed [$F(1,59) = 20.749, p < 0.05$] from day 1 to day 4, and increased with the reversal trial [$p = 0.0001 - 0.0034$] (Fig 3.1C). Similarly, the distance traveled (Fig 3.1D) was not significantly different between groups, but changed across all groups over time [$F(1,61) = 22.036, p < 0.05$], with decreasing distance from days 1 to four, and an increase in the reversal trial [$p = 0.0001 - 0.0296$]. While no significant interactions were noted in the average velocity of the animals, independent main effects of drug [$F(1,61) = 5.366, p < 0.05$] and time [$F(1,61) = 4.116, p < 0.05$] are present (Fig 3.1E). Placebo treated animals move at

higher velocity across all trials [$p = 0.0239$], and all groups move at a lower velocity on Day 4 compared to day 1, with a return to baseline velocity in the reversal trial [$p = 0.0142 - 0.002$].

Electrophysiological analysis of Tat and drug effects on CA1 pyramidal cells

In order to assess the effects of Tat and morphine on physiological function of CA1 pyramidal cells as the functional output of CA1, a planned comparisons testing paradigm was designed to test the differences between six sets of conditions: Groups A and B consisted of Tat⁻ and Tat⁺ placebo-treated animals (n = 13 cells from 3 animals, and 11-12 cells from 3 animals respectively). Groups C and D consisted of Tat⁻ and Tat⁺ morphine-treated mice in which the *ex vivo* slices were maintained in 500 nM morphine-containing physiological solutions during recordings and referred to as 'morphine maintained' (n = 19 cells from 4 animals, and 13 cells from 4 animals, respectively) and were compared to groups A and B. Groups E and F consisted of Tat⁻ and Tat⁺ morphine-treated mice in which morphine was withheld from the *ex vivo* slices that were maintained in physiological solutions lacking morphine during recordings and referred to as 'morphine withheld' (n = 29 cells from 8 animals, and 22 cells from 7 animals). Groups A and B were independently compared to groups C and D ('morphine maintained') or to groups E and F ('morphine withheld'; Fig 3.3), but C and D and E and F were not directly compared to one another.

In the comparison between Tat⁻ and Tat⁺ placebo-treated animals vs. Tat⁻ and Tat⁺ morphine maintained animals, several effects were observed. Assessments of firing frequency showed a significant interaction between current step and Tat genotype [$F(1,52) = 3.037, p < 0.05$]; however, no other interactions occurred (Fig 3.4A-D). One-

way ANOVA revealed that between the 50 pA and 150 pA current steps, pyramidal cells from Tat+ mice fired at a lower frequency than those from Tat- mice [$p = 0.0024 - 0.0461$] (Fig. 3.4C). Intrinsic membrane properties were assessed by two-way ANOVA. An interaction between Tat and morphine exposure was observed in the resting membrane potential of the CA1 pyramidal cells [$F(1,53) = 7.341, p < 0.05$]. Pairwise comparisons using the Bonferroni correction for multiple comparisons (significance threshold set at $p < 0.0083$) revealed that only placebo-treated Tat- and Tat+ mice differed (Fig. 3.5A), with Tat+ placebo-treated animals having significantly more depolarized resting membrane potentials [$p = 0.0057$]. In addition, a main effect of morphine was observed on the firing threshold of CA1 pyramidal cells [$F(1,53) = 15.812, p < 0.05$], with morphine-treated cells firing at a more hyperpolarized potential than placebo-treated mice [$p = 0.0001$] (Fig 3.5C). No significant effects were noted for rheobase, however, Tat treatment caused a trend toward increased rheobase compared to controls [$F(1,53) = 3.367, p = 0.0622$] (fig 3.5B). Notably, no significant differences were seen between any groups in the values of input resistance or capacitance (Table 3.3).

To assess the effects of withholding morphine in our model, we compared the physiological response of CA1 pyramidal cells in Tat- and Tat+ placebo treated animals with those of Tat- and Tat+ morphine treated animals, in which physiological recordings took place in solutions lacking morphine, so as to induce a withdrawal-like state in the tissue slices. Assessment of firing frequency revealed two interactions, one between Tat and current step [$F(1,71) = 3.465, p < 0.05$], and another between drug treatment and current step [$F(1,71) = 6.425, p < 0.05$]. Tat and morphine treatment did not show any

interactions (Fig 3.6A-D). To independently test the effects the Tat induction and morphine on the firing rates pyramidal cells exposed to increasing amounts of current, the Bonferroni corrected significance threshold was set at $p < 0.025$. Collapsing across genotype and ignoring the effects of morphine, Tat exposure altered the firing rate of pyramidal cells depending on the amount of the stimulating current. Tat+ pyramidal cells fired at a lower frequency than Tat- neurons [$p = 0.0013 - 0.0208$] (Fig 3.6C) at 25 pA to 200 pA, but firing rates did not differ at other current levels. Collapsing across drug treatment, without considering the effects of genotype, showed that when morphine was withheld from slices from morphine-treated mice, pyramidal cells fired at a significantly lower frequency than those in placebo-treated mice when stimulated with 275 pA to 375 pA [$p = 0.0069 - 0.0204$] (Fig 3.6D). Intrinsic membrane properties were again compared by using two-way ANOVA. An interaction between Tat and drug treatment was observed in the resting membrane potential [$F(1,72) = 37.989, p < 0.05$]. Pairwise comparisons using the Bonferroni correction for multiple comparisons (significance at $p < 0.0083$) revealed that only the resting membrane potential of Tat- and placebo- and Tat+ and placebo-treated mice differed (Fig 3.7A), with Tat+ placebo-treated animals having significantly more depolarized resting membrane potentials [$p = 0.0031$]. Additionally, a Tat effect was noted in the observed rheobase [$F(1,72) = 7.704, p < 0.05$], where Tat positive cells required more current to reach threshold [$p = 0.0039$] (Fig 3.7B). No significant effects were observed on the firing threshold CA1 pyramidal cells (Fig 3.7D). As in the previous comparison, neither the resistance nor capacitance was affected by Tat and/or morphine, suggesting that the effects of Tat and morphine on CA1 pyramidal cells are indirect (e.g., through alterations in presynaptic inputs

originating from interneurons, circuits outside CA1, and/or glial activity), rather than direct/intrinsic effects of Tat and/or morphine on the pyramidal cells themselves (Table 3.4).

Morphological analyses

The morphological effects of Tat on CA1 pyramidal cells have previously been analyzed as whole cells or larger segments without consideration to the sublamina divisions within CA1 (Fitting et al, 2013), which may result in subtler effects of Tat being missed, as distinct structural and functional differences exist between, and within, the dendritic compartments occupying different CA1 sublamina (Megías et al, 2001). To better assess the regional variations within CA1 dendritic structure, analyses of morphology were broken down by sublamina (Figs 3.8, 3.9A, 3.10A, 3.11A). The cells and dendrite segments used for morphological analysis were all used in the electrophysiological analysis of Tat and morphine (n for all groups = 10-12; figs 3.8, 3.9B, 3.10B, 3.11B).

The effects of Tat and morphine on the density of dendritic spines differed in each layer of hippocampal area CA1. In the SO, there was a main effect of morphine on spine density [$F(1,41) = 8.402, p < 0.05$], where cells from morphine treated animals had fewer spines per 10 μM segment [$p = 0.0069$] (Fig 3.9C). No effects on spine density were observed in SR (Fig 3.10C); however, a significant effect of Tat was observed in SL-M [$F(1,38) = 5.015, p < 0.05$], with Tat+ cells having a higher spine density than Tat- cells [$p = 0.0252$] (Fig 3.11C). A trend toward an interaction between Tat and morphine was also observed in SL-M [$F(1,38) = 3.465, p = 0.0704$]. With this in mind, the effects of morphine were examined further in pyramidal cells in Tat- and Tat+

mice separately. Significant effects were observed in Tat⁻ cells [$F(1,20) = 7.075, p < 0.05$], but not Tat⁺ cells. Morphine-treated pyramidal cells in Tat⁻ mice had fewer SL-M spines than in placebo-treated mice [$p = 0.0150$]. With the lack of change in pyramidal cells in the Tat⁺ mice by comparison considered with the trend toward interaction, it is likely that the main effect of Tat on SL-M spine density is actually driven by a reducing effect of morphine that is present only in Tat⁻ cells.

As with regional spine density, the effects of Tat and morphine on the morphologic types of spines present on dendrites varied by sublamina. Significant interactions between Tat and morphine were observed in the SO (Fig 3.9D) for the percentage of mushroom spines [$F(1,40) = 6.932, p < 0.05$] and stubby spines [$F(1,40) = 8.764, p < 0.05$], and SL-M (Fig 3.11D) for the percent of mushroom spines [$F(1,35) = 6.140, p < 0.05$]. SO mushroom spines were found to be reduced in Tat⁺ morphine-treated animals compared to Tat⁻ placebo-treated animals [$p = 0.0028$], and Tat⁻ morphine-treated animals [$p < 0.0001$]. Tat⁺ placebo-treated animals had more mushroom-type spines than Tat⁻ morphine-treated animals [$p = 0.0034$], but only showed a trend toward increase from Tat⁻ placebo-treated animals [$p = 0.0865$]. Additionally, Tat⁺ morphine-treated animals trended toward decreased mushroom spines in comparison to Tat⁻ morphine-treated animals [$p = 0.0563$]. Stubby spines in the SO were reduced in Tat⁺ placebo-treated mice [$p = 0.0115$], as well as both Tat⁻ and Tat⁺ morphine-treated mice [$p = 0.0001 - 0.0062$]. SL-M mushroom spines were reduced in Tat⁺ morphine-treated animals compared to all other groups [$p = 0.0005 - 0.0112$]. In addition to interactive effects, main effects of morphine were observed on the mushroom-type spines of SR (Fig 3.10D) [$F(1,43) = 7.027, p < 0.05$], with morphine-

treated animals having fewer mushroom-type spines than placebo-treated animals [$p = 0.0107$], and on the stubby-type spines of SLM [$F(1,35) = 5.867, p < 0.05$], with morphine-treated animals having more stubby-type spines than placebo-treated animals [$p = 0.0129$]. Finally, a main of Tat was seen on the percentage of thin/filopodial type spines in SR [$F(1,43) = 5.043, p < 0.05$], with an increase seen in Tat+ animals compared to Tat- animals [$p = 0.0274$]

Differing levels of dendritic damage were observed in SO, SR, and SL-M. Tat and morphine had an interactive effect on the percent of SO dendrites with varicosities [$F(1,43) = 5.125, p < 0.05$] (Fig 3.9E). This interaction was driven by all Tat+ groups and morphine-treated groups being higher than the Tat- and placebo-treated controls [$p = <0.0001-0.0004$]. In the SR, there were independent Tat [$F(1,43) = 13.571, p < 0.05$] and morphine effects [$F(1,43) = 13.100, p < 0.05$] on the percentage of dendrites exhibiting varicosities (Fig 3.10E), and a trend toward an interaction between them [$F(1,43) = 3.093, p = 0.0857$]. Pyramidal cells in Tat+ mice had more dendrites with varicosities than those in Tat- mice [$p = 0.0006$], and morphine-exposed pyramidal cells had more dendrites with varicosities than those in placebo-treated mice [$p = 0.0005$]. In addition to damage in the terminal dendrites, some degenerative effects were evident on the main axis dendritic shaft (Fig 3.10F). The nonparametric Kruskal-Wallis test was used because, unlike pyramidal cells in Tat+ mice, Tat- placebo-treated animals displayed no varicosities along the main axis of their dendrites. Because of the lack of variance in the Tat- placebo-treated animals compared to other groups, the ANOVA is an improper test. A significant effect was observed between the four group medians ($H' = 16.993, p < 0.05$). Mann-Whitney testing (with significance threshold set at $p < 0.0083$)

revealed that Tat⁺ and placebo-treated animals and Tat⁺ or Tat⁻ mice receiving morphine had more dendritic varicosities than control neurons [$p < 0.0001-0.0025$]. Additionally in SL-M, a significant effect of morphine was observed in the percentage of terminal dendrites with varicosities [$F(1,38) = 11.142, p < 0.05$], with morphine-exposed cells having more dendrites with varicosities than in placebo-treated mice [$p = 0.0019$] (Fig 3.11E).

Assessment of the number of inhibitory postsynaptic puncta within pyramidal cells was performed to further explore the loss of Syt2 expression and increase of gephyrin previously observed in the hippocampus (Fitting et al, 2013). The number of puncta was quantified along the aspiny portions of the basilar and apical dendrites as they emerged from the soma, as this is the region known to have the highest percentage of inhibitory contacts onto pyramidal cells (Megías et al, 2001). The results show no significant interactions between or main effects of either Tat or morphine on the number of inhibitory puncta within the basilar [$p = 0.3145-0.7208$] or apical [$p = 0.1287-0.5430$] dendritic shafts in the perisomatic region (Fig 3.12).

Correlational analysis

A number of correlations were observed between morphological outcomes, and electrophysiological outcomes. Several noteworthy correlations between the morphological features in discrete dendritic compartments and electrophysiological function were observed, and are presented with statistical results in Table 3.3. Negative correlations between the density of spines in SR and the firing frequency of pyramidal cells between 50 and 300 pA were observed. SR spine density also positively correlated with rheobase. The percentage of mushroom spines in SO was seen to positively

correlate with firing threshold, and negatively with firing frequency at the 100, 125, and 150 pA current steps. The percentage of mushroom spines in SL-M positively correlated with resting membrane potential, and the percentage of thin spines in SL-M positively correlated with firing frequency between the 275-300 pA and 350-400 pA current steps. Measures of dendritic damage did not correlate with electrophysiological function.

Discussion

In a variety of cell types, Tat is known to cause neuronal excitotoxicity (Yu et al, 1997; Mattson et al, 2005; Eugenin et al, 2007; Soulas et al, 2009; King et al, 2010). While Hippocampal pyramidal cells have been shown to be vulnerable to excitotoxic injury induced by excessive NMDA agonism (Avignone et al, 2005), the present study, and previous studies of CA1 pyramidal cell function and morphology, suggest that direct effects on CA1 pyramidal cells by Tat are minimal (Fitting et al, 2013) and that there is an effect on local circuitry that impinges on CA1 pyramidal cells (Marks et al, 2016). Indeed, there are more routes to excitotoxic injury than simple excess activation of NMDA receptors (Bouilleret et al, 2000; Avignone et al, 2005). The excitotoxic effects of Tat seem to mimic the syndrome caused in the kainite-induced injury model used to examine temporal lobe epilepsy rather than exposure to NMDA, as the effects appear to be more pronounced in subsets of CA1 interneurons rather than in CA1 pyramidal cells (Bouilleret et al, 2000; Avignone et al, 2005; Marks et al, 2016). This variation in excitotoxic disease could be due to interactions with multiple signaling pathways beyond NMDA receptor activation (Cossart et al, 2001; Oliva et al, 2002; Avignone et al, 2005), which is not surprising in the case of Tat considering how many interactions it can have

with intra- and extracellular targets (Eugenin et al, 2007; King et al, 2010; Debaisieux et al, 2012).

Physiologically, a Tat effect is seen in the analyses of Tat vs. morphine, and Tat vs. pyramidal cells in which morphine was withheld, in which firing frequency is significantly reduced at low current stimulation intensities. If direct excitotoxic activity of Tat on CA1 pyramidal cells was sufficiently great, or occurring in isolation, it could be expected that there would be an increase in their firing frequency, rather than a decrease, as has been shown in pyramidal cells isolated from upstream circuitry and exposed to excitotoxic insult (Avignone et al, 2005). Moreover, in the present study, the decrease in firing frequency was accompanied by an increase in the amount of current for pyramidal cells in Tat+ mice needed to reach their firing threshold. Although the firing frequency of pyramidal cells from Tat+ animals is decreased, the resting membrane potential of these cells is significantly elevated. This finding suggests that while Tat-exposed pyramidal cells may tend to be hyperexcitable, Tat may sufficiently overactivate the surrounding presynaptic inhibitory inputs to negate any intrinsic excitatory effects of Tat on the pyramidal cells themselves.

Disparate effects occurred when comparing the active presence of morphine against the effects of prolonged exposure followed by removal of morphine on CA1 pyramidal cells. Most interestingly, the only measure on which Tat and a morphine paradigm interacted was the resting membrane potential, and in each case, the difference is largely driven by the difference between the Tat- and Tat+ placebo-treated population, with morphine exposure appearing to obviate the effect, as we observe in both the Barnes maze results, and in the cytokine data. When morphine is present

during recordings of animals previously exposed to morphine, there is no observed morphine effect on firing, and it appears again that the presence of morphine obviates the Tat effect. There is, however, a reduction in the firing threshold of morphine-treated cells. By contrast, however, when tissues from morphine-treated animals are tested in solutions lacking morphine the firing frequency of withdrawn CA1 pyramidal cells is lower at high current stimulations (275-375 pA), but there is no effect of withholding morphine on the firing threshold.

HIV-1 Tat has been shown to cause changes in dendritic spines throughout the brain, indicating aberrations in normal patterns of plasticity. Reductions of spine density have been observed in the cortex, striatum, and hippocampus (Fitting et al, 2013; Raybuck et al, 2017; Schier et al, 2017), and alterations in the type of dendritic spines present on dendrites in the striatum have been observed (Schier et al, 2017). Decreased long term potentiation has also been seen in the hippocampus independently with Tat and morphine exposure (Bao et al, 2007; Fitting et al, 2013). Additionally, HIV-1 Tat and morphine exposure have an interactive negative effect on spine density in the striatum (Fitting et al, 2010a). The present study shows morphine-driven reductions in the spine density of dendrites in SO that do not interact with Tat, and differential morphine effects in the SL-M on Tat- and Tat+ pyramidal cells, with no change in the SR. In comparison, an eleven percent reduction in CA1 pyramidal cell spines was described by Fitting et al (2013) and attributed to Tat alone, differences in the methodology and quantification are present in this study which may give a more nuanced view by looking at discrete dendritic compartments rather than the cell as a whole. The analysis of dendritic spine loss is complemented by observations of regional shifts in spine types, which reflect

region specific shifts in plasticity. The excitatory systems, however, do not act alone. Our data show no differences in the amount of gephyrin puncta within dendrites near the soma (fig 3.12), which could suggest that the previously-found increase in gephyrin expression is related to inhibitory contacts onto other interneurons (Fitting et al, 2013; Marks et al, 2016). In any case, it is likely that in each of the CA1 lamina, a subtle balancing between excitatory and inhibitory processes is occurring independently of the other layers. The changes observed in spine number and morphology, as well as measures of dendritic damage were more pronounced in SO and SL-M, while SR remained comparatively stable, indicating systems interacting within SR may be more stable or better able to adapt. Dendritic damage observed in this study did not appear in previous work (Fitting et al, 2013), which may indicate that added insults, such as the manipulations under the hours-long sectioning, patching recording, and immersion fixation processes employed here might expose underlying pathology that is not readily visible given the relatively acute exposure to Tat in the prior experiments.

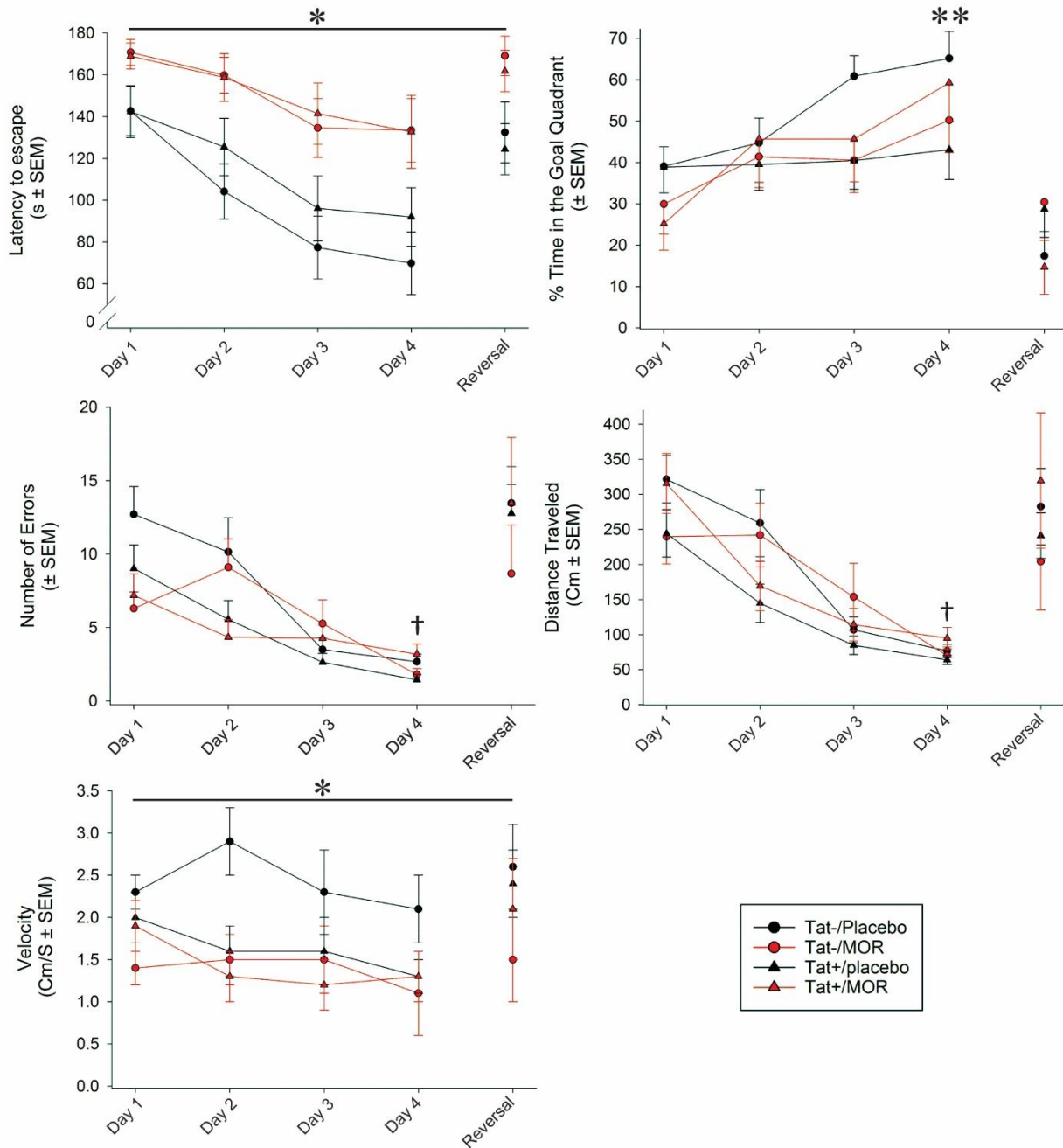
Results from previous studies have shown that Tat attenuates spatial memory as assessed by the Barnes maze task. This includes an increased latency to escape, a decreased time in the correct quadrant, and altered search strategies, as well decreased performance in working memory and phase dependent alterations in reversal learning (Kesby et al, 2016; Marks et al, 2016). The attenuation of spatial memory by Tat is still evident, with Tat+ placebo-treated animals performing significantly worse than Tat- placebo-treated animals according to post-hoc testing. Morphine treatment appeared to obviate the negative effects of Tat, with morphine treated mice performing at levels between the Tat- and Tat+ placebo-treated animals, regardless of genotype.

Interestingly, there is only an observed effect of morphine on latency to escape, with morphine-treated animals taking longer to escape than placebo-treated counterparts regardless of genotype. While both Tat and morphine independently can impair spatial memory function (Zhu et al, 2011; Kitanaka et al, 2015 ; Kesby et al, 2016; Marks et al, 2016), the present study shows no interaction between these factors, and even points toward a morphine-based attenuation of the deleterious effects of Tat. Morphine has been shown to have both stimulating and depressive effects on motor behavior depending on dose, with higher doses generating a biphasic response in which activity first decreases, then increases before returning to baseline. Tolerance to the depressive effects, however, develops more rapidly than the stimulant effects with chronic high dose administration. (Vasko & Domino, 1978; Ling et al, 1989; Le Marec et al, 2011) raising the possibility of motor confound in the present study. Other studies, however, have suggested that the effect of morphine on spatial memory is not attributable to locomotor effects (Kitanaka et al, 2015). This is likely considering that there is an observed effect of morphine on the overall velocity of travel (but not distance travelled), and could be a consequence of the drug delivery method used in the present studies. Additionally, it is possible that post-surgical inflammation, which can be expected from any surgical procedure, may affect behavioral function (Chen et al, 2008; Vizcaychipi et al, 2014). Also of note is that the testing protocol employed here used 2 fewer training trials than in Marks et al (2016) to eliminate the problem of overtraining the animals, as in the previous study we observed that after four days of training trials, a number of the animals became habituated to the aversive stimulus used to drive the task and stopped performing. It is possible that the risk of overtraining was outweighed by the

confounding effects of morphine, and that the present study would have benefited from more training trials. Further studies should be directed towards examining the behavioral outcomes of Tat and morphine interactions

The results of this study suggest that despite the general observation that morphine exposure exacerbates Tat toxicity in the brain (Hauser et al, 2012), the hippocampus as a discrete region may not be as susceptible to this phenomenon. This might be related to the Tat induced reduction of MOR expression, which could result in a subtle shift between the deleterious effects of chronic MOR activation, and the counter effects of DOR or KOR activation (Fitting et al, 2010a; Fitting et al, 2015b).

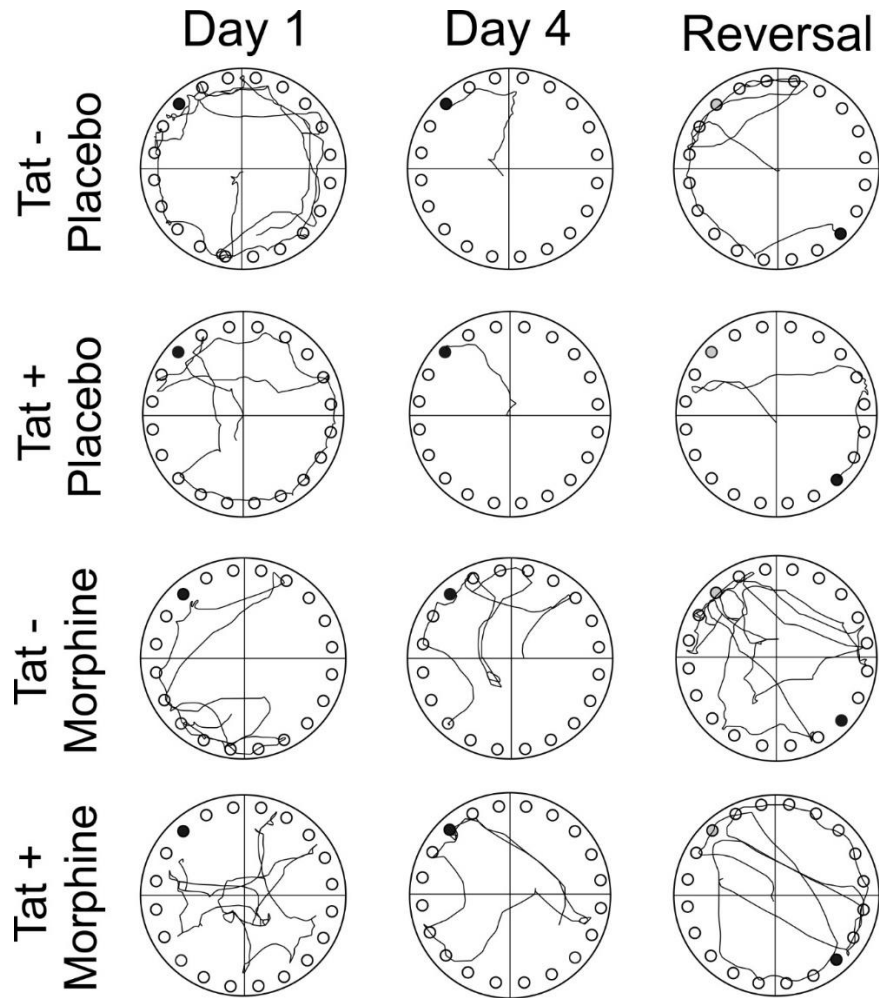
Figure 3. 1: Effects of Tat and morphine on Barnes maze performance in mice



Barnes maze performance of Tat+ animals compared to Tat- animals, with either placebo or morphine pellets implanted. **(A)** Animals given morphine took longer to escape than mice given placebo pellets, regardless of genotype ($p = 0.00002$). **(B)** A significant interaction was observed between Tat and morphine in the percent of

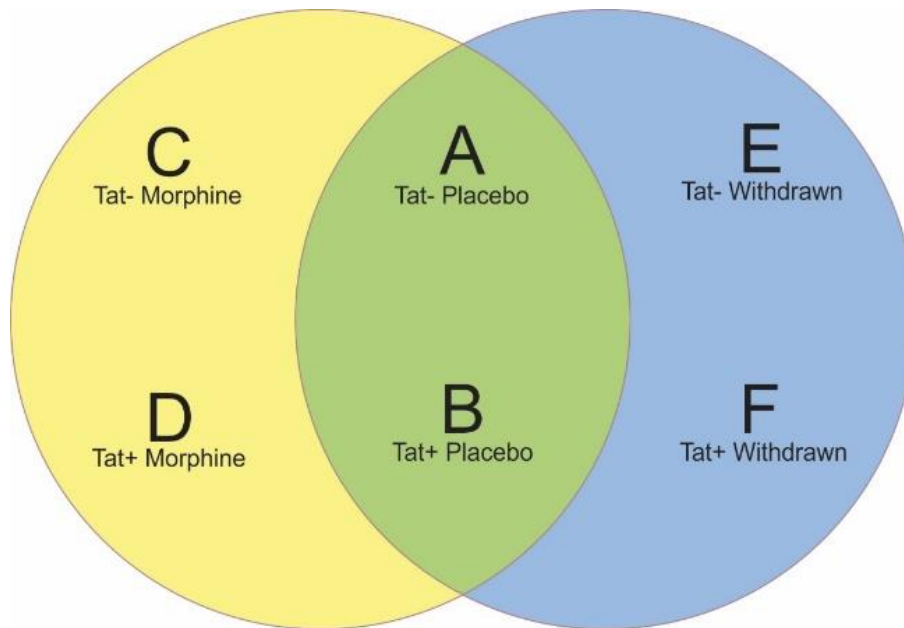
time spent in the correct quadrant ($p < 0.05$), with placebo-treated Tat⁻ mice performing better than placebo-treated Tat⁺ animals ($p = 0.0402$). Mice treated with morphine performed at an intermediate level regardless of genotype. No significant differences in the number of errors made (**C**), or the distance traveled (**D**), were observed between groups; however, these measures decreased from Day 1 to day 4, returning to Day 1 levels during the reversal probe ($p = .00001-0.0209$). The velocity differed across all days between mice given placebo pellets and morphine pellets (**E**), with morphine pellet-treated mice moving more slowly than placebo-treated animals ($p = 0.0142-0.002$).

Figure 3. 2: Representative Barnes maze track traces



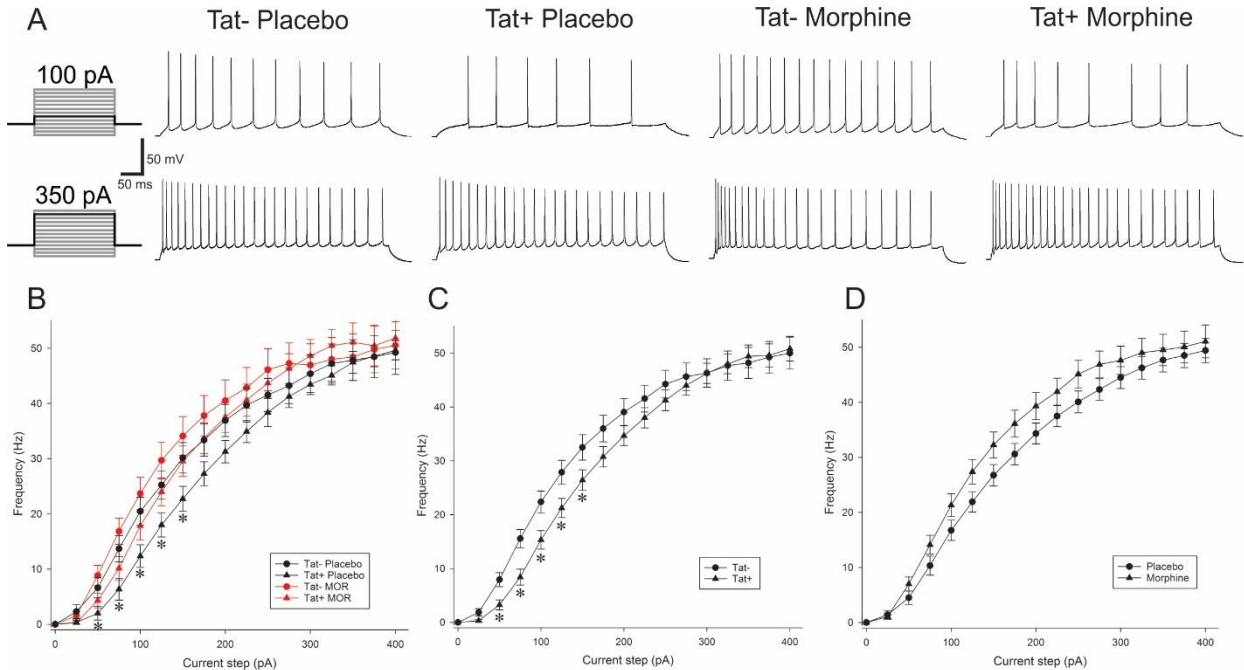
Representative track plots of the movements of male mice taken during 3 min (180 Sec) performance of the Barnes Maze spatial memory test. Track plots represented show the performance of Tat- and Tat+ mice, with either a morphine- or placebo-pellet implanted subcutaneously in the subscapular region.

Figure 3. 3: Visual representation of planned comparisons design for electrophysiological analysis



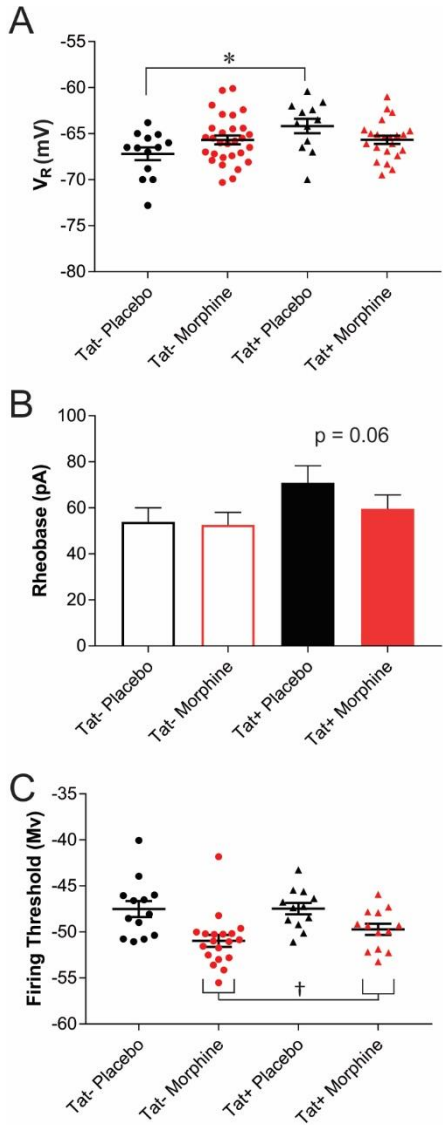
Visual representation of the planned comparisons design described in the methods section to assess the physiological activity of morphine naive Tat⁻ and Tat⁺ CA1 pyramidal, and cells exposed to morphine in a morphine maintained state, and a morphine deprived state independently. Briefly, six separate groups of mice were generated contemporaneously for electrophysiological recordings. Intended comparisons were between pyramidal cells from Tat⁻ and Tat⁺ placebo treated mice, and recorded in unsupplemented physiological solutions (**A, B**) and Tat⁻ and Tat⁺ mice treated with morphine, and recorded in physiological solutions supplemented with morphine (**C, D**). The second intended comparison was between groups A, and B as in the first comparison, and Groups **E** and **F** (Tat⁻ and Tat⁺ mice treated with morphine, but recorded in unsupplemented physiological solutions).

Figure 3. 4: Firing frequency of CA1 pyramidal cells after exposure to Tat and/or morphine-treated mice (*in vivo*) in which morphine is present during electrophysiological recordings (*ex vivo*)



Analysis of the firing frequency of CA1 pyramidal cells from Tat– or Tat+ mice treated with either a placebo or morphine. Slices from morphine-treated animals were recorded in artificial CSF containing 500 nM morphine to continue to expose the hippocampal slices to morphine *ex vivo*. Patched cells were stimulated with escalating current pulses 500 ms in duration starting at –100 pA and escalating to 400 pA in 25 pA steps. Representative traces (**A**) for each group are depicted at the 100 and 350 pA current steps. An interaction between Tat genotype and the amount of current applied was observed in the repeated measures ANOVA ($p < 0.05$) (**B**). CA1 pyramidal cells from Tat+ mice fired at a lower frequency than those of Tat– animals at between 50 and 150 pA ($p = 0.0024 - 0.0461$; **C**), but were unaffected by the sustained exposure to morphine during recordings (**D**).

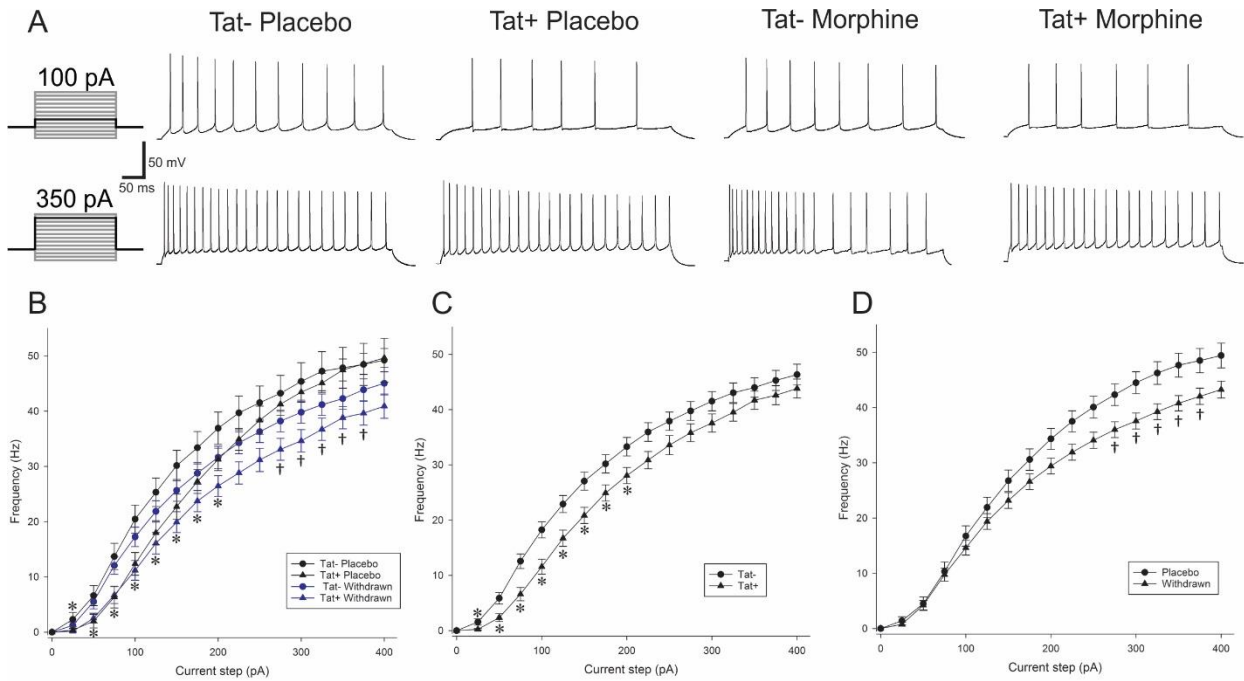
Figure 3. 5: Membrane properties of CA1 pyramidal cells in Tat and/or morphine-treated mice (*in vivo*) in which morphine is present during electrophysiological recordings (*ex vivo*)



Further analysis of the excitability of CA1 pyramidal cells from Tat– or Tat+ mice treated with either a placebo- or morphine-pelleted implants for 5 days *in vivo*. Slices derived from morphine-treated animals were isolated and recorded in physiological solutions containing 500 nM morphine to maintain receptor occupancy and morphine

effects on the tissue. A significant interaction between Tat and morphine was observed for the resting membrane potential (V_R) of CA1 pyramidal cells (**A**). Post hoc analysis showed that the differences were driven by a significant increase in the resting membrane potential of pyramidal cells from Tat+ and placebo-treated mice relative to those from Tat- and placebo-treated mice ($p = 0.0057$). Morphine treatment appears to obviate the effects of Tat. While no significant effects were noted in the rheobase, there was a trend ($p = 0.0619$) for pyramidal cells from Tat+ animals to require a greater amount of current (pA) to reach threshold for firing compared to cells from Tat- mice (**B**). A main effect of drug observed on firing threshold. The threshold for firing (mV) is significantly reduced in cells from morphine-treated animals ($p = 0.0622$; **C**).

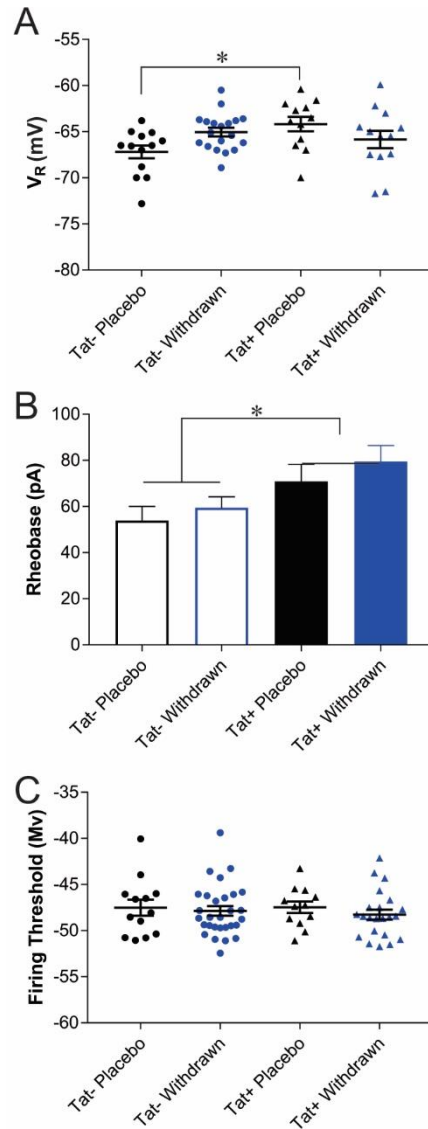
Figure 3. 6: Firing frequency of CA1 pyramidal cells from Tat and/or morphine-treated mice (*in vivo*) in which morphine is withheld during electrophysiological recordings (*ex vivo*)



Analysis of the firing frequency of CA1 pyramidal cells from Tat– or Tat+ mice treated with either a placebo or morphine. Slices from morphine-treated mice and morphine naïve mice were recorded in physiological solutions which did not contain morphine. Patched cells were stimulated with escalating current pulses 500 ms in duration starting at –100 pA and escalating to 400 pA in 25 pA steps. Representative traces (**A**) for each group are depicted at the 100 and 350 pA current steps. Interactions between Tat and current step, and morphine withdrawal and current step were observed in the repeated measures ANOVA ($p < 0.05$; **B**). Tat and morphine removal did not interact at any level of the analysis. At stimulating currents between 25 and 2,000 pA, CA1 pyramidal cells in slices from Tat+ mice fired at a lower frequency than those from Tat– mice ($p = 0.0013-0.0208$; **C**). Withholding morphine from pyramidal

cells slices isolated from morphine-exposed mice resulted in significantly lower firing rates at stimulating currents from 275 pA to 375 pA compared to morphine-naïve pyramidal cells ($p = 0.0069-0204$; **D**).

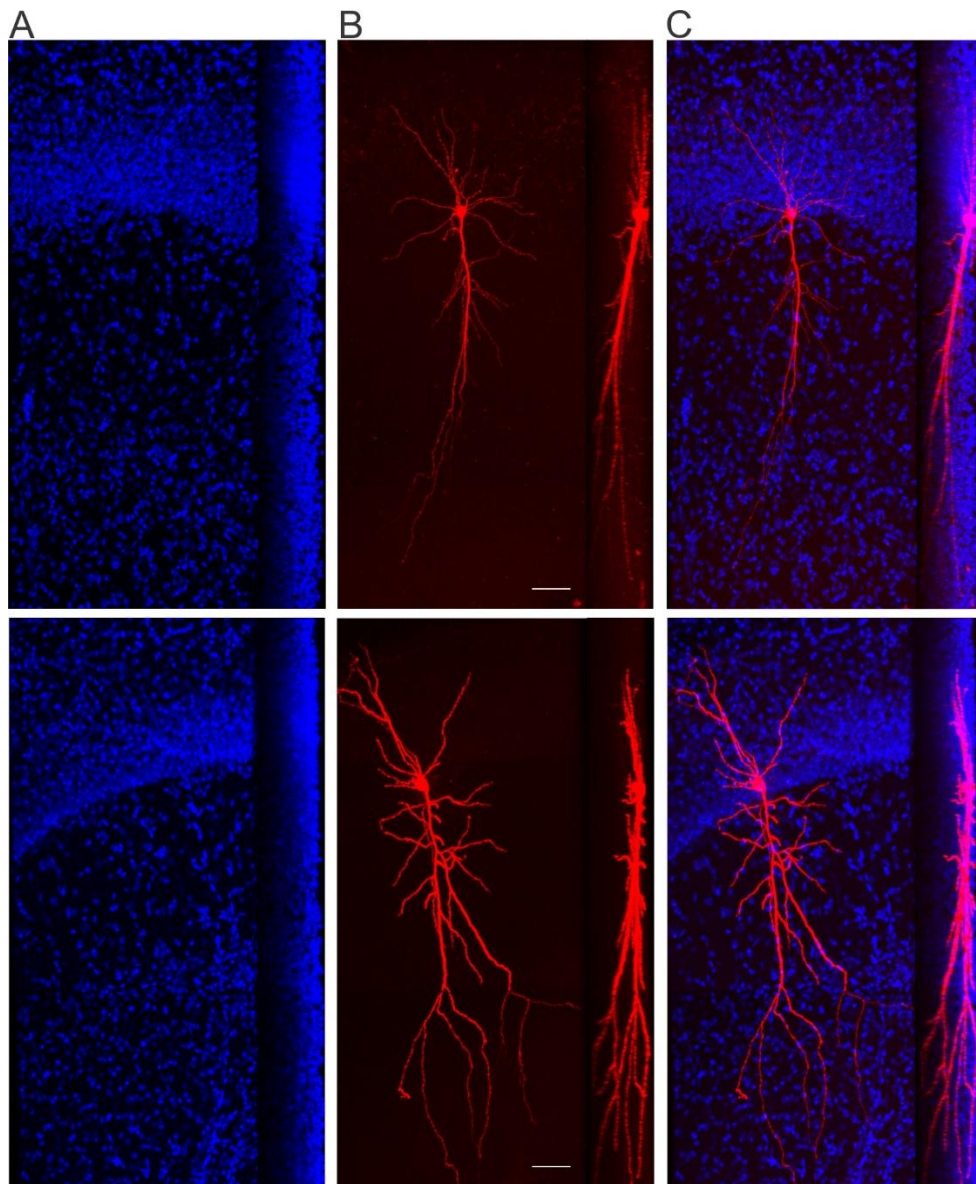
Figure 3. 7: Membrane properties of CA1 pyramidal cells from Tat and/or morphine-treated mice (*in vivo*) in which morphine is withheld during electrophysiological recordings (*ex vivo*)



Analysis of the firing frequency of CA1 pyramidal cells from Tat- or Tat+ mice treated with either a placebo or morphine. Morphine-treated and morphine-naive mice in this analysis were recorded in physiological solutions that did not contain morphine. A significant interaction between Tat and morphine was again observed for the resting membrane potential (V_R) of CA1 pyramidal cells (**A**). Post hoc analysis showed that the

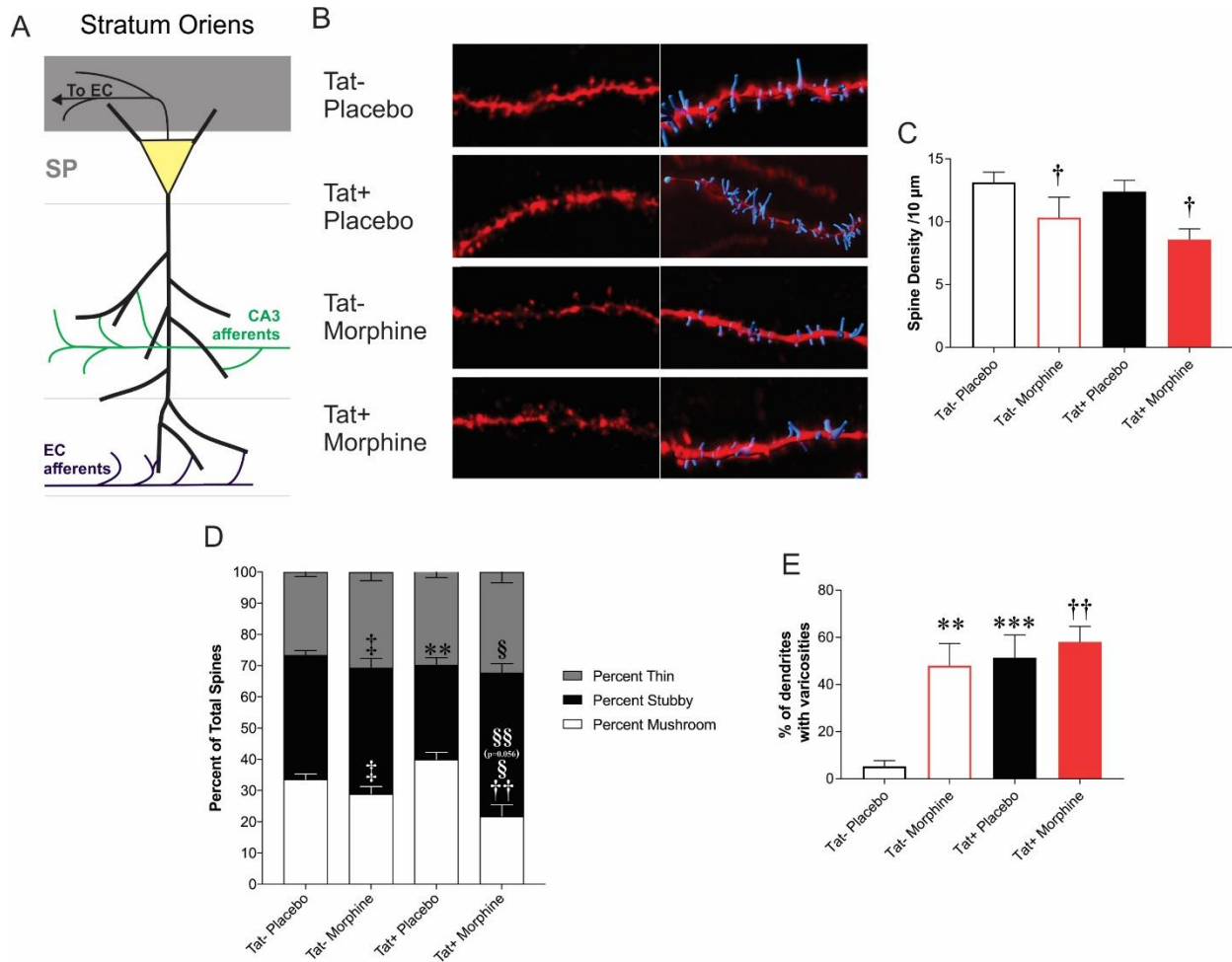
differences resulted from a significant increase in the resting membrane potential in pyramidal cells from Tat⁺ than Tat⁻ mice treated with placebo pellets ($p = 0.0031$). There was a significant effect of Tat on rheobase. Independent of morphine presence or withholding, pyramidal cells in Tat⁺ mice required a greater amount of current (pA) to reach the threshold potential for firing compared to Tat⁻ mice ($p = 0.0039$; **B**), despite the fact that the firing threshold (mV) of CA1 pyramidal cells was unaffected by Tat or morphine exposure (**C**).

Figure 3. 8: Examples of a 3D-reconstructed biocytin-filled CA1 pyramidal cells



Reconstructions of Z-stack images of biocytin-filled pyramidal cells within hippocampal area CA1. Z-stack images were used for analysis of morphological characteristics following exposure to Tat and morphine. Scale bars = 50 μ M.

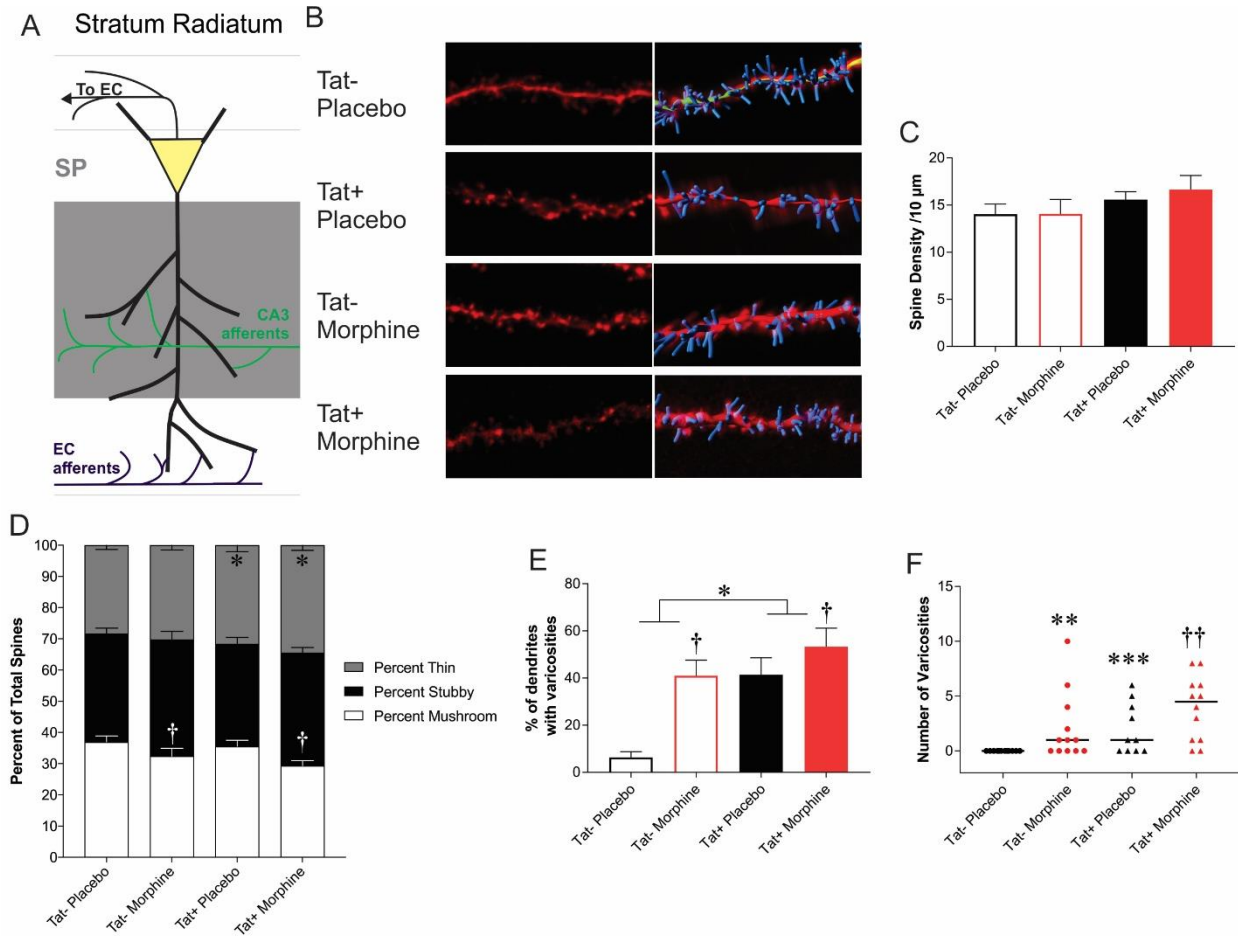
Figure 3. 9: Effects of Tat and morphine on the morphology of the portion of the pyramidal cell dendrite within the stratum oriens (SO)



Morphological effects of Tat and morphine on the portion of the CA1 pyramidal cell dendrite within the stratum oriens (**SO**) (**A**). (**B**) Sample SO dendrites and 3D reconstructions from each of the four experimental groups (**C**) An overall reduction in spine density was attributed to the effects of morphine ($p = 0.0069$). (**D**) There were also significant shifts in the morphologic types of spines present on SO dendrites. The percentage of stubby spines was reduced in Tat+/placebo-treated animals when compared to all other groups ($p = 0.0001-0.0115$). The percentage of mushroom spines was reduced in Tat+/morphine-treated animals compared to both placebo-treated

groups ($p = 0.0034$), and was trending toward being significantly lower than Tat-/morphine-treated animals ($p = 0.0563$). There was evidence of an increase in dendrites with varicosities in all groups compared to control animals ($p = 0.0001-0.004$;
E). Multiple symbols are used in this figure for a $p < 0.05$ due to the complexity of panel D; (*) denotes a main effect of Tat, (†) denotes a main effect of morphine, (**) denotes a difference between Tat-/placebo and Tat+/placebo, (***) represents a difference between Tat-/placebo and Tat-/morphine, (††) represents significance between Tat-/placebo and Tat+ morphine, the difference between Tat+/placebo and Tat-/morphine is shown by (‡), Significance between Tat+/placebo and Tat+/morphine is denoted with (§), and finally The differences between Tat-/morphine and Tat+/morphine are denoted as (§§).

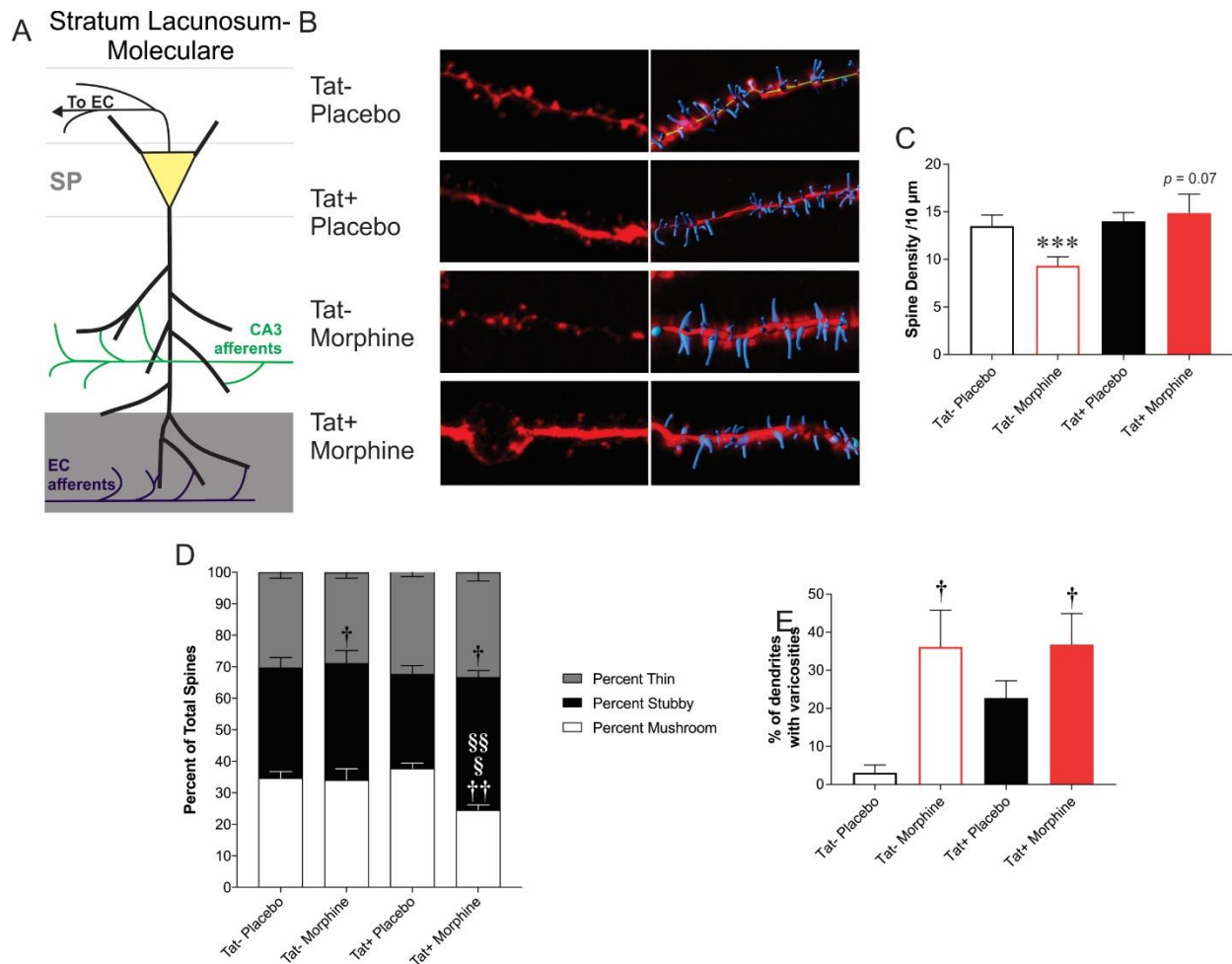
Figure 3. 10: Effects of Tat and morphine on the morphology of the portion of the pyramidal cell dendrite within the stratum radiatum (SR)



Morphological effects of Tat and morphine on the portion of the CA1 pyramidal cell dendrite within the stratum radiatum (SR) (A). (B) Sample SR dendrites from each of the four experimental groups. No differences were observed in spine density in SR dendrites (C). (D) Tat and morphine caused shifts in the spine morphology on SR dendrites. The percentage of thin type spines was increased by Tat ($p = 0.0107$), while the percentage of mushroom-type spines was decreased by morphine ($p = 0.0274$). There were non-interacting effects of Tat ($p = 0.0006$) and morphine ($p = 0.0004$) to increase the amount of varicosity formation along peripheral SR dendrites (E).

Additionally, significant increases in the number of varicosities along the main axis of pyramidal cells were observed in all groups compared to controls ($p = 0.0001-0.0025$; **F**)
̄. Parametric statistics were used except where noted in parenthesis. Multiple symbols are used in this figure for to denote significance; (*) denotes a main effect of Tat, (**†**) denotes a main effect of morphine, (**) denotes a difference between Tat-/placebo and Tat+/placebo (Mann-Whitney U test), (***) represents a difference between Tat-/placebo and Tat-/morphine (Mann-Whitney U test), (**††**) represents significance between Tat-/placebo and Tat+/morphine (Mann-Whitney U test), the difference between Tat+/placebo and Tat-/morphine is shown by (**‡**), Significance between Tat+/placebo and Tat+/morphine is denoted with (**§**), and finally The differences between Tat-/morphine and Tat+/morphine are denoted as (**§§**).

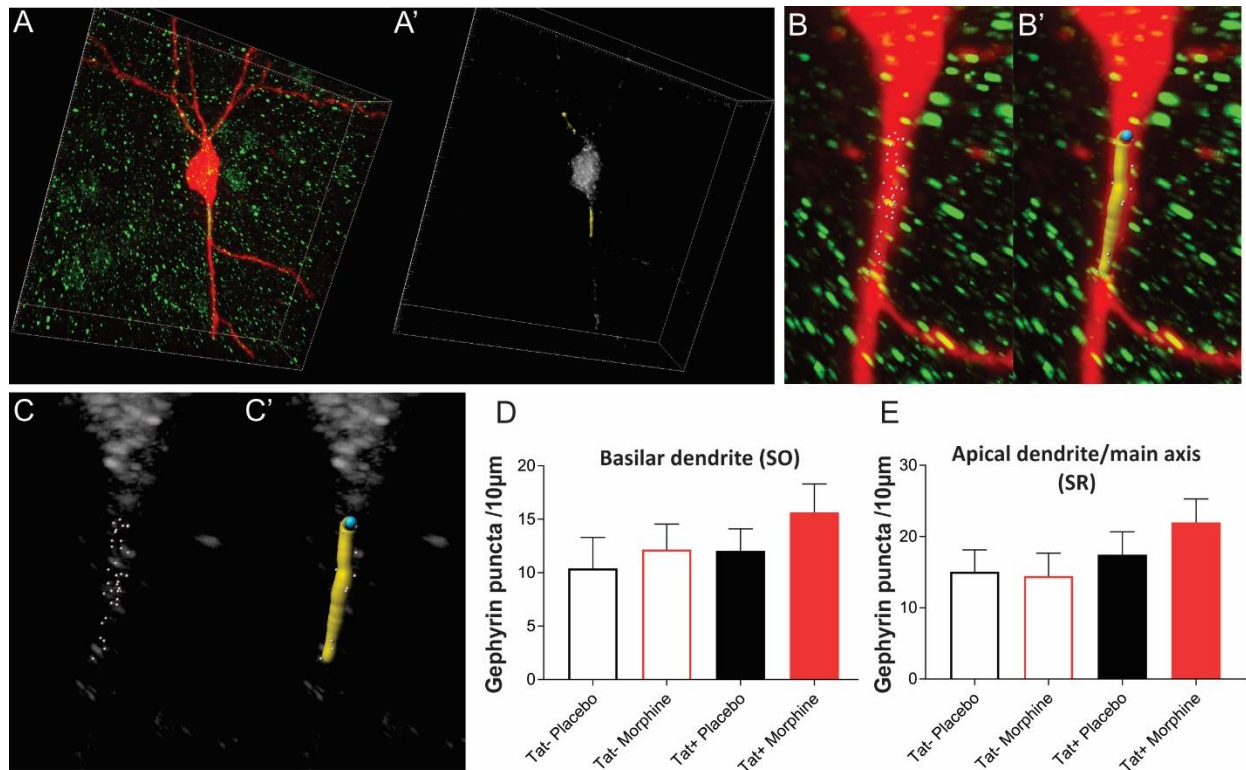
Figure 3. 11: Effects of Tat and morphine on the morphology of the portion of the pyramidal cell dendrite within the stratum lacunosum-moleculare (SL-M)



Morphological effects of Tat and morphine on the portion of CA1 pyramidal cell dendrite within the stratum lacunosum-moleculare (SL-M) (A). (B) Sample SL-M dendrites from each of the four experimental groups. Morphine caused a reduction of dendritic spine density in pyramidal cells from Tat-, but not Tat+, mice. In fact, there was a trend for Tat to reverse morphine-dependent reductions in dendritic spine density, albeit not significant ($p = 0.07$), suggesting that the Tat and morphine may uniquely interact to increase spine numbers on the SL-M (C). Spine morphology was observed to change with Tat and morphine exposure (D). Morphine caused an increase in the

percentage of stubby-type spines ($p = 0.0129$), and Tat+/morphine-treated animals had fewer mushroom-type spines than all other groups ($p = 0.0005-0.0112$). Increases in dendritic damage observed with the percentage of dendrites with varicosities increasing in morphine-treated animals ($p = 0.0019$; **E**). Multiple symbols are used in this figure for a $p < 0.05$; (*) denotes a main effect of Tat, (†) denotes a main effect of morphine, (**) denotes a difference between Tat-/placebo and Tat+/placebo, (***) represents a difference between Tat-/placebo and Tat-/morphine, (††) represents significance between Tat-/placebo and Tat+/morphine, the difference between Tat+/placebo and Tat-/morphine is shown by (‡), Significance between Tat+/placebo and Tat+/morphine is denoted with (§), and finally The differences between Tat-/morphine and Tat+/morphine are denoted as (§§).

Figure 3. 12: Assessment of gephyrin puncta within the aspiny portion of pyramidal cell basilar and apical dendrites



Assessment of gephyrin puncta within the perisomatic dendrites of CA1 pyramidal cells. Biocytin filled pyramidal cells labeled with an Alexa 594-conjugated streptavidin probe (red) and gephyrin puncta (green) were analyzed in Imaris Bitplane 9.0.0. (**A, B, B'**), and a third channel was created which contained only green voxels which overlapped in the space occupied by red voxels (**A', C, C'**). The number of co-localized puncta (**B, C**) was quantified in a region of interest of a defined length (**B', C'**) to generate a value reflecting the number of co-localized puncta per 10 μ M. No changes in the number of gephyrin puncta were observed occurring on the aspiny portions of the basilar (**D**) or apical (**E**) dendrites in the perisomatic region following Tat expression or exposure to morphine.

	Tat- Placebo n = 13	Tat+ Placebo n = 12	Tat- Morphine n = 19	Tat+ Morphine n = 13
Capacitance (pF)	29.42 ± 2.8	32.59 ± 3.65	30.77 ± 2.8	31.44 ± 2.72
Resistance (MΩ)	19.858 ± 2.2	22.86 ± 3.06	23.81 ± 1.96	21.98 ± 2.06

Table 3. 1: Membrane properties of CA1 pyramidal cells after exposure to Tat and morphine

Table 3.1 lists the Capacitance and resistance values for the comparison of Tat- and Tat+ animals treated with placebo against those treated with morphine. No significant changes were observed. All values are shown as mean ± SEM.

	Tat- Placebo n = 13	Tat+ Placebo n = 12	Tat- Withdrawn n = 29	Tat+ Withdrawn n = 22
Capacitance (pF)	29.42 ± 2.8	32.59 ± 3.65	43.13 ± 7.66	35.89 ± 3.5
Resistance (MΩ)	19.86 ± 2.2	22.86 ± 3.06	24.12 ± 1.54	22. ± 1.49

Table 3. 2: Membrane properties of CA1 pyramidal cells from Tat- and Tat+ animals in a withdrawal like state

Table 3.2 lists the Capacitance and resistance values for the comparison of Tat- and Tat+ animals treated with placebo against those treated with morphine and then forced into a withdrawal-like state. No significant changes were observed. All values are shown as mean ± SEM.

Morphological Data	Physiological Data	Correlation	N	Z	p	
SO % Mushroom	Threshold	.348	43	2.298	0.0216	
	Frequency 100 pA	-0.311	43	2.033	0.0421	
	Frequency 125 pA	-0.313	43	2.045	0.0408	
	Frequency 150 pA	-0.331	43	2.174	0.0297	
SR spine density	Rheobase	0.422	45	2.918	0.0035	
	Frequency 50 pA	-0.347	45	2.347	0.0189	
	Frequency 75 pA	-0.433	45	3.001	0.0027	
	Frequency 100 pA	-0.393	45	2.692	0.0071	
	Frequency 125 pA	-0.403	45	2.771	0.0056	
	Frequency 150 pA	-0.393	45	2.691	0.0071	
	Frequency 175 pA	-0.407	45	2.803	0.0051	
	Frequency 200 pA	-0.382	45	2.611	0.0090	
	Frequency 225 pA	-0.371	45	2.521	0.0117	
	Frequency 250 pA	-0.351	45	2.376	0.0175	
	Frequency 275 pA	-0.337	45	2.275	0.0229	
	Frequency 300 pA	-0.319	45	2.142	0.0322	
	SL-M % Mushroom	V _R	.396	38	2.291	0.0219
	SL-M % Thin	Frequency 275 pA	.344	38	2.122	0.0339
Frequency 300 pA		.326	38	2.004	0.0451	
Frequency 350 pA		.352	38	2.176	0.0295	
Frequency 375 pA		.375	38	2.330	0.0189	
Frequency 400 pA		.406	38	2.548	0.0108	

Table 3. 3 Correlations between morphological and electrophysiological findings

Table 3.3 presents a selection of relevant correlations between morphological observations and electrophysiological data. The data presented here include samples from 4 groups: Tat⁻ and Tat⁺ placebo-treated animals, and Tat⁻ and Tat⁺ morphine-treated animals that had been maintained in morphine containing physiological solutions.

Chapter 4: General Discussion and future directions

Clarification of contributions: Dr. Virginia McLane performed the Bioplex assay.

HIV infection and HIV-1 have been demonstrated as having profound effects on the hippocampus. There is also a preponderance of evidence that shows concurrent exposure to opiates exacerbates progression of HIV or HIV protein-related pathology immunologically and neurologically (Hriso et al, 1991; Anthony et al, 2005; Bruce-Keller et al, 2008; Fitting et al, 2010a; Byrd et al, 2011; Hauser et al, 2012; Xu & Fitting, 2016); however, few of these studies have been performed specifically in the hippocampus, and those that do tend to focus on biochemical or morphological effects rather than hippocampal function (Guo et al, 2012; Hauser et al, 2012; McLane et al, 2014). The collected aim of the studies discussed here is to determine the effects of HIV-1 Tat and/or morphine on the circuitry of the hippocampus morphologically, and to assess the disruptions to functional outputs of the hippocampus behaviorally and electrophysiologically in order to understand the etiology, and ultimately inform the development of treatment options, of the spatial memory deficits commonly seen in HIV patients suffering from HAND (Antinori et al, 2007; Stark, 2007; Byrd et al, 2011; Bilgrami & O'Keefe, 2014).

While multiple inputs and outputs play a critical role in hippocampal function, the studies presented herein focus on the CA1 subfield as the final step in the hippocampal tripartite circuit before passing information to other brain regions (Ranson, 1932; Amaral & Lavenex, 2007; Stark, 2007). Particularly, the focus is on the CA1 pyramidal cells and

the circuitry affecting pyramidal cell function is important since this is a major excitatory output of the hippocampus. The pyramidal cells do not act alone, and are supported by a diverse array of network interactions (Acsady et al, 1996b; Ali et al, 1998; Klausberger et al, 2004; Klausberger & Somogyi, 2008; Kelley et al, 2009; Leão et al, 2012; Tyan et al, 2014; Pelkey et al, 2017). Both Tat and chronic morphine exposure impair spatial learning concomitantly where LTP is inhibited (McQuiston, 2008; Fitting et al, 2013; Zhou et al, 2015). Prolonged exposure to Tat and/or morphine have both been shown to impair LTP in CA1 with (Fitting et al, 2013; Heidari et al, 2013; Wen et al, 2014; Zhou et al, 2015) and the acquisition of spatial memory, which is closely associated with LTP (Carey et al, 2012; Kitanaka et al, 2015; Marks et al, 2016; Raybuck et al, 2017). The action of morphine within the CA1 system varies depending upon the context in which morphine is given, reflecting the adaptation of the hippocampus to chronic exposure to morphine (McQuiston & Saggau, 2003; Zhu et al, 2011; Fakira et al, 2014; Portugal et al, 2014; Kitanaka et al, 2015). Reductions in LTP caused by Tat and morphine independently (Fitting et al, 2013; Wen et al, 2014; Zhou et al, 2015) likely result from a shift in the functionality of the interneuron network and the disinhibition of discrete sets of interneurons (Pelkey et al, 2017). Over time, compensatory processes may occur as tolerance develops, or as Tat exposure continues, through alterations in the expression of ion channels, opioid and/or other receptor types, or other signaling events (Hall et al, 1991; Fakira et al, 2014; Portugal et al, 2014; Sadegh & Fathollahi, 2014; Zhou et al, 2015). GABAergic interneurons in the hippocampus are comparatively more susceptible to excitotoxic damage, one of the main hallmarks of HIV associated neurocognitive

damage, than pyramidal cells (Avignone et al, 2005; Chandra et al, 2005; Hoskison et al, 2007), and are often also a target for morphine (Drake & Milner, 2002).

The net effect of morphine in CA1 is to decrease GABA release, resulting in increased pyramidal cell excitability under acute activation paradigms (McQuiston & Saggau, 2003), mediated through primarily GABA_A receptors, but also through GABA_B receptors (McQuiston & Saggau, 2003; McQuiston, 2007). It is important to note that the exposure paradigm can have a significant effect on the outcome of experiments, with acute, chronic, and withdrawal administration pattern effecting the results of experiments (McQuiston & Saggau, 2003). In our experiments, morphine administration via subscapular pellet implantation results in a continuous release of morphine over a 5-day period, which is more than sufficient for development of tolerance in the hippocampus. In hippocampal slice physiology preparations, tolerance has been observed to develop within 2-6 hours of the initiation of morphine exposure (Lue et al, 1999). Tolerance will develop to different aspects of morphine's effects (e.g. analgesic first, locomotor second) at different rates (Vasko & Domino, 1978; Hall et al, 1991; Bodnar, 2012), and the development of tolerance has been shown to proceed at different rates for the different opioid receptors (Angelopoulos et al, 1995). The effects of tolerance in the present studies may be more pronounced, but harder to discern than in wild type mice; however, as Tat⁺ mice induced with doxycycline show increased tolerance to the analgesic and locomotor effects of morphine, while paradoxically exhibiting less pronounced withdrawal symptoms (Fitting et al, 2012; Fitting et al, 2016). This may be related to Tat-induced changes in the expression or activity of MOR and its cognate endogenous ligands (Fitting et al, 2010a; Hahn et al, 2016). The observations

of acute increases in excitability mediated both through loss of GABAergic inhibition and increase of extracellular glutamate levels (Wimpey et al, 1989; Farahmandfar et al, 2011a; Farahmandfar et al, 2011b) give way to a re-established homeostasis. In the pyramidal cells, as evidenced by the lack of difference between the firing rate of morphine-treated cells and placebo-treated cells shown in chapter 3. Subsequent removal of morphine likely releases the MOR expressing interneurons to re-inhibit the disinhibited pyramidal cells, which have become acclimated to a new homeostasis with lower inhibition. As a result, their excitability becomes reduced (Fig 3.3B). A similar effect has been observed in the reduction of LTP in animals following withdrawal of chronic morphine application during which tolerance is likely to have developed, which can be restored with reperfusion of the drug (Bao et al, 2007).

The distribution of MOR expression in CA1 is mainly in the pyramidal layer. MOR expression is also observed on SO and SR, while the lowest levels are in the SL-M (Drake & Milner, 2002; McQuiston, 2008). MOR expression can be further localized to GABAergic interneurons (McQuiston, 2007), with differential expression and therefore morphine effects on different CA1 interneuron subsets. Morphine exposure increases excitatory post synaptic potentials (EPSPs) strongly in CA1 SO, SP, and SR; but weakly in SL-M, indicating the effects of MOR activation on local excitatory/inhibitory balance differs among hippocampal layers depending on differences in presynaptic inputs from MOR-expressing interneurons or from MOR-expressing afferents from other brain regions (McQuiston, 2008; Sadegh & Fathollahi, 2014). The laminar effects depend on the projections of varying interneuron subsets to other layers (McQuiston, 2007), where changes in GABA release act to increase excitation through diminished action at both

the GABA_A and GABA_B receptors (McQuiston & Saggau, 2003; McQuiston, 2007). A substantial portion of CA1 network interactions come from inhibitory interneurons, of which there is an ever-expanding classification of subtypes (Cenquizca & Swanson, 2006; Klausberger & Somogyi, 2008; Wheeler et al, 2015; Hamilton et al, 2017b). I have found Tat exposure disrupts the hippocampal interneuron network which we believe is in part responsible for the behavioral and physiological deficits observed in our data and in previous publications (Fitting et al, 2013; Marks et al, 2016). Considering that morphine acts in part through the disinhibition of GABAergic inputs (Liao et al, 2005), and that Tat damages the interneuron network, it is reasonable to conclude that combining morphine with Tat will more strongly disrupt the normal functioning of the hippocampus, making the present findings more surprising.

Of the 21+ types of interneurons found within the hippocampal area CA1 (Cenquizca & Swanson, 2006; Klausberger & Somogyi, 2008; Wheeler et al, 2015), we have found selective vulnerability in two discrete subtypes and vulnerability within two other interneuron families that we have not yet fully defined. Induction of Tat expression in our mouse model resulted in losses of nNOS⁺/NPY⁻ interneurons in the stratum pyramidale (IS3s) and in the SR (neurogliaform cells) (Acsady et al, 1996a; Acsady et al, 1996b; Chamberland et al, 2010; Tricoire et al, 2010; Armstrong et al, 2012; Tricoire & Vitalis, 2012; Tyan et al, 2014; Marks et al, 2016). We also observed reductions in the total population of PV⁺ interneurons within the pyramidal layer, and SST⁺ interneurons within the SO. While our data did not show conclusively which subsets are affected, they suggest that the major contributor to these losses are the bistratified cells and OL-Ms, respectively (Buhl et al, 1996; Muller & Remy, 2014). The initial definition of Tat

effects in the hippocampus can now be used alongside what we know about the endogenous opioid system in the hippocampus to help inform our understanding of their potential interactions. MOR, DOR, and KOR are expressed with some, but not complete, overlap in subsets of GABAergic interneurons (Drake & Milner, 1999; Halasy et al, 2000; Pelkey et al, 2017), and are usually found presynaptically, with lower levels expressed postsynaptically on dendrites (Lambert et al, 1991; Drake & Milner, 1999; Pelkey et al, 2017). Pyramidal cells also express low levels of DOR (Stumm et al, 2004). While the hippocampus as a whole responds to morphine, there is differential sensitivity, with CA3 being more affected at low doses of morphine, and CA1 effects emerging with higher receptor occupancy (Jones et al, 1994). MOR immunoreactivity is found in PV+ and SST+ cells, including the OL-M cells and IS3s (Acsady et al, 1996a; Acsady et al, 1996b; Drake & Milner, 2002; Stumm et al, 2004), as well as Ivy cells and neurogliaform cells (Lafourcade & Alger, 2008; McQuiston, 2008; Krook-Magnuson et al, 2011). DOR expression occurs primarily in NPY+ and SST+ projections to the pyramidal layer, generally on cells originating in SO (Commons & Milner, 1996; Stumm et al, 2004). With KOR tending to overlap with DOR expression (Svoboda et al, 1999). The connectivity between interneurons and the localization of the opioid receptors on processes is critical to the way they modulate CA1 synaptic events. MOR and DOR/KOR systems appear to fill separate but complimentary roles, with MOR activity modulating feed-forward inhibition, and DOR/KOR modulating feedback inhibition (Pelkey et al, 2017). DOR activity appears to hyperpolarize both bistratified cells and OLMs, which can unbalance the normal gating of inputs to favor activation of pyramidal cells by the EC (Svoboda et al, 1999). MOR activity, by contrast, tends to regulate the

activity of terminals synapsing onto pyramidal cells rather than hyperpolarizing interneurons and reducing firing in that way, although this process still occurs in Ivy cells (Glickfeld et al, 2008; Krook-Magnuson et al, 2011).

IS3s and OL-Ms play a strong role in spatial memory, which is affected in HAND (Antinori et al, 2007). Tat has been shown to worsen spatial learning and memory in the Morris water maze and Barnes maze tasks, and to limit memory in contextual fear-conditioning and novel object recognition tasks, as has Gp120 (Sanchez-Alavez et al, 2000; Carey et al, 2012; Fitting et al, 2013; Kesby et al, 2016; Marks et al, 2016). The diversity of interneurons and their interconnections underlie the processing power of the hippocampus, which is revealed in the complexity of integrated interneuronal input into CA1 pyramidal neurons (Buhl et al, 1994; Acsady et al, 1996a; Acsady et al, 1996b; Sik et al, 1997; Ali et al, 1998; Drake & Milner, 2002; Klausberger et al, 2004; Cenquizca & Swanson, 2006; Klausberger & Somogyi, 2008; Tricoire et al, 2010; Leão et al, 2012; Tricoire & Vitalis, 2012; Lovett-Barron et al, 2014; Muller & Remy, 2014; Sun et al, 2014; Marks et al, 2016). It is the modulation of the complex interneuron-pyramidal cell interface that appears to be specifically affected by Tat, resulting in the observed behavioral deficits (Drake & Milner, 2002; Cenquizca & Swanson, 2006; Klausberger & Somogyi, 2008; Fitting et al, 2013; Lovett-Barron et al, 2014; Tyan et al, 2014; Marks et al, 2016). For example, the vulnerable interneuron subsets we identified reportedly play a strong role in mnemonic and spatial memory processes (Sik et al, 1997; Cenquizca & Swanson, 2006; Leão et al, 2012; Lovett-Barron et al, 2014) and form a unique microcircuit (Tricoire & Vitalis, 2012; Muller & Remy, 2014; Tyan et al, 2014; Marks et al, 2016) within the larger CA1 subfield. We believe this microcircuit is critical in the

etiology of HIV-related mnemonic disorders (Buhl et al, 1994; Acsady et al, 1996a; Acsady et al, 1996b; Sik et al, 1997; Ali et al, 1998; Drake & Milner, 2002; Klausberger et al, 2004; Cenquizca & Swanson, 2006; Klausberger & Somogyi, 2008; Tricoire et al, 2010; Carey et al, 2012; Leão et al, 2012; Tricoire & Vitalis, 2012; Lovett-Barron et al, 2014; Muller & Remy, 2014; Sun et al, 2014; Kesby et al, 2016; Marks et al, 2016). The IS3s play a crucial role in setting the rhythm and tone in a key inhibitory circuit that regulates output from CA1 pyramidal cells, acting as a feedback control mechanism through control of other interneurons (Chamberland & Topolnik, 2012; Tyan et al, 2014). This feedback occurs by regulating the disinhibition of OL-M cells, which inhibit pyramidal cells and have significant cross interaction with bistratified cells (Chamberland et al, 2010; Chamberland & Topolnik, 2012; Tyan et al, 2014). The optogenetic activation of IS3s decreases OL-M cell firing and stimulating IS3s can produce activity in OL-Ms mimicking theta oscillations (Tyan et al, 2014). OL-Ms will have significant crosstalk with bistratified cells, which can also be inhibited by IS3s (Leão et al, 2012; Muller & Remy, 2014). This interaction defines a gating mechanism, in which dendrites receiving inputs from CA3 (in the SR) or entorhinal cortex (in the SL-M) will be preferentially inhibited, while negating the effects of opposing inputs (Leão et al, 2012; Lovett-Barron et al, 2014; Muller & Remy, 2014).

Tat and opiate-induced functional imbalances in the interneuron network profoundly affect the output of pyramidal cells independently, but the question remains to what extent they will interact. The data seems to support the notion that despite Tat and morphine having the tendency to alter hippocampal function, the interactions between them from a functional perspective are limited (Figs 3.4-3.8). That does not

necessarily mean, however, that they do not interact at a deeper level which might mask a simple identification of the effect. Tat has previously been shown to lower the expression of the mu opiate receptor in the hippocampus, while not effecting the expression of DOR or KOR (Fitting et al, 2010a), and MOR signaling activity in the striatum and amygdala also appear to be altered by Tat (Hahn et al, 2016). This shift in the balance of receptors/receptor activation could underlie a genuine interaction between Tat and morphine that would not manifest as an explicit worsening of function. It has been demonstrated that mild neuroprotective effects of morphine and other MOR antagonists can occur at low doses, or rather, with low level activation of MOR, likely due to the relative levels of MOR, DOR, and KOR activation (Zhao et al, 2006; Ammon-Treiber et al, 2007; Fitting et al, 2010a; Kawalec et al, 2011). At the same time, it is known that the activation of DOR and KOR can have different effects on cellular processes and that the effects mediated by DOR and KOR often run counter to the effects of MOR (Loacker et al, 2007; Saboory et al, 2007; Lutz & Kieffer, 2013). Additionally, MOR and DOR/KOR systems appear to operate in separate but complimentary systems in the hippocampal GABAergic network (Valentino et al, 1982; Plager & Vogt, 1988; Drake & Milner, 2002; Loacker et al, 2007; McQuiston, 2008; Krook-Magnuson et al, 2011; Williams & Milner, 2011; Pelkey et al, 2017), and most importantly, many MOR agonists can also act at DOR and KOR with lower efficacy, but a non-zero effect (Beckman, 2014). It is a possibility that the reduced levels of MOR expression caused by Tat, coupled with the moderate neuroprotective effects achievable by activating the right combinations of opioid receptors, begins to explain why independent Tat and morphine/morphine withdrawal effects are evident, but

interactive effects are not. It might be that a genuine interaction is occurring, but the effect is actually neuroprotective, and could explain why it appears that morphine treatment ameliorates or obviates the observed effects of Tat in Barnes maze performance and resting membrane potential. This question could be tested by administering MOR, DOR, and KOR antagonists to mice, and repeating the physiological studies performed in the presence of these same antagonists. Ideally, a dose response curve could be generated for each of these antagonist categories for physiological functionality and Tat interactions, with the degree of antagonism of DOR and KOR systems likely to reveal interactive functional pathology due to Tat and morphine interactions.

Despite all of these observations in support of alterations in the GABAergic interneuron network by both HIV-1 Tat and by morphine, it is not possible to attribute this to an actual loss of inhibitory innervation. Previous studies of the effects of Tat in the hippocampus showed that the amount of Syt2, the presynaptic organizer of GABAergic synapses was decreased in CA1. The Syt2 loss was specifically in the SR, while the overall amount of gephyrin in CA1 was increased (Fitting et al, 2013). Our data shows that the density of gephyrin puncta within the regions of the pyramidal cell with typically high levels of inhibitory contacts do not change with Tat or morphine treatments (Fig 3.12). Nevertheless, this observation does not necessarily contradict the previous finding. One potential explanation is that the increase in gephyrin, believed to be compensatory for the loss of Syt2 expression, was sufficient to maintain inhibitory presynaptic contacts on the aspiny portions of pyramidal cell dendrites. Another potential explanation would be that the increase in gephyrin and loss of Syt2 is limited to

specific types of inhibitory presynaptic contacts, either local (ISI type 1, 2, or 3) interneurons or from extrahippocampal regions (septohippocampal projections). In either case, it would not necessarily be the lack of synaptic contacts onto pyramidal cells, but alterations in the network activity, that would be responsible for the observed physiological effects.

Beyond questions about the contribution of damage to the inhibitory interneuronal network to the disturbances in functional output, mention also must be made about the observed structural and functional changes to the excitatory systems within CA1. In the present studies, there were differential effects of Tat and morphine on the spine density and spine types present across the dendrites occupying SO, SR, and SL-M. Moreover, interactions between Tat and morphine were evident in SO and SL-M, where decreases as well as increases in different spine types were observed. Increases in spine density or a particular spine type can be just as disruptive to the overall balance of a complex circuit as a reduction. The excitatory presynaptic inputs onto pyramidal cell dendrites differ within each layer and region of the hippocampus. The degree to which spine density or spine type changes may reflect some alteration in the excitatory input being given or received by these areas. The largest contributors to excitatory input in CA1 pyramidal cells are the Shaffer collateral inputs onto SR and the temporoammonic inputs from entorhinal cortex that form presynaptic contacts throughout SL-M (Amaral & Lavenex, 2007; Agster & Burwell, 2013). Both the Shaffer collaterals and temporoammonic pathway possess collateral fibers that split from the main fiber tract and synapse onto the dendrites in SO, where their excitatory activity is directly modulated by cholinergic inputs from the septal nuclei (Seress et al, 2002; Buño et al,

2006; Zheng et al, 2011). In addition to cholinergic inputs from the septal nuclei, afferents from the diagonal band of Broca also modulate the activity of Interneurons in SO (Gulyás et al, 1991; Amaral & Lavenex, 2007; McQuiston, 2014; Bell et al, 2015). Although there is some evidence of direct excitation by septohippocampal inputs, the observation may simply be a reflection of the net disinhibition driven by GABAergic action of the septohippocampal inputs, resulting in increased pyramidal cell activity (Oka & Yoshida, 1985; Toth et al, 1993). Interestingly, some of the excitatory inputs from EC to SO appear to come from nNOS positive pyramidal cells (Seress et al, 2002), along with observations of the contributions of NO to excitotoxicity and morphine tolerance, might be a good target for further study (Lue et al, 1999; Eugenin et al, 2007; King et al, 2010; Sanchez-Blazquez et al, 2010; Garzon et al, 2011; Marks et al, 2016). In addition to the intrahippocampal excitatory inputs, there are several extrahippocampal regions which send excitatory inputs onto CA1 pyramidal cells. Afferents from the basomedial nuclei of the amygdala synapse onto dendrites throughout CA1 along the temporal hippocampus, and receive some input from CA1 (Pikkarainen et al, 1999; Amaral & Lavenex, 2007; Kim & Cho, 2017). More specifically, SL-M receives inputs from the accessory basal nucleus, while both SO and SR receive inputs from the caudomedial region of the parvicellular division (Pikkarainen et al, 1999). The Perirhinal cortex synapses onto the dendrites in SL-M, and receives inputs from CA1 resulting in synchronous activation under certain oscillation patterns (Supcun et al, 2012; Agster & Burwell, 2013; Vinck et al, 2015). The perirhinal cortex also interacts directly with the amygdala (Supcun et al, 2012). Finally, excitatory inputs from the nucleus reuniens (NR) synapse onto dendrites within SL-M, as well as SL-M interneurons (Dolleman-Van

der Weel et al, 1997; Amaral & Lavenex, 2007). The NR is part of a circuit involved in spatial memory consolidation in which (1) pyramidal cells in CA1 project to the PFC, (2) pyramidal neurons in the PFC project to the NR, and (3) the NR then projects back to CA1 (Cassel et al, 2013; Griffin, 2015).

Alterations to any of these inputs to CA1 could profoundly change the net effect of hippocampal processing (Lee & Park, 2013; Newmark et al, 2013; Wu et al, 2014a; Benetti et al, 2015), and are likely to be directly affected by Tat and/or morphine (Table 1.1 lists the large number of brain regions affected by Tat and morphine). However, even in the absence of direct neuropathology causing decreased excitatory input, the inputs to CA1 from each of these regions are likely disrupted by local disturbances in synaptodendritic structure and function depending on the combination of Tat and morphine. A general observation can be made that morphine is known to modulate spine shape. The endogenous opioid system plays a role in maintaining the integrity of dendritic spines; however, the application of morphine can overwhelm the normal function of the endogenous system, and result in a loss of spine stability (Liao et al, 2005). More specific observations can be made, however, when considering the complexity of local microcircuits and inter-regional connections. First, it is notable that across all three regions, the least amount of change was seen in SR, where there was no observation of a shift in spine density following exposure to Tat or morphine, and comparatively fewer shifts in the type of spines present. The fact that the spines in SR remain comparatively stable despite the Tat and opiate insults is intriguing. There are some shifts in the types of spines seen in the region; yet, there is no evidence of interactive effects of Tat and morphine. A main effect of Tat to increase thin/filopodia

type spines, and a main effect of morphine to decrease mushroom-type spines are both observed in SR. The Tat-induced increases in the proportion of thin/filopodia type spines is unexpected, as LTP is known to be reduced in Tat+ animals (Li et al, 2004; Fitting et al, 2013). Nonetheless, increases the filopodia are though represent newly formed connections and coincide with learning and plasticity (Rocheffort & Konnerth, 2012; Bailey et al, 2015). In the SL-M, there is an interesting occurrence where a statistically significant Tat effect upon further examination appears to be more due to differential effects of morphine to reduce spine density on pyramidal cells in Tat-, but not Tat+, mice (Fig 3.11C). This is of particular interest considering that the amygdala is known to send projections onto this layer, and that Tat has been seen to differentially modulate MOR activity in the amygdala, with Tat decreasing MOR signaling (Pikkarainen et al, 1999; Hahn et al, 2016). In this case, it makes sense that if Tat reduces MOR signaling, morphine itself will have less inhibitory activity on outputs from the amygdala to SL-M in Tat+ than Tat- animals, coinciding well with the observations of spine density in SL-M. While the amygdalar component is of note, it is also important to recall the existence of inputs from EC onto SL-M dendrites, and that the amygdala and perirhinal cortex have been shown to interact with each other and contribute to spatial memory processing with the perirhinal cortex and EC projections overlapping in the SL-M (Supcun et al, 2012; Agster & Burwell, 2013; Lee & Park, 2013). Beyond changes in the density of spines in SL-M, morphine treatment was observed to reduce the amount of thin spines in the layer, suggesting a shift away from stable connections toward formation of new synapses, a notion supported by the fact that Tat and morphine interacted to reduce the amount of mushroom spines in SL-M (Fig 3.11D) (Rocheffort &

Konnerth, 2012; Bailey et al, 2015). In the SO, there was another differing pattern of spine morphology perturbation, with morphine reducing spine density regardless of Tat, and shifts in the amount of mushroom and stubby spines, but not thin spines. Like the SL-M, the SO also receives amygdalar inputs; however, the specific nuclei that project to these regions are different. More likely to be a contributing factor to SO morphology would be the modulation of septohippocampal inputs and their effects on the glutamatergic inputs from EC and CA3 (Seress et al, 2002; Amaral & Lavenex, 2007). Morphine has been shown to reduce the spontaneous firing of GABAergic neurons in the septum and diagonal band, which would then have an effect on the modulation of activity in the hippocampus and spatial memory formation (Alreja et al, 2000). This may explain in part the morphine-induced reductions in spine density. The change in morphologic types of dendritic spines is more difficult to draw conclusions from, as the shifts were between mushroom- and stubby- shaped spine types; both associated with stable synapses (Rochefort & Konnerth, 2012; Bailey et al, 2015). Variations in spine neck diameter may still have effects on the amount of calcium able to flow through the spine, allowing for subtle changes in input processing to occur with changes in the representation of stable spine types (Noguchi et al, 2005). Overall, while interesting to consider, the complexity of these local and regional networks makes pinpointing the exact cause of the changes in spinous morphology impossible given the current dataset, with further conclusions necessitating a more focused circuit based approach with a focus on extrahippocampal afferent projections.

Increased dendritic damage was seen across all three major dendritic compartments in response to Tat expression and to morphine, with SO and SL-M being

more affected than SR, mirroring the ways in which these regions changed or did not change spine density and spine types. The observation of damage (Figs 3.9B,E, 3.10B,E-F, 3.11 B,E) stands in contrast to the notable lack of damage observed in pyramidal cells by Fitting et al (2013). It is possible that differences in the technique used to process the images made damage appear more evident in the present study. Alternatively, it is possible that the cellular trauma induced by the act of patching onto the cells themselves caused a strong enough perturbation to make damage appear in neurons that were already unhealthy or disrupted as a result of exposure to Tat and morphine, whereas the healthy control neurons were not damaged by the patching process.

Future directions

In light of the discovery of selectively vulnerable interneuron populations within the CA1, further studies on the physiological effects on these cells might be appropriate (Marks et al, 2016). When it is considered that previous studies in the hippocampus showed no increase in the number of apoptotic cells within the CA1 subfield following Tat exposure (Fitting et al, 2013), and that chromatolytic damage observed in the hippocampus with HIV infection is not necessarily lethal, and can in fact be reversible (Kim et al, 2008; Torres & Noel, 2014), it is reasonable to conclude that the missing interneurons observed in these studies may not be dead, but merely damaged; performing at sub optimal levels, and expressing various markers below the biochemical detection threshold of fluorescent immunohistochemical techniques. If this is the case, pharmacological rescue of these cells may be possible, in addition to more focused studies on their pathology. In the studies presented here, however, some interneurons

of the identified vulnerable subgroups remain in the tissue, which also begs the questions of why they are not affected as much as other cells of the same class, and what role the subtle variations in populations play in their resilience. Since the publication of the interneuron studies presented here, a broader understanding of the hippocampal interneuron complement was unveiled in the hippocampome project (Wheeler et al, 2015; Rees et al, 2016). The hippocampome is a compendium of cell types within the hippocampus based on gene expression patterns, with estimates of cell type categories which go far beyond the previously touted 21+ types of interneurons within the CA1. Recent improvements and additions to the hippocampome project have been aimed at clarifying disparate naming conventions of interneuron populations, identifying more subtypes of hippocampal principal cells, and exploring the network connectivity of the hippocampus (Rees et al, 2016; Hamilton et al, 2017a; Hamilton et al, 2017b; Rees et al, 2017). The idea that there are subtypes within existing interneuron groups is not new. Variations within the expression of proteins and of localization within the CA1 subfield have been noted within the bistratified cells, O-LMs, and neurogliaform cells (Tricoire et al, 2010; Chittajallu et al, 2013; Muller & Remy, 2014; Pelkey et al, 2017), and in fact, many of the classifications that existed prior to the hippocampome project were based on one or two subtle differences, as in the case of IS3s (Acsady et al, 1996a; Acsady et al, 1996b; Tricoire et al, 2010). It is not unreasonable to expect that functional differences which were previously undetected, less defined, or unexplored within the cell types identified as being vulnerable to Tat may play a causal role in that phenomenon. Our observation of putative losses of O-LM cells and bistratified cells might be better explained with this in mind. O-LMs have been

demonstrated to have 2 distinct subtypes, with one expressing 5HT3RA, and the other lacking. In addition, these subsets of O-LMs may either express parvalbumin at low levels, or not at all (Chittajallu et al, 2013). While the earlier discussed results did demonstrate a loss of somatostatin positive cells in the SO, and while there was no significant reduction in cells that co-express somatostatin and parvalbumin in this region, there was a trend toward significance was observed when the population of somatostatin positive cells that lacked parvalbumin expression were examined. This suggests that the total loss of somatostatin positive interneurons, while containing individual neurons from both subpopulations, is mostly comprised of parvalbumin negative O-LMs. A similar observation can be made regarding the loss of parvalbumin positive interneurons in the pyramidal layer which I have suggested are putative bistratified cells. The broad class of bistratified cells may or may not express somatostatin, and can even have some subtle variations in their relative depth within the CA1 subfield, and so may encompass several similar neuron varieties (Chittajallu et al, 2013; Marks et al, 2016; Pelkey et al, 2017).

A project to assess the firing properties of IS3 cells in the CA1 was begun, but terminated for technical reasons. Tat mice were bred with a live of tdTomato VIP reporter mice to enable targeted patch clamping of VIP positive cells, with the intention of identifying VIP+ IS3 cells within the pyramidal layer for physiological and morphological analysis. Several cells were successfully patched and subsequently identified as putative IS3s by confirming morphological and basic physiological properties (Tyan et al, 2014). This project had to be terminated due to a problem with the TdTomato construct association with the VIP promoter, which caused TdTomato to

be expressed constitutively in the mice (Fig 4.1), rendering it impossible to identify any one cell under excitation. Necropsy revealed that the only materials/tissues that did not glow under excitation were the fur, bones, and blood. This project is a logical next step in continuing the exploration of the effects of Tat and morphine on the functionality of the CA1, and is in fact commonly asked for by individuals who learn of the study on the effects of Tat on the interneuron network. A few additional components that should be added to the study for comprehensiveness include the expansion of the scope to include multiple subtypes of interneurons beyond the IS3s, and the inclusion of MOR, DOR, and KOR agonists/antagonists to determine the role of opioids in the functionality of these interneurons following Tat exposure. Additionally, a paired recording system in which recordings are made from pyramidal cells and identified interneurons simultaneously under these conditions would further clarify the interactions between Tat and the presence of opioids in the CA1 system.

Further mechanistic studies of the physiology of the pyramidal cells themselves would be beneficial in which pyramidal cells are systematically isolated from the surrounding circuits by sequential application of specific antagonists. This study was attempted with inhibition of AMPA and NMDA with AP5 and CNQX respectively, CGP55845 was added to the AP5 and CNQX containing solutions to inhibit GABA_B receptors, and finally Bicuculline was added to the other antagonists to inhibit GABA_A receptors, with a final goal of isolating the pyramidal cells from glutamatergic and GABAergic neurotransmission. While this study was attempted, technical errors resulted in the failure of the experiment. Moving forward, some alterations to the design would be useful in clarifying the outcomes further. First, in the original experiment, application

of the GABA_B antagonist CGP 55845 always occurred before application of bicuculline to antagonize GABA_A. It would be better to alternate which GABA antagonist is applied first in case there is any additive effect of GABA receptor types. This would be important moving forward, and both GABA_A and GABA_B receptors are involved in the functionality of CA1 regional circuitry (McQuiston, 2007; Pelkey et al, 2017). Additionally, this study would benefit greatly from the acquisition of mini EPSPs/IPSPs and paired pulse facilitation experiments in conjunction with the isolation of pyramidal cells from the surrounding circuitry and various morphine exposure/withdrawal paradigms. In order to better investigate the link between circuit function and behavior, it would also be useful to observe the effects of Tat and morphine/morphine withdrawal on LTP in the hippocampus (Bao et al, 2007; Fitting et al, 2013; Portugal et al, 2014).

Behaviorally, additional studies into the effects of Tat and morphine on spatial memory acquisition would be worth pursuing. In the present studies (Figs 3.1, 3.2), Morphine administration is achieved by the implantation of an indwelling pellet resulting in continuous morphine release over several days. This presents a few confounding factors, including the potential for peripheral inflammation resulting from the pelleting surgery itself affecting behavioral outputs, even with proper post-surgical care (Chen et al, 2008; Vizcaychipi et al, 2014). Additionally, continuous morphine application does not adequately mirror the usage pattern of opioid abusers, who will go through a series of highs and lows in their pursuit and use of opioid drugs (Eitan et al, 2017). The results of this experiment may be easier to interpret, and more translational if a paradigm of repeated morphine injections were used rather than the implantation of a morphine pellet. While this is not without its own problems, including confounds from the

repetitious injections and the increased amount of handling that would be necessary, contrasting these data with the continuous administration might yield valuable insight. It may also be useful to isolate MOR, DOR, and KOR effects by including their respective antagonists through the duration of treatment to see if the effects of the differential contribution hypothesis I have laid out here are indeed observable in behavioral outcomes (Ammon-Treiber et al, 2007; Fitting et al, 2014; Fitting et al, 2015b; Hahn et al, 2016).

A pilot study was performed to examine the degree of hippocampal inflammation associated with HIV-1 Tat and morphine. The effects of Tat and morphine on cytokine levels were examined in hippocampi isolated from randomly selected mice following behavioral analysis discussed in chapter 3, with 3 to 4 animals in each of four groups (Table 4.1) utilizing the Bioplex cytokine assay (Bioplex, Catalog #M60009RDPD). A main effect of Tat was observed for levels of GM-CSF [$F(1,9) = 6.525, p < 0.05$], with Tat+ mice having lower levels of this cytokine than Tat- mice. Similarly, there was a trend for Tat+ animals to display reduced levels of CCL2 than Tat- animals [Main effect; $F(1,10) = 4.718, p = 0.055$]. Of the 23 cytokines assayed, no other cytokines were significantly affected by Tat and/or morphine. G-CSF, was unable to be analyzed due several samples being excluded for errors in data acquisition (table 4.2). The observation that Tat+ animals had a decreased expression of GM-CSF was surprising, as the expression of this cytokine tends to increase with inflammatory insult rather than decrease (Choi et al, 2014). GM-CSF is usually considered a pro-inflammatory cytokine because it acts as a growth factor for macrophages, it is involved in the differentiation of immune cells, and its levels increase with inflammation (Bhattacharya et al, 2015). The

reasons why GM-CSF is not elevated in the hippocampus of Tat+ mice is uncertain, although it may be due to timing or perhaps result from the development of innate immune tolerance in response to unrelenting Tat exposure (Gonek et al, 2017). Alternatively, some elevation in baseline levels of cytokines might occur in our control mice during surgical implantation of the placebo pellets. It has previously been shown that peripheral inflammation can trigger the inflammation in the CNS (DiSabato et al, 2016) .

A study in progress is further examining the interactive effects of HIV-1 Tat and the effects of morphine withdrawal on cytokine levels. Tat transgenic animals are being exposed to doxycycline for 5 days, prior to receiving either a placebo or 25-mg morphine pellet implant, which remains in place concurrently with doxycycline administration for an additional 5 days. On the last day, animals are given a subcutaneous injection of either saline, or 10 mg/kg naloxone 1 hour before harvesting the tissue to induce precipitated withdrawal in morphine-treated mice, yielding a balanced study design with 8 groups; placebo/saline, morphine/saline, placebo/naloxone, and morphine/naloxone in both Tat- and + mice. It is difficult to predict the outcome of this study due to several potentially opposing observations in our mouse model. HIV-1 Tat may directly affect the function of the endogenous opioid system. Notably, in the hippocampus, MOR transcript levels are reduced, but not DOR and KOR (Fitting et al, 2010a), which may result in alterations in morphine responsiveness in the region (Fitting et al, 2010a; Razavi et al, 2014). Tat+ mice have been shown to develop greater tolerance to morphine, and less severe withdrawal behaviors. These effects coincide with the temporal expression of Tat (Fitting et al, 2012; Fitting et al, 2016). While the withdrawal behaviors in Tat+ mice may be

diminished, the severity of functional effects within specific brain tissues are likely to be more heterogeneous (Fitting et al, 2010a; Fitting et al, 2010b; Gelman et al, 2012; Nath, 2015). MOR expression is observed in astrocytes, and there are astrocyte specific splice variants (Dever et al, 2012), and similar to the broader CNS expression of MOR, HIV can cause a shift in the expression levels of different splice variants, likely causing alterations in the normal balance of functions modulated by those receptors by the endogenous opioid system (Fitting et al, 2010a; Dever et al, 2012). Fitting et al (2010b) showed that HIV Tat increased in the production of cytokines and chemokines in culture from multiple regions of the brain, while neither gp120 or morphine affected cytokine release; however, the hippocampus was not included in that study. Interestingly, there was no interaction between Tat and morphine on the production of cytokines and chemokines. Alternatively, the pilot data shows that most cytokines did not change when assayed from the entire hippocampus from Tat+ mice, nor was there any observed effect of morphine. The only cytokine that did change (GM-CSF) was decreased. Although there is no extant hippocampal screen to compare this data against, the near global effect of Tat on cultured astrocytes from varying CNS regions makes this possibility very unlikely (Fitting et al, 2010b). This could indicate that the sample size in the pilot data was not sufficient, but more likely suggest that the pattern of cytokines released from an intact, adult hippocampal system treated over time with Tat and morphine differs from pattern of cytokines seen in an artificial in vitro system in which neonatal astrocytes are cultured in isolation and treated acutely with Tat and morphine (Fitting et al, 2010b). Since the mice used for the withdrawal component of this project had been exposed to morphine for several days, it is not expected that any

morphine effect will be seen in light of the pilot data as the 5 day exposure period is long enough for tolerance to develop. Nevertheless, there is a chance that the inflammatory cytokine response to spontaneous withdrawal, which is less abrupt than precipitated withdrawal caused by giving an opioid receptor antagonist such as naloxone, may qualitatively differ from the cytokine response after 5 days of chronic morphine exposure.

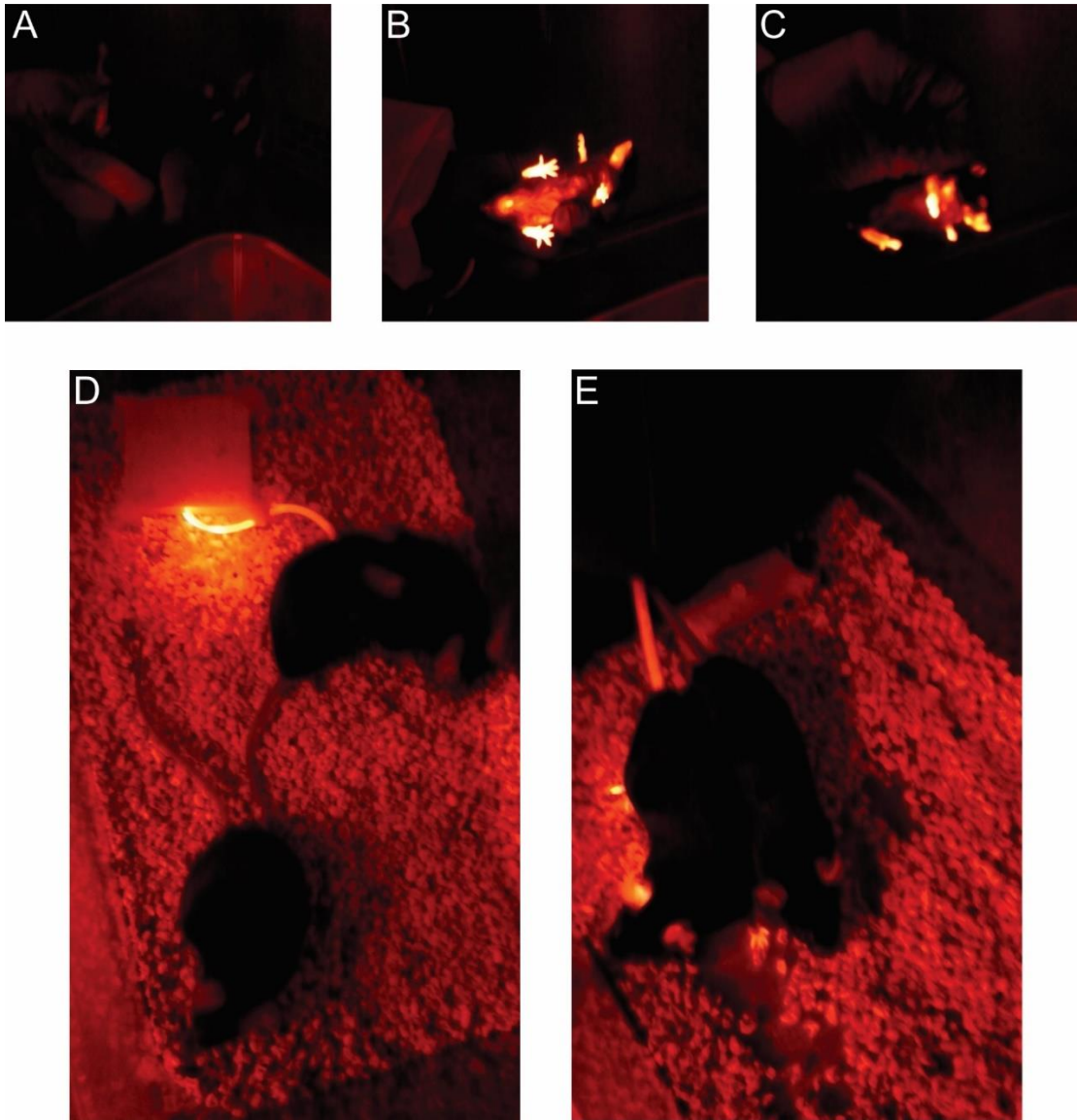
An added layer of complexity to all the above-mentioned future directions would come with adjustments to the timing of experiments and treatment periods. The studies presented and proposed in this document all have a relatively acute Tat exposure paradigm, with experiments occurring after 10-12 days of DOX administration, and any morphine exposure happening within the last 5 days of that 10-12 day window. With the consideration of the temporal component of neuroinflammatory processes (Schwartz & Baruch, 2014), and the effects of HIV in aging populations (Ances et al, 2012), Many more questions relevant to discrete populations of both HIV+ individuals and opioid users can be addressed, and questions regarding the timing of the development of observable behavioral effects vs underlying circuit pathology can be addressed in greater detail (Norman et al, 2007; Vander Jagt et al, 2008; Schier et al, 2017).

Concluding remarks

The effects of HIV infection and more specifically the Tat protein in the hippocampus are less well studied than other regions of the CNS like the striatum or the cortex, and relatively few studies have focused on the effects of HIV infection on the neural circuitry and resultant functional activity of the hippocampus or any other region of the brain. The studies performed here are among the first observations of the effects

of HIV infection on the physiological activity of the hippocampus, and the first studies of their kind exploring interactions of Tat and morphine on the physiological outputs of the hippocampus. The results of these studies have revealed selective vulnerability of interneuron subsets to HIV-1 Tat, shown electrophysiological deficits related to HIV-1 Tat, and perhaps most importantly, suggest that HIV-1 Tat and morphine do not synergistically interact to worsen pathology in the hippocampus despite the prevailing wisdom that morphine exposure exacerbates the progression of HIV induced neuropathology throughout the brain. These new data open the door to circuitry-based inquiry in the context of both neuroAIDS and opiate abuse, form a starting point for many new questions to be studied, and ultimately stand as a novel insight into the etiology of HAND development that will hopefully be useful in informing the treatment of these disorders in patients.

Figure 4. 1: TdTomato x VIP expressing mice



Images depicting transgenic mice expressing TdTomato under the control of the VIP promoter (**A, D, E**), or constitutively (**B-E**) under excitation under blue light using the Nightsea fluorescence visualization system (Nightsea, Bedford, MA).

Cytokine	Tat- Placebo n = 3	Tat+ Placebo n = 3-4	Tat- Morphine n = 3-4	Tat+ Morphine n = 3-4
IL-1a	5.17 ± 0.16	5.93 ± 0.46	6.74 ± 1.07	6.08 ± 0.87
IL-1b	25.97 ± 0.2	32.58 ± 2.65	31.57 ± 3.12	30.69 ± 3.08
IL-2	51.01 ± 3.1	67.91 ± 7.21	70.78 ± 9.65	65.41 ± 7.85
IL-3	3.56 ± 0.3	3.3 ± 0.48	3.923 ± 0.46	2.662 ± 0.78
IL-4	1.84 ± 0.32	1.26 ± 0.04	1.76 ± 0.16	5.34 ± 4.23
IL-5	2.5 ± 0.41	2.58 ± 0.33	4.06 ± 0.73	2.85 ± 0.28
IL-6	4.2 ± 0.27	4.63 ± 0.22	4.1 ± 0.79	4.29 ± 0.67
IL-9	27.99 ± 2.5	24.52 ± 1.47	28.83 ± 4.26	21.81 ± 4.67
IL-10	10.33 ± 0.83	8.87 ± 0.11	12.15 ± 1.56	9.54 ± 1.58
IL-12 p40	11.25 ± 0.88	11.45 ± 1.74	11.93 ± 1.36	11.85 ± 2.24
IL-12 p70	228.14 ± 3.59	211.56 ± 41.4	228.26 ± 14.43	240.92 ± 19.09
IL-13	90.21 ± 7.76	142.34 ± 20.23	138.27 ± 31.25	138.16 ± 24.43
IL-17	61.22 ± 6.22	55.34 ± 4.65	69.92 ± 5.13	50.78 ± 10.84
Eotaxin	130.13 ± 18.23	128.53 ± 4.99	136.16 ± 12.14	121.38 ± 13.12
GM-CSF	27.12 ± 1.58	15.91 ± 4.96*	26.46 ± 1.77	22.377 ± 3.11*
IFN-γ	120.23 ± 13	135 ± 45.54	141.88 ± 16.16	132.64 ± 27.46
KC	3.56 ± 0.3	3.2 ± 0.48	3.92 ± 0.46	2.66 ± 0.78
MCP-1	46.05 ± 3.81	35.01 ± 4.91^b	45.73 ± 2.36	39.44 ± 5.4^b
MIP-1α	2.12 ± 0.27	1.75 ± 0.41	2.26 ± 0.26	1.56 ± 0.58
MIP-1β	30.56 ± 3.48	37.1 ± 0.95	30 ± 2.73	29.97 ± 4.13
RANTES	12.91 ± 1.28	12.81 ± 0.33	14.81 ± 1.64	11.74 ± 1.37
TNF-α	404.12 ± 61.59	495.42 ± 104.82	386.32 ± 96.27	553.38 ± 8.93

Table 4. 1: Effects of Tat and morphine on hippocampal cytokine levels

Table 4.1 lists the levels of multiple cytokines assayed using the Bioplex analysis. * indicates a significant main effect of Tat ($p < 0.05$). ^bindicates a trend toward a main effect of Tat ($p = 0.055$). Values are expressed as mean $\mu\text{g/ml} \pm \text{SEM}$.

Sample ID#	Tat	Drug	Concentration (µg/mL)	Desired Final Concentration (ug/mL)	Volume Sample (µL)	Volume IP Buffer (µL)	Final protein content
1	-	Placebo	4099.92	500	15.244	47.26	62.5
2	-	Placebo	5476.04	500	11.41	51.09	62.5
3	-	Placebo	4658.41	500	13.417	49.08	62.5
4	-	Morphine	2000.93	500	31.23	31.26	62.5
5	-	Morphine	3982.01	500	15.7	46.8	62.5
6	-	Morphine	5028.84	500	12.428	50.07	62.5
7	-	Morphine	5375.62	500	11.627	50.87	62.5
8	+	Placebo	365.66	200	68.37	-5.87	50.8
9	+	Placebo	2858.09	500	21.87	40.632	62.5
10	+	Placebo	4568.35	500	13.68	48.82	62.5
11	+	Placebo	3163.41	500	19.76	42.74	62.5
12	+	Morphine	3320.84	500	18.82	43.67	62.5
13	+	Morphine	4798.52	500	13.025	49.48	62.5
14	+	Morphine	4040.32	500	15.47	47.03	62.5
15	+	Morphine	3088.98	500	20.23	42.27	62.5

Table 4. 2: Protein extracted from hippocampal samples

Records of the amount of protein extracted from hippocampal tissue samples as recorded by the BCA analysis. Dilution factors to achieve the desired protein concentration, the amount of additional buffer needed, and the final protein concentration for each sample are listed. Sample 8 (Tat+ / placebo) was excluded from all analyses due to low protein yield.

References

- Abe H, Mehraein P, Weis S. 1996. Degeneration of the cerebellar dentate nucleus and the inferior olivary nuclei in HIV-1-infected brains: a morphometric analysis. *Acta Neuropathol* 92: 150-155
- Acharjee S, Branton WG, Vivithanaporn P, Maingat F, Paul AM, et al. 2014. HIV-1 Nef expression in microglia disrupts dopaminergic and immune functions with associated mania-like behaviors. *Brain Behav Immun* 40: 74-84
- Achim CL, Adame A, Dumaop W, Everall IP, Masliah E, Neurobehavioral Research C. 2009. Increased accumulation of intraneuronal amyloid beta in HIV-infected patients. *J Neuroimmune Pharmacol* 4: 190-199
- Acsady L, Arabadzisz D, Freund TF. 1996a. Correlated morphological and neurochemical features identify different subsets of vasoactive intestinal polypeptide-immunoreactive interneurons in rat hippocampus. *Neuroscience* 73: 299-315
- Acsady L, Gorcs TJ, Freund TF. 1996b. Different populations of vasoactive intestinal polypeptide-immunoreactive interneurons are specialized to control pyramidal cells or interneurons in the hippocampus. *Neuroscience* 73: 317-334
- Agrawal L, Louboutin JP, Marusich E, Reyes BA, Van Bockstaele EJ, Strayer DS. 2010. Dopaminergic neurotoxicity of HIV-1 gp120: reactive oxygen species as signaling intermediates. *Brain Res* 1306: 116-130
- Agster KL, Burwell RD. 2013. Hippocampal and subicular efferents and afferents of the perirhinal, postrhinal, and entorhinal cortices of the rat. *Behav Brain Res* 254: 50-64
- Aksenov MY, Hasselrot U, Bansal AK, Wu G, Nath A, et al. 2001. Oxidative damage induced by the injection of HIV-1 Tat protein in the rat striatum. *Neurosci Lett* 305: 5-8
- Ali AB, Deuchars J, Pawelzik H, Thomson AM. 1998. CA1 pyramidal to basket and bistratified cell EPSPs: dual intracellular recordings in rat hippocampal slices. *J Physiol* 507 (Pt 1): 201-217
- Almolda B, Villacampa N, Manders P, Hidalgo J, Campbell IL, et al. 2014. Effects of astrocyte-targeted production of interleukin-6 in the mouse on the host response to nerve injury. *Glia* 62: 1142-1161
- Alreja M, Shanabrough M, Liu W, Leranath C. 2000. Opioids suppress IPSCs in neurons of the rat medial septum/diagonal band of Broca: involvement of mu-opioid receptors and septohippocampal GABAergic neurons. *J Neurosci* 20: 1179-1189

- Amaral D, Lavenex P. 2007. Hippocampal Neuroanatomy In *The Hippocampus Book*, ed. P Anderson, R Morris, D Amaral, T Bliss, J O'Keefe, pp. 37-109. New York: Oxford University Press
- Ammon-Treiber S, Stolze D, Holtt V. 2007. Differential effects of mu-opioid receptor agonists in a hippocampal hypoxia/hypoglycemia model. *Brain Res* 1183: 60-65
- An SF, Groves M, Gray F, Scaravilli F. 1999. Early entry and widespread cellular involvement of HIV-1 DNA in brains of HIV-1 positive asymptomatic individuals. *J Neuropathol Exp Neurol* 58: 1156-1162
- Ances BM, Ortega M, Vaida F, Heaps J, Paul R. 2012. Independent effects of HIV, aging, and HAART on brain volumetric measures. *J Acquir Immune Defic Syndr* 59: 469-477
- Andras IE, Pu H, Deli MA, Nath A, Hennig B, Toborek M. 2003. HIV-1 Tat protein alters tight junction protein expression and distribution in cultured brain endothelial cells. *J Neurosci Res* 74: 255-265
- Andronikou S, Ackermann C, Laughton B, Cotton M, Tomazos N, et al. 2014. Correlating brain volume and callosal thickness with clinical and laboratory indicators of disease severity in children with HIV-related brain disease. *Childs Nerv Syst* 30: 1549-1557
- Angelopoulos E, Koutsoukos E, Maillis A, Zioudrou C, Stefanis C. 1995. Acute tolerance to the excitatory effects of opioids in the rat hippocampus. *J Neurosci Res* 40: 72-78
- Anthony IC, Ramage SN, Carnie FW, Simmonds P, Bell JE. 2005. Does drug abuse alter microglial phenotype and cell turnover in the context of advancing HIV infection? *Neuropathol Appl Neurobiol* 31: 325-338
- Anthony IC, Arango JC, Stephens B, Simmonds P, Bell JE. 2008. The effects of illicit drugs on the HIV infected brain. *Front Biosci* 13: 1294-1307
- Antinori A, Arendt G, Becker JT, Brew BJ, Byrd DA, et al. 2007. Updated research nosology for HIV-associated neurocognitive disorders. *Neurology* 69: 1789-1799
- Antonucci F, Alpar A, Kacza J, Caleo M, Verderio C, et al. 2012. Cracking down on inhibition: selective removal of GABAergic interneurons from hippocampal networks. *J Neurosci* 32: 1989-2001
- Armstrong C, Krook-Magnuson E, Soltesz I. 2012. Neurogliaform and Ivy Cells: A Major Family of nNOS Expressing GABAergic Neurons. *Front Neural Circuits* 6: 23

- Avignone E, Frenguelli BG, Irving AJ. 2005. Differential responses to NMDA receptor activation in rat hippocampal interneurons and pyramidal cells may underlie enhanced pyramidal cell vulnerability. *Eur J Neurosci* 22: 3077-3090
- Avraham HK, Jiang S, Fu Y, Rockenstein E, Makriyannis A, et al. 2015. Impaired neurogenesis by HIV-1-Gp120 is rescued by genetic deletion of fatty acid amide hydrolase enzyme. *Br J Pharmacol* 172: 4603-4614
- Bailey CH, Kandel ER, Harris KM. 2015. Structural Components of Synaptic Plasticity and Memory Consolidation. *Cold Spring Harb Perspect Biol* 7: a021758
- Bajic D, Commons KG, Soriano SG. 2013. Morphine-enhanced apoptosis in selective brain regions of neonatal rats. *Int J Dev Neurosci* 31: 258-266
- Bao G, Kang L, Li H, Li Y, Pu L, et al. 2007. Morphine and heroin differentially modulate in vivo hippocampal LTP in opiate-dependent rat. *Neuropsychopharmacology* 32: 1738-1749
- Barnes CA. 1979. Memory deficits associated with senescence: a neurophysiological and behavioral study in the rat. *J Comp Physiol Psychol* 93: 74-104
- Barre-Sinoussi F, Chermann J, Rey F, Nugeyre M, Chamaret S, et al. 1983. Isolation of a T-lymphotropic retrovirus from a patient at risk for acquired immune deficiency syndrome (AIDS). *Science* 220: 868-871
- Bayer P, Kraft M, Ejchart A, Westendorp M, Frank R, Rosch P. 1995. Structural studies of HIV-1 Tat protein. *J Mol Biol* 247: 529-535
- Becker KM, Heinrichs-Graham E, Fox HS, Robertson KR, Sandkovsky U, et al. 2013. Decreased MEG beta oscillations in HIV-infected older adults during the resting state. *J Neurovirol* 19: 586-594
- Beckman BS. 2014. The Opioids In *Drugs and Their Actions*, pp. 139-144. Acton, MA: XanEdu
- Behnisch T, Francesconi W, Sanna PP. 2004. HIV secreted protein Tat prevents long-term potentiation in the hippocampal CA1 region. *Brain Res* 1012: 187-189
- Bell JE, Brettle RP, Chiswick A, Simmonds P. 1998. HIV encephalitis, proviral load and dementia in drug users and homosexuals with AIDS. Effect of neocortical involvement. *Brain* 121 (Pt 11): 2043-2052

- Bell LA, Bell KA, McQuiston AR. 2015. Activation of muscarinic receptors by ACh release in hippocampal CA1 depolarizes VIP but has varying effects on parvalbumin-expressing basket cells. *The Journal of Physiology* 593: 197-215
- Benetti F, Furini CR, de Carvalho Myskiw J, Provensi G, Passani MB, et al. 2015. Histamine in the basolateral amygdala promotes inhibitory avoidance learning independently of hippocampus. *Proc Natl Acad Sci U S A* 112: E2536-2542
- Berger EA, Doms RW, Fenyo EM, Korber BT, Littman DR, et al. 1998. A new classification for HIV-1. *Nature* 391: 240
- Bertin J, Jalaguier P, Barat C, Roy MA, Tremblay MJ. 2014. Exposure of human astrocytes to leukotriene C4 promotes a CX3CL1/fractalkine-mediated transmigration of HIV-1-infected CD4(+) T cells across an in vitro blood-brain barrier model. *Virology* 454-455: 128-138
- Bhattacharya P, Budnick I, Singh M, Thiruppathi M, Alharshawi K, et al. 2015. Dual Role of GM-CSF as a Pro-Inflammatory and a Regulatory Cytokine: Implications for Immune Therapy. *J Interferon Cytokine Res* 35: 585-599
- Bikoff JB, Gabitto MI, Rivard AF, Drobac E, Machado TA, et al. 2016. Spinal Inhibitory Interneuron Diversity Delineates Variant Motor Microcircuits. *Cell* 165: 207-219
- Bilgrami M, O'Keefe P. 2014. Neurologic diseases in HIV-infected patients. *Handb Clin Neurol* 121: 1321-1344
- Bobardt MD, Salmon P, Wang L, Esko JD, Gabuzda D, et al. 2004. Contribution of proteoglycans to human immunodeficiency virus type 1 brain invasion. *J Virol* 78: 6567-6584
- Bodnar RJ. 2012. Endogenous opiates and behavior: 2011. *Peptides* 38: 463-522
- Bodzon-Kulakowska A, Suder P, Drabik A, Kotlinska JH, Silberring J. 2010. Constant activity of glutamine synthetase after morphine administration versus proteomic results. *Anal Bioanal Chem* 398: 2939-2942
- Bohlius J, Valeri F, Maskew M, Prozesky H, Garone D, et al. 2014. Kaposi's Sarcoma in HIV-infected patients in South Africa: Multicohort study in the antiretroviral therapy era. *Int J Cancer* 135: 2644-2652
- Bouilleret V, Schwaller B, Schurmans S, Celio MR, Fritschy JM. 2000. Neurodegenerative and morphogenic changes in a mouse model of temporal lobe epilepsy do not depend on the

- expression of the calcium-binding proteins parvalbumin, calbindin, or calretinin. *Neuroscience* 97: 47-58
- Brack-Werner R. 1999. Astrocytes: HIV cellular reservoirs and important participants in neuropathogenesis. *AIDS* 13: 1-22
- Bruce-Keller AJ, Turchan-Cholewo J, Smart EJ, Geurin T, Chauhan A, et al. 2008. Morphine causes rapid increases in glial activation and neuronal injury in the striatum of inducible HIV-1 Tat transgenic mice. *Glia* 56: 1414-1427
- Bruce RD, Altice FL. 2007. Clinical care of the HIV-infected drug user. *Infect Dis Clin North Am* 21: 149-179, ix
- Buhl EH, Halasy K, Somogyi P. 1994. Diverse sources of hippocampal unitary inhibitory postsynaptic potentials and the number of synaptic release sites. *Nature* 368: 823-828
- Buhl EH, Szilagy T, Halasy K, Somogyi P. 1996. Physiological properties of anatomically identified basket and bistratified cells in the CA1 area of the rat hippocampus in vitro. *Hippocampus* 6: 294-305
- Buño W, Cabezas C, de Sevilla DF. 2006. Presynaptic Muscarinic Control of Glutamatergic Synaptic Transmission. *Journal of Molecular Neuroscience* 30: 161-164
- Butour J-L, Moisan C, Mazarguil H, Mollereau C, Meunier J-C. 1997. Recognition and activation of the opioid receptor-like ORL1 receptor by nociceptin, nociceptin analogs and opioids. *European Journal of Pharmacology* 321: 97-103
- Byrd D, Murray J, Safdieh G, Morgello S. 2012. Impact of opiate addiction on neuroinflammation in HIV. *J Neurovirol* 18: 364-373
- Byrd DA, Fellows RP, Morgello S, Franklin D, Heaton RK, et al. 2011. Neurocognitive impact of substance use in HIV infection. *J Acquir Immune Defic Syndr* 58: 154-162
- Camara ML, Corrigan F, Jaehne EJ, Jawahar MC, Anscomb H, et al. 2013. TNF-alpha and its receptors modulate complex behaviours and neurotrophins in transgenic mice. *Psychoneuroendocrinology* 38: 3102-3114
- Carey AN, Sypek EI, Singh HD, Kaufman MJ, McLaughlin JP. 2012. Expression of HIV-Tat protein is associated with learning and memory deficits in the mouse. *Behav Brain Res* 229: 48-56

- Cassel JC, Pereira de Vasconcelos A, Loureiro M, Cholvin T, Dalrymple-Alford JC, Vertes RP. 2013. The reuniens and rhomboid nuclei: neuroanatomy, electrophysiological characteristics and behavioral implications. *Prog Neurobiol* 111: 34-52
- Castelo JM, Sherman SJ, Courtney MG, Melrose RJ, Stern CE. 2006. Altered hippocampal-prefrontal activation in HIV patients during episodic memory encoding. *Neurology* 66: 1688-1695
- CDC. 1987. Recommendations for prevention of HIV transmission in health-care settings. *MMWR* 1987;36 (suppl no. 2S).
- CDC. 2016. HIV Transmission. <https://www.cdc.gov/hiv/basics/transmission.html>. May 15, 2017
- CDC. 2017. About HIV/AIDS. <https://www.cdc.gov/hiv/basics/whatishiv.html>. Oct 17
- Cenquizca LA, Swanson LW. 2006. Analysis of direct hippocampal cortical field CA1 axonal projections to diencephalon in the rat. *J Comp Neurol* 497: 101-114
- Chaboub LS, Deneen B. 2012. Developmental origins of astrocyte heterogeneity: the final frontier of CNS development. *Dev Neurosci* 34: 379-388
- Chamberland S, Salesse C, Topolnik D, Topolnik L. 2010. Synapse-specific inhibitory control of hippocampal feedback inhibitory circuit. *Front Cell Neurosci* 4: 130
- Chamberland S, Topolnik L. 2012. Inhibitory control of hippocampal inhibitory neurons. *Front Neurosci* 6: 165
- Chana G, Everall IP, Crews L, Langford D, Adame A, et al. 2006. Cognitive deficits and degeneration of interneurons in HIV+ methamphetamine users. *Neurology* 67: 1486-1489
- Chandra T, Maier W, Konig HG, Hirzel K, Kogel D, et al. 2005. Molecular interactions of the type 1 human immunodeficiency virus transregulatory protein Tat with N-methyl-d-aspartate receptor subunits. *Neuroscience* 134: 145-153
- Chang JR, Mukerjee R, Bagashev A, Del Valle L, Chabrashvili T, et al. 2011. HIV-1 Tat protein promotes neuronal dysfunction through disruption of microRNAs. *J Biol Chem* 286: 41125-41134
- Chatterjee N, Callen S, Seigel GM, Buch SJ. 2011. HIV-1 Tat-mediated neurotoxicity in retinal cells. *J Neuroimmune Pharmacol* 6: 399-408

- Chen H, Wood C, Petito CK. 2000. Comparisons of HIV-1 viral sequences in brain, choroid plexus and spleen: potential role of choroid plexus in the pathogenesis of HIV encephalitis. *J Neurovirol* 6: 498-506
- Chen J, Buchanan JB, Sparkman NL, Godbout JP, Freund GG, Johnson RW. 2008. Neuroinflammation and disruption in working memory in aged mice after acute stimulation of the peripheral innate immune system. *Brain Behav Immun* 22: 301-311
- Cheng S, Klein H, Bartsch DU, Kozak I, Marcotte TD, Freeman WR. 2011. Relationship between retinal nerve fiber layer thickness and driving ability in patients with human immunodeficiency virus infection. *Graefes Arch Clin Exp Ophthalmol* 249: 1643-1647
- Chiang MC, Dutton RA, Hayashi KM, Lopez OL, Aizenstein HJ, et al. 2007. 3D pattern of brain atrophy in HIV/AIDS visualized using tensor-based morphometry. *Neuroimage* 34: 44-60
- Chitnis A, Rawls D, Moore J. 2000. Origin of HIV type 1 in colonial French Equatorial Africa? *AIDS Res Hum Retroviruses* 16: 5-8
- Chittajallu R, Craig MT, McFarland A, Yuan X, Gerfen S, et al. 2013. Dual origins of functionally distinct O-LM interneurons revealed by differential 5-HT(3A)R expression. *Nat Neurosci* 16: 1598-1607
- Choi SS, Lee HJ, Lim I, Satoh J, Kim SU. 2014. Human astrocytes: secretome profiles of cytokines and chemokines. *PLoS One* 9: e92325
- Christopherson KS, Hillier BJ, Lim WA, Brecht DS. 1999. PSD-95 Assembles a Ternary Complex with the N-Methyl-D-aspartic Acid Receptor and a Bivalent Neuronal NO Synthase PDZ Domain. *Journal of Biological Chemistry* 274: 27467-27473
- Churchill MJ, Wesselingh SL, Cowley D, Pardo CA, McArthur JC, et al. 2009. Extensive astrocyte infection is prominent in human immunodeficiency virus-associated dementia. *Ann Neurol* 66: 253-258
- Clavel F, Guetard D, Brun-Vezinet F, Chamaret S, Rey M, et al. 1986. Isolation of a new human retrovirus from West African patients with AIDS. *Science* 233: 343-346
- Coakley E, Petropoulos CJ, Whitcomb JM. 2005. Assessing chemokine co-receptor usage in HIV. *Current Opinion in Infectious Diseases* 18: 9-15
- Cohen-Avrahami M, Shames AI, Ottaviani MF, Aserin A, Garti N. 2014. HIV-TAT enhances the transdermal delivery of NSAID drugs from liquid crystalline mesophases. *J Phys Chem B* 118: 6277-6287

- Coleman P, Federoff H, Kurlan R. 2004. A focus on the synapse for neuroprotection in Alzheimer disease and other dementias. *Neurology* 63: 1155-1162
- Commons KG, Milner TA. 1996. Cellular and subcellular localization of delta opioid receptor immunoreactivity in the rat dentate gyrus. *Brain Res* 738: 181-195
- Cossart R, Dinocourt C, Hirsch JC, Merchan-Perez A, De Felipe J, et al. 2001. Dendritic but not somatic GABAergic inhibition is decreased in experimental epilepsy. *Nat Neurosci* 4: 52-62
- Covelo A, Araque A. 2016. Lateral regulation of synaptic transmission by astrocytes. *Neuroscience* 323: 62-66
- Crum-Cianflone N, Eberly L, Zhang Y, Ganesan A, Weintrob A, et al. 2009. Is HIV becoming more virulent? Initial CD4 cell counts among HIV seroconverters during the course of the HIV epidemic: 1985-2007. *Clin Infect Dis* 48: 1285-1292
- Cui H, Hayashi A, Sun HS, Belmares MP, Cobey C, et al. 2007. PDZ protein interactions underlying NMDA receptor-mediated excitotoxicity and neuroprotection by PSD-95 inhibitors. *J Neurosci* 27: 9901-9915
- Dawes S, Suarez P, Casey CY, Cherner M, Marcotte TD, et al. 2008. Variable patterns of neuropsychological performance in HIV-1 infection. *J Clin Exp Neuropsychol* 30: 613-626
- de Sousa JD, Muller V, Lemey P, Vandamme AM. 2010. High GUD incidence in the early 20 century created a particularly permissive time window for the origin and initial spread of epidemic HIV strains. *PLoS One* 5: e9936
- Debaisieux S, Rayne F, Yezid H, Beaumelle B. 2012. The ins and outs of HIV-1 Tat. *Traffic* 13: 355-363
- Deng W, Aimone JB, Gage FH. 2010. New neurons and new memories: how does adult hippocampal neurogenesis affect learning and memory? *Nat Rev Neurosci* 11: 339-350
- Dere E, Huston JP, De Souza Silva MA. 2007. The pharmacology, neuroanatomy and neurogenetics of one-trial object recognition in rodents. *Neurosci Biobehav Rev* 31: 673-704
- Desagher S, Glowinski J, Premont J. 1996. Astrocytes protect neurons from hydrogen peroxide toxicity. *J Neurosci* 16: 2553-2562
- Dever SM, Xu R, Fitting S, Knapp PE, Hauser KF. 2012. Differential expression and HIV-1 regulation of mu-opioid receptor splice variants across human central nervous system cell types. *J Neurovirol* 18: 181-190

- Di JH, Li C, Yu HM, Zheng JN, Zhang GY. 2012. nNOS downregulation attenuates neuronal apoptosis by inhibiting nNOS-GluR6 interaction and GluR6 nitrosylation in cerebral ischemic reperfusion. *Biochem Biophys Res Commun* 420: 594-599
- DiSabato DJ, Quan N, Godbout JP. 2016. Neuroinflammation: the devil is in the details. *J Neurochem* 139 Suppl 2: 136-153
- Dolleman-Van der Weel MJ, Lopes da Silva FH, Witter MP. 1997. Nucleus Reunions Thalami Modulates Activity in Hippocampal Field CA1 through Excitatory and Inhibitory Mechanisms. *The Journal of Neuroscience* 17: 5640-5650
- Drake CT, Milner TA. 1999. Mu opioid receptors are in somatodendritic and axonal compartments of GABAergic neurons in rat hippocampal formation. *Brain Res* 849: 203-215
- Drake CT, Milner TA. 2002. Mu opioid receptors are in discrete hippocampal interneuron subpopulations. *Hippocampus* 12: 119-136
- Drury PP, Davidson JO, Mathai S, van den Heuvel LG, Ji H, et al. 2014. nNOS inhibition during profound asphyxia reduces seizure burden and improves survival of striatal phenotypic neurons in preterm fetal sheep. *Neuropharmacology* 83: 62-70
- Dugladze T, Vida I, Tort AB, Gross A, Otahal J, et al. 2007. Impaired hippocampal rhythmogenesis in a mouse model of mesial temporal lobe epilepsy. *Proc Natl Acad Sci U S A* 104: 17530-17535
- Edelman EJ, So-Armah K, Cheng DM, Doyle MF, Coleman SM, et al. 2017. Impact of illicit opioid use on T cell subsets among HIV-infected adults. *PLoS One* 12: e0176617
- Eitan S, Emery MA, Bates MLS, Horrax C. 2017. Opioid addiction: Who are your real friends? *Neurosci Biobehav Rev*
- Elliot T, Casey A, Lambert PA, Sandoe J. 2012. *Lecture Notes: Medical Microbiology and Infection*. pp. P. 273. John Wiley & Sons.
- Ellis R, Langford D, Masliah E. 2007. HIV and antiretroviral therapy in the brain: neuronal injury and repair. *Nat Rev Neurosci* 8: 33-44
- Ennaceur A, Delacour J. 1988. A new one-trial test for neurobiological studies of memory in rats. 1: Behavioral data. *Behav Brain Res* 31: 47-59

- Ensoli B, Barillari G, Salahuddin SZ, Gallo RC, Wong-Staal F. 1990. Tat protein of HIV-1 stimulates growth of cells derived from Kaposi's sarcoma lesions of AIDS patients. *Nature* 345: 84-86
- Erbs E, Faget L, Ceredig RA, Matifas A, Vonesch JL, et al. 2016. Impact of chronic morphine on delta opioid receptor-expressing neurons in the mouse hippocampus. *Neuroscience* 313: 46-56
- Esiri MM, Biddolph SC, Morris CS. 1998. Prevalence of Alzheimer plaques in AIDS. *J Neurol Neurosurg Psychiatry* 65: 29-33
- Eugenin EA, King JE, Nath A, Calderon TM, Zukin RS, et al. 2007. HIV-tat induces formation of an LRP-PSD-95- NMDAR-nNOS complex that promotes apoptosis in neurons and astrocytes. *Proc Natl Acad Sci U S A* 104: 3438-3443
- Everall I, Vaida F, Khanlou N, Lazzaretto D, Achim C, et al. 2009. Cliniconeuropathologic correlates of human immunodeficiency virus in the era of antiretroviral therapy. *J Neurovirol* 15: 360-370
- Everall IP, Barnes H. 1999. Reduction in phosphorylated heavy neurofilament in the cerebellum in HIV disease. *J NeuroAIDS* 2: 43-55
- Everall IP, Salaria S, Atkinson JH, Young C, Corbeil J, et al. 2006. Diminished somatostatin gene expression in individuals with HIV and major depressive disorder. *Neurology* 67: 1867-1869
- Fakira AK, Portugal GS, Carusillo B, Melyan Z, Moron JA. 2014. Increased small conductance calcium-activated potassium type 2 channel-mediated negative feedback on N-methyl-D-aspartate receptors impairs synaptic plasticity following context-dependent sensitization to morphine. *Biol Psychiatry* 75: 105-114
- Fan J, Vasuta OC, Zhang LY, Wang L, George A, Raymond LA. 2010. N-methyl-D-aspartate receptor subunit- and neuronal-type dependence of excitotoxic signaling through post-synaptic density 95. *J Neurochem* 115: 1045-1056
- Fan W, Fu T. 2014. Somatostatin modulates LTP in hippocampal CA1 pyramidal neurons: differential activation conditions in apical and basal dendrites. *Neurosci Lett* 561: 1-6
- Farahmandfar M, Karimian SM, Zarrindast MR, Kadivar M, Afrouzi H, Naghdi N. 2011a. Morphine sensitization increases the extracellular level of glutamate in CA1 of rat hippocampus via mu-opioid receptor. *Neurosci Lett* 494: 130-134
- Farahmandfar M, Zarrindast MR, Kadivar M, Karimian SM, Naghdi N. 2011b. The effect of morphine sensitization on extracellular concentrations of GABA in dorsal hippocampus of male rats. *Eur J Pharmacol* 669: 66-70

- Fazeli PL, Crowe M, Ross LA, Wadley V, Ball K, Vance DE. 2014. Cognitive Functioning in Adults Aging with HIV: A Cross-Sectional Analysis of Cognitive Subtypes and Influential Factors. *J Clin Res HIV AIDS Prev* 1: 155-169
- Ferrucci A, Nonnemacher MR, Wigdahl B. 2013. Extracellular HIV-1 viral protein R affects astrocytic glyceraldehyde 3-phosphate dehydrogenase activity and neuronal survival. *J Neurovirol* 19: 239-253
- Fitting S, Booze RM, Hasselrot U, Mactutus CF. 2006. Intrahippocampal injections of Tat: effects on prepulse inhibition of the auditory startle response in adult male rats. *Pharmacol Biochem Behav* 84: 189-196
- Fitting S, Booze RM, Hasselrot U, Mactutus CF. 2008. Differential long-term neurotoxicity of HIV-1 proteins in the rat hippocampal formation: a design-based stereological study. *Hippocampus* 18: 135-147
- Fitting S, Xu R, Bull C, Buch SK, El-Hage N, et al. 2010a. Interactive comorbidity between opioid drug abuse and HIV-1 Tat: chronic exposure augments spine loss and sublethal dendritic pathology in striatal neurons. *Am J Pathol* 177: 1397-1410
- Fitting S, Zou S, Chen W, Vo P, Hauser KF, Knapp PE. 2010b. Regional heterogeneity and diversity in cytokine and chemokine production by astroglia: differential responses to HIV-1 Tat, gp120, and morphine revealed by multiplex analysis. *J Proteome Res* 9: 1795-1804
- Fitting S, Scoggins KL, Xu R, Dever SM, Knapp PE, et al. 2012. Morphine efficacy is altered in conditional HIV-1 Tat transgenic mice. *Eur J Pharmacol* 689: 96-103
- Fitting S, Ignatowska-Jankowska BM, Bull C, Skoff RP, Lichtman AH, et al. 2013. Synaptic dysfunction in the hippocampus accompanies learning and memory deficits in human immunodeficiency virus type-1 Tat transgenic mice. *Biol Psychiatry* 73: 443-453
- Fitting S, Knapp PE, Zou S, Marks WD, Bowers MS, et al. 2014. Interactive HIV-1 Tat and morphine-induced synaptodendritic injury is triggered through focal disruptions in Na(+) influx, mitochondrial instability, and Ca(2)(+) overload. *J Neurosci* 34: 12850-12864
- Fitting S, Ngwainmbi J, Kang M, Khan FA, Stevens DL, et al. 2015a. Sensitization of enteric neurons to morphine by HIV-1 Tat protein. *Neurogastroenterol Motil* 27: 468-480
- Fitting S, Zou S, El-Hage N, Suzuki M, Paris J, et al. 2015b. Opiate Addiction Therapies and HIV-1 Tat: Interactive Effects on Glial [Ca²⁺]_i, Oxyradical and Neuroinflammatory Chemokine Production and Correlative Neurotoxicity. *Current HIV Research* 12: 424-434

- Fitting S, Stevens DL, Khan FA, Scoggins KL, Enga RM, et al. 2016. Morphine Tolerance and Physical Dependence Are Altered in Conditional HIV-1 Tat Transgenic Mice. *J Pharmacol Exp Ther* 356: 96-105
- Fox L, Alford M, Achim C, Mallory M, Masliah E. 1997. Neurodegeneration of somatostatin-immunoreactive neurons in HIV encephalitis. *J Neuropathol Exp Neurol* 56: 360-368
- Francis H. 2003. Substance abuse and HIV infection. *Top HIV Med* 11: 20-24
- Frankel AD, Pabo CO. 1988. Cellular uptake of the tat protein from human immunodeficiency virus. *Cell* 55: 1189-1193
- Freund TF, Buzsáki G. 1998. Interneurons of the hippocampus. *Hippocampus* 6: 347-470
- Friedland GH. 1985. Intravenous Drug Abusers and the Acquired Immunodeficiency Syndrome (AIDS). *Archives of Internal Medicine* 145
- Fu X, Lawson MA, Kelley KW, Dantzer R. 2011. HIV-1 Tat activates indoleamine 2,3 dioxygenase in murine organotypic hippocampal slice cultures in a p38 mitogen-activated protein kinase-dependent manner. *J Neuroinflammation* 8: 88
- Fuentealba P, Begum R, Capogna M, Jinno S, Marton LF, et al. 2008. Ivy cells: a population of nitric-oxide-producing, slow-spiking GABAergic neurons and their involvement in hippocampal network activity. *Neuron* 57: 917-929
- Gallo R, Sarin P, Gelmann E, Robert-Guroff M, Richardson E, et al. 1983. Isolation of human T-cell leukemia virus in acquired immune deficiency syndrome (AIDS). *Science* 220: 865-867
- Garvey LJ, Pavese N, Politis M, Ramlackhansingh A, Brooks DJ, et al. 2014. Increased microglia activation in neurologically asymptomatic HIV-infected patients receiving effective ART. *AIDS* 28: 67-72
- Garzon J, Rodriguez-Munoz M, Vicente-Sanchez A, Bailon C, Martinez-Murillo R, Sanchez-Blazquez P. 2011. RGS22 binds to the neural nitric oxide synthase PDZ domain to regulate mu-opioid receptor-mediated potentiation of the N-methyl-D-aspartate receptor-calmodulin-dependent protein kinase II pathway. *Antioxid Redox Signal* 15: 873-887
- Gelbard HA, Nottet HS, Swindells S, Jett M, Dzenko KA, et al. 1994. Platelet-activating factor: a candidate human immunodeficiency virus type 1-induced neurotoxin. *J Virol* 68: 4628-4635

- Gelman BB, Chen T, Lisinicchia JG, Soukup VM, Carmical JR, et al. 2012. The National NeuroAIDS Tissue Consortium brain gene array: two types of HIV-associated neurocognitive impairment. *PLoS One* 7: e46178
- Gelman BB, Lisinicchia JG, Morgello S, Masliah E, Commins D, et al. 2013. Neurovirological correlation with HIV-associated neurocognitive disorders and encephalitis in a HAART-era cohort. *J Acquir Immune Defic Syndr* 62: 487-495
- Ghafari S, Golalipour MJ. 2014. Prenatal morphine exposure reduces pyramidal neurons in CA1, CA2 and CA3 subfields of mice hippocampus. *Iran J Basic Med Sci* 17: 155-161
- Ghorpade A, Persidsky Y, Swindells S, Borgmann K, Persidsky R, et al. 2005. Neuroinflammatory responses from microglia recovered from HIV-1-infected and seronegative subjects. *J Neuroimmunol* 163: 145-156
- Gilbert PB, McKeague IW, Eisen G, Mullins C, Gueye NA, et al. 2003. Comparison of HIV-1 and HIV-2 infectivity from a prospective cohort study in Senegal. *Stat Med* 22: 573-593
- Gilmore NJ, Beaulieu R, Steben M, Laverdiere M. 1983. AIDS: acquired immunodeficiency syndrome. *Can Med Assoc J* 128: 1281-1284
- Glass JD, Fedor H, Wesselingh SL, McArthur JC. 1995. Immunocytochemical quantitation of human immunodeficiency virus in the brain: correlations with dementia. *Ann Neurol* 38: 755-762
- Glickfeld LL, Atallah BV, Scanziani M. 2008. Complementary modulation of somatic inhibition by opioids and cannabinoids. *J Neurosci* 28: 1824-1832
- Goldin M, Epsztein J, Jorquera I, Represa A, Ben-Ari Y, et al. 2007. Synaptic kainate receptors tune oriens-lacunosum moleculare interneurons to operate at theta frequency. *J Neurosci* 27: 9560-9572
- Gonek M, McLane VD, Stevens DL, Lippold K, Akbarali HI, et al. 2017. CCR5 mediates HIV-1 Tat-induced neuroinflammation and influences morphine tolerance, dependence, and reward. *Brain Behav Immun*
- Gongvatana A, Schweinsburg BC, Taylor MJ, Theilmann RJ, Letendre SL, et al. 2009. White matter tract injury and cognitive impairment in human immunodeficiency virus-infected individuals. *J Neurovirol* 15: 187-195
- Gongvatana A, Harezlak J, Buchthal S, Daar E, Schifitto G, et al. 2013. Progressive cerebral injury in the setting of chronic HIV infection and antiretroviral therapy. *J Neurovirol* 19: 209-218

- González-Scarano F, Martín-García J. 2005. The neuropathogenesis of AIDS. *Nature Reviews Immunology* 5: 69-81
- Grabert K, Michael T, Karavolos MH, Clohisey S, Baillie JK, et al. 2016. Microglial brain region-dependent diversity and selective regional sensitivities to aging. *Nat Neurosci* 19: 504-516
- Green M, Loewenstein PM. 1988. Autonomous functional domains of chemically synthesized human immunodeficiency virus tat trans-activator protein. *Cell* 55: 1179-1188
- Griffin AL. 2015. Role of the thalamic nucleus reuniens in mediating interactions between the hippocampus and medial prefrontal cortex during spatial working memory. *Front Syst Neurosci* 9: 29
- Grima G, Benz B, Do KQ. 2001. Glial-derived arginine, the nitric oxide precursor, protects neurons from NMDA-induced excitotoxicity. *Eur J Neurosci* 14: 1762-1770
- Guillemin GJ, Kerr SJ, Brew BJ. 2005. Involvement of quinolinic acid in AIDS dementia complex. *Neurotox Res* 7: 103-123
- Gulyas AI, Hajos N, Freund TF. 1996. Interneurons containing calretinin are specialized to control other interneurons in the rat hippocampus. *J Neurosci* 16: 3397-3411
- Gulyás AI, Seress L, Tóth K, Acsády L, Antal M, Freund TF. 1991. Septal GABAergic neurons innervate inhibitory interneurons in the hippocampus of the macaque monkey. *Neuroscience* 41: 381-390
- Gundersen HJ, Bendtsen TF, Korbo L, Marcussen N, Møller A, et al. 1988. Some new, simple and efficient stereological methods and their use in pathological research and diagnosis. *AMPIS* 96: 379-394
- Guo M, Bryant J, Sultana S, Jones O, Royal W, 3rd. 2012. Effects of vitamin A deficiency and opioids on parvalbumin + interneurons in the hippocampus of the HIV-1 transgenic rat. *Curr HIV Res* 10: 463-468
- Gutstein HB, Akil H. 2006. Opioid Analgesics In *Goodman and Gillman's The Pharmacological Basis of Therapeutics*, ed. LL Brunton, JS Lazo, KL Parker, pp. 547-590. New York: McGraw Hill
- Gyorkey F, Melnick JL, Gyorkey P. 1987. Human immunodeficiency virus in brain biopsies of patients with AIDS and progressive encephalopathy. *J Infect Dis* 155: 870-876
- Haase AT. 1986. Pathogenesis of lentivirus infections. *Nature* 322: 130-136

- Hahn YK, Paris JJ, Lichtman AH, Hauser KF, Sim-Selley LJ, et al. 2016. Central HIV-1 Tat exposure elevates anxiety and fear conditioned responses of male mice concurrent with altered mu-opioid receptor-mediated G-protein activation and beta-arrestin 2 activity in the forebrain. *Neurobiol Dis* 92: 124-136
- Halasy K, Rácz B, Maderspach K. 2000. Kappa opioid receptors are expressed by interneurons in the CA1 area of the rat hippocampus: a correlated light and electron microscopic immunocytochemical study. *Journal of Chemical Neuroanatomy* 19: 233-241
- Hall NR, O'Grady MP, Menzies RA. 1991. Neuroimmunopharmacologic effects of drugs of abuse. *Adv Exp Med Biol* 288: 13-23
- Hamilton DJ, Wheeler DW, White CM, Rees CL, Komendantov AO, et al. 2017a. Name-calling in the hippocampus (and beyond): coming to terms with neuron types and properties. *Brain Inform* 4: 1-12
- Hamilton DJ, White CM, Rees CL, Wheeler DW, Ascoli GA. 2017b. Molecular fingerprinting of principal neurons in the rodent hippocampus: A neuroinformatics approach. *J Pharm Biomed Anal*
- Hargus NJ, Thayer SA. 2013. Human immunodeficiency virus-1 Tat protein increases the number of inhibitory synapses between hippocampal neurons in culture. *J Neurosci* 33: 17908-17920
- Harouse JM, Wroblewska Z, Laughlin MA, Hickey WF, Schonwetter BS, Gonzalez-Scarano F. 1989. Human choroid plexus cells can be latently infected with human immunodeficiency virus. *Ann Neurol* 25: 406-411
- Harricharan R, Thaver V, Russell VA, Daniels WM. 2015. Tat-induced histopathological alterations mediate hippocampus-associated behavioural impairments in rats. *Behav Brain Funct* 11: 3
- Harris A, Bolus NE. 2008. HIV/AIDS: an update. *Radiol Technol* 79: 243-252; quiz 253-245
- Harris KM, Jensen FE, Tsao B. 1992. Three-dimensional structure of dendritic spines and synapses in rat hippocampus (CA1) at postnatal day 15 and adult ages: implications for the maturation of synaptic physiology and long-term potentiation [published erratum appears in J Neurosci 1992 Aug;12(8):following table of contents]. *The Journal of Neuroscience* 12: 2685
- Harrison JM, Allen RG, Pellegrino MJ, Williams JT, Manzoni OJ. 2002. Chronic Morphine Treatment Alters Endogenous Opioid Control of Hippocampal Mossy Fiber Synaptic Transmission. *Journal of Neurophysiology* 87: 2464-2470

- Hatzoglou A, Ouafik L, Bakogeorgou E, Thermos K, Castanas E. 1995. Morphine Cross-React with Somatostatin Receptor SSTRs in the T4D Human Breast Cancer Cell line and Decreases Cell Growth. *Cancer Research* 55: 5632-5636
- Haughey NJ, Nath A, Mattson MP, Slevin JT, Geiger JD. 2001. HIV-1 Tat through phosphorylation of NMDA receptors potentiates glutamate excitotoxicity. *Journal of Neurochemistry* 78: 457-467
- Haughey NJ, Mattson MP. 2002. Calcium dysregulation and neuronal apoptosis by the HIV-1 proteins Tat and gp120. *J Acquir Immune Defic Syndr* 31 Suppl 2: S55-61
- Hauser KF, Hahn YK, Adjan VV, Zou S, Buch SK, et al. 2009. HIV-1 Tat and morphine have interactive effects on oligodendrocyte survival and morphology. *Glia* 57: 194-206
- Hauser KF, Fitting S, Dever SM, Podhaizer EM, Knapp PE. 2012. Opiate Drug Use and the Pathophysiology of NeuroAIDS. *Current HIV Research* 10: 435-452
- Hazra A, Gu F, Aulakh A, Berridge C, Eriksen JL, Ziburkus J. 2013. Inhibitory neuron and hippocampal circuit dysfunction in an aged mouse model of Alzheimer's disease. *PLoS One* 8: e64318
- He J, Chen Y, Farzan M, Choe H, Ohagen A, et al. 1997. CCR3 and CCR5 are co-receptors for HIV-1 infection of microglia. *Nature* 385: 645-649
- Heaton RK, Franklin DR, Ellis RJ, McCutchan JA, Letendre SL, et al. 2011. HIV-associated neurocognitive disorders before and during the era of combination antiretroviral therapy: differences in rates, nature, and predictors. *J Neurovirol* 17: 3-16
- Heidari MH, Amini A, Bahrami Z, Shahriari A, Movafag A, Heidari R. 2013. Effect of Chronic Morphine Consumption on Synaptic Plasticity of Rat's Hippocampus: A Transmission Electron Microscopy Study. *Neurol Res Int* 2013: 290414
- Heyes MP, Ellis RJ, Ryan L, Childers ME, Grant I, et al. 2001. Elevated cerebrospinal fluid quinolinic acid levels are associated with region-specific cerebral volume loss in HIV infection. *Brain* 124: 1033-1042
- Hochstim C, Deneen B, Lukaszewicz A, Zhou Q, Anderson DJ. 2008. Identification of positionally distinct astrocyte subtypes whose identities are specified by a homeodomain code. *Cell* 133: 510-522
- Hoskison MM, Yanagawa Y, Obata K, Shuttleworth CW. 2007. Calcium-dependent NMDA-induced dendritic injury and MAP2 loss in acute hippocampal slices. *Neuroscience* 145: 66-79

- Hossain MI, Kamaruddin MA, Cheng HC. 2012. Aberrant regulation and function of Src family tyrosine kinases: their potential contributions to glutamate-induced neurotoxicity. *Clin Exp Pharmacol Physiol* 39: 684-691
- Hriso E, Kuhn T, Masdeu JC, Grundman M. 1991. Extrapyrimal symptoms due to dopamine-blocking agents in patients with AIDS encephalopathy. *Am J Psychiatry* 148: 1558-1561
- Hsu YC, Chang YC, Lin YC, Sze CI, Huang CC, Ho CJ. 2014. Cerebral microvascular damage occurs early after hypoxia-ischemia via nNOS activation in the neonatal brain. *J Cereb Blood Flow Metab* 34: 668-676
- Hu M, Sun YJ, Zhou QG, Chen L, Hu Y, et al. 2008. Negative regulation of neurogenesis and spatial memory by NR2B-containing NMDA receptors. *J Neurochem* 106: 1900-1913
- Hua X, Boyle CP, Harezlak J, Tate DF, Yiannoutsos CT, et al. 2013. Disrupted cerebral metabolite levels and lower nadir CD4 + counts are linked to brain volume deficits in 210 HIV-infected patients on stable treatment. *Neuroimage Clin* 3: 132-142
- Huang Y, Zhao L, Jia B, Wu L, Li Y, et al. 2011. Glutaminase dysregulation in HIV-1-infected human microglia mediates neurotoxicity: relevant to HIV-1-associated neurocognitive disorders. *J Neurosci* 31: 15195-15204
- Iragui VJ, Kalmijn J, Plummer DJ, Sample PA, Trick GL, Freeman WR. 1996. Pattern electroretinograms and visual evoked potentials in HIV infection: evidence of asymptomatic retinal and postretinal impairment in the absence of infectious retinopathy. *Neurology* 47: 1452-1456
- Iskander S, Walsh KA, Hammond RR. 2004. Human CNS cultures exposed to HIV-1 gp120 reproduce dendritic injuries of HIV-1-associated dementia. *J Neuroinflammation* 1: 7
- Jacobson LP, Kirby AJ, Polk S, Phair JP, Besley DR, et al. 1993. Changes in survival after acquired immunodeficiency syndrome (AIDS): 1984-1991. *Am J Epidemiol* 138: 952-964
- Jinno S, Aika Y, Fukuda T, Kosaka T. 1999. Quantitative analysis of neuronal nitric oxide synthase-immunoreactive neurons in the mouse hippocampus with optical disector. *J Comp Neurol* 410: 398-412
- Jinno S, Kosaka T. 2000. Colocalization of parvalbumin and somatostatin-like immunoreactivity in the mouse hippocampus: Quantitative analysis with optical disector. *The Journal of Comparative Neurology* 428: 377-388

- Jinno S, Kosaka T. 2002. Patterns of expression of calcium binding proteins and neuronal nitric oxide synthase in different populations of hippocampal GABAergic neurons in mice. *J Comp Neurol* 449: 1-25
- Jinno S, Kosaka T. 2004. Patterns of colocalization of neuronal nitric oxide synthase and somatostatin-like immunoreactivity in the mouse hippocampus: quantitative analysis with optical disector. *Neuroscience* 124: 797-808
- Johann-Liang R, Lin K, Cervia J, Stavola J, Noel G. 1998. Neuroimaging findings in children perinatally infected with the human immunodeficiency virus. *Pediatr Infect Dis J* 17: 753-754
- Johnson TP, Patel K, Johnson KR, Maric D, Calabresi PA, et al. 2013. Induction of IL-17 and nonclassical T-cell activation by HIV-Tat protein. *Proc Natl Acad Sci U S A* 110: 13588-13593
- Jones LS, Grooms SY, Salvadori S, Lazarus LH. 1994. Dermorphin-induced hyperexcitability in hippocampal CA3 and CA1 in vitro. *Eur J Pharmacol* 264: 39-48
- Jorand R, Biswas S, Wakefield DL, Tobin SJ, Golfetto O, et al. 2016. Molecular signatures of mu opioid receptor and somatostatin receptor 2 in pancreatic cancer. *Mol Biol Cell* 27: 3659-3672
- Kallianpur KJ, Kirk GR, Sailasuta N, Valcour V, Shiramizu B, et al. 2012. Regional cortical thinning associated with detectable levels of HIV DNA. *Cereb Cortex* 22: 2065-2075
- Kaul M, Garden GA, Lipton SA. 2001. Pathways to neuronal injury and apoptosis in HIV-associated dementia. *Nature* 410: 988-994
- Kawalec M, Kowalczyk JE, Beresewicz M, Lipkowski AW, Zablocka B. 2011. Neuroprotective potential of biphalin, multireceptor opioid peptide, against excitotoxic injury in hippocampal organotypic culture. *Neurochem Res* 36: 2091-2095
- Kelley JB, Balda MA, Anderson KL, Itzhak Y. 2009. Impairments in fear conditioning in mice lacking the nNOS gene. *Learn Mem* 16: 371-378
- Kerr SJ, Armati PJ, Guillemin GJ, Brew BJ. 1998. Chronic exposure of human neurons to quinolinic acid results in neuronal changes consistent with AIDS dementia complex. *AIDS* 12: 355-363
- Kesby JP, Markou A, Semenova S, Group T. 2016. Effects of HIV/TAT protein expression and chronic selegiline treatment on spatial memory, reversal learning and neurotransmitter levels in mice. *Behav Brain Res* 311: 131-140

- Keutmann MK, Gonzalez R, Maki PM, Rubin LH, Vassileva J, Martin EM. 2017. Sex differences in HIV effects on visual memory among substance-dependent individuals. *J Clin Exp Neuropsychol* 39: 574-586
- Khanlou N, Moore DJ, Chana G, Cherner M, Lazzaretto D, et al. 2009. Increased frequency of alpha-synuclein in the substantia nigra in human immunodeficiency virus infection. *J Neurovirol* 15: 131-138
- Kim HJ, Martemyanov KA, Thayer SA. 2008. Human immunodeficiency virus protein Tat induces synapse loss via a reversible process that is distinct from cell death. *J Neurosci* 28: 12604-12613
- Kim JB, Sharp PA. 2001. Positive transcription elongation factor B phosphorylates hSPT5 and RNA polymerase II carboxyl-terminal domain independently of cyclin-dependent kinase-activating kinase. *J Biol Chem* 276: 12317-12323
- Kim TA, Avraham HK, Koh YH, Jiang S, Park IW, Avraham S. 2003. HIV-1 Tat-mediated apoptosis in human brain microvascular endothelial cells. *J Immunol* 170: 2629-2637
- Kim WB, Cho JH. 2017. Synaptic Targeting of Double-Projecting Ventral CA1 Hippocampal Neurons to the Medial Prefrontal Cortex and Basal Amygdala. *J Neurosci* 37: 4868-4882
- King JE, Eugenin EA, Hazleton JE, Morgello S, Berman JW. 2010. Mechanisms of HIV-tat-induced phosphorylation of N-methyl-D-aspartate receptor subunit 2A in human primary neurons: implications for neuroAIDS pathogenesis. *Am J Pathol* 176: 2819-2830
- King SR. 1994. HIV: Virology and mechanisms of disease. *Annals of Emergency Medicine* 24: 443-449
- Kirchner L, Weitzdoerfer R, Hoeger H, Url A, Schmidt P, et al. 2004. Impaired cognitive performance in neuronal nitric oxide synthase knockout mice is associated with hippocampal protein derangements. *Nitric Oxide* 11: 316-330
- Kitanaka J, Kitanaka N, Hall FS, Fujii M, Goto A, et al. 2015. Memory impairment and reduced exploratory behavior in mice after administration of systemic morphine. *J Exp Neurosci* 9: 27-35
- Klausberger T, Marton LF, Baude A, Roberts JD, Magill PJ, Somogyi P. 2004. Spike timing of dendrite-targeting bistratified cells during hippocampal network oscillations in vivo. *Nat Neurosci* 7: 41-47
- Klausberger T, Somogyi P. 2008. Neuronal diversity and temporal dynamics: the unity of hippocampal circuit operations. *Science* 321: 53-57

- Kokotis P, Schmelz M, Skopelitis EE, Kordossis T, Karandreas N. 2007. Differential sensitivity of thick and thin fibers to HIV and therapy-induced neuropathy. *Auton Neurosci* 136: 90-95
- Kolesnikov YA, Pick CG, Ciszewska G, Pasternak GW. 1993. Blockade of tolerance to morphine but not to kappa opioids by a nitric oxide synthase inhibitor. *PNAS* 90: 5162-5166
- Korotkova T, Fuchs EC, Ponomarenko A, von Engelhardt J, Monyer H. 2010. NMDA receptor ablation on parvalbumin-positive interneurons impairs hippocampal synchrony, spatial representations, and working memory. *Neuron* 68: 557-569
- Kosaka T, Katsumaru H, Hama K, Wu JY, Heizmann CW. 1987. GABAergic neurons containing the Ca²⁺-binding protein parvalbumin in the rat hippocampus and dentate gyrus. *Brain Res* 419: 119-130
- Kramer-Hammerle S, Rothenaigner I, Wolff H, Bell JE, Brack-Werner R. 2005. Cells of the central nervous system as targets and reservoirs of the human immunodeficiency virus. *Virus Res* 111: 194-213
- Krishnan G, Chatterjee N. 2014. Endocannabinoids affect innate immunity of Muller glia during HIV-1 Tat cytotoxicity. *Mol Cell Neurosci* 59: 10-23
- Krogh KA, Wydeven N, Wickman K, Thayer SA. 2014. HIV-1 protein Tat produces biphasic changes in NMDA-evoked increases in intracellular Ca²⁺ concentration via activation of Src kinase and nitric oxide signaling pathways. *J Neurochem* 130: 642-656
- Krook-Magnuson E, Luu L, Lee SH, Varga C, Soltesz I. 2011. Ivy and neurogliaform interneurons are a major target of mu-opioid receptor modulation. *J Neurosci* 31: 14861-14870
- Kruman, II, Nath A, Mattson MP. 1998. HIV-1 protein Tat induces apoptosis of hippocampal neurons by a mechanism involving caspase activation, calcium overload, and oxidative stress. *Exp Neurol* 154: 276-288
- Kuiken C, Foley B, Leitner T, Apetrei C, Hahn B, et al. 2010. HIV Sequence Compendium 2010, Office of Scientific and Technical Information (OSTI)
- Kumar AM, Ownby RL, Waldrop-Valverde D, Fernandez B, Kumar M. 2011. Human immunodeficiency virus infection in the CNS and decreased dopamine availability: relationship with neuropsychological performance. *J Neurovirol* 17: 26-40
- Lackner P, Kuenz B, Reindl M, Morandell M, Berger T, et al. 2010. Antibodies to myelin oligodendrocyte glycoprotein in HIV-1 associated neurocognitive disorder: a cross-sectional cohort study. *J Neuroinflammation* 7: 79

- Lafourcade CA, Alger BE. 2008. Distinctions among GABAA and GABAB responses revealed by calcium channel antagonists, cannabinoids, opioids, and synaptic plasticity in rat hippocampus. *Psychopharmacology (Berl)* 198: 539-549
- Lambert NA, Harrison NL, Teyler TJ. 1991. Evidence for mu opiate receptors on inhibitory terminals in area CA1 of rat hippocampus. *Neurosci Lett* 124: 101-104
- Lane JH, Sasseville VG, Smith MO, Vogel P, Pauley DR, et al. 1996. Neuroinvasion by simian immunodeficiency virus coincides with increased numbers of perivascular macrophages/microglia and intrathecal immune activation. *J Neurovirol* 2: 423-432
- Lapray D, Lasztocki B, Lagler M, Viney TJ, Katona L, et al. 2012. Behavior-dependent specialization of identified hippocampal interneurons. *Nat Neurosci* 15: 1265-1271
- Le Marec T, Marie-Claire C, Noble F, Marie N. 2011. Chronic and intermittent morphine treatment differently regulates opioid and dopamine systems: a role in locomotor sensitization. *Psychopharmacology (Berl)* 216: 297-303
- Leão RN, Mikulovic S, Leão KE, Munguba H, Gezelius H, et al. 2012. OLM interneurons differentially modulate CA3 and entorhinal inputs to hippocampal CA1 neurons. *Nature Neuroscience* 15: 1524-1530
- Lecoeur H, Borgne-Sanchez A, Chaloin O, El-Khoury R, Brabant M, et al. 2012. HIV-1 Tat protein directly induces mitochondrial membrane permeabilization and inactivates cytochrome c oxidase. *Cell Death Dis* 3: e282
- Lee I, Park SB. 2013. Perirhinal cortical inactivation impairs object-in-place memory and disrupts task-dependent firing in hippocampal CA1, but not in CA3. *Front Neural Circuits* 7: 134
- Lee MH, Wang T, Jang MH, Steiner J, Haughey N, et al. 2011. Rescue of adult hippocampal neurogenesis in a mouse model of HIV neurologic disease. *Neurobiol Dis* 41: 678-687
- Leibrand CR, Paris JJ, Ghandour MS, Knapp PE, Kim WK, et al. 2017. HIV-1 Tat disrupts blood-brain barrier integrity and increases phagocytic perivascular macrophages and microglia in the dorsal striatum of transgenic mice. *Neurosci Lett*
- Leite JP, Chimelli L, Terra-Bustamante VC, Costa ET, Assirati JA, et al. 2002. Loss and sprouting of nitric oxide synthase neurons in the human epileptic hippocampus. *Epilepsia* 43 Suppl 5: 235-242

- Levenga J, Krishnamurthy P, Rajamohamedsait H, Wong H, Franke TF, et al. 2013. Tau pathology induces loss of GABAergic interneurons leading to altered synaptic plasticity and behavioral impairments. *Acta Neuropathol Commun* 1: 34
- Levine AJ, Soontornniyomkij V, Achim CL, Maslah E, Gelman BB, et al. 2016. Multilevel analysis of neuropathogenesis of neurocognitive impairment in HIV. *J Neurovirol* 22: 431-441
- Levy JA, Shimabukuro J, Hollander H, Mills J, Kaminsky L. 1985. Isolation of AIDS-associated retroviruses from cerebrospinal fluid and brain of patients with neurological symptoms. *Lancet* 2: 586-588
- Li Q, Bian S, Hong J, Kawase-Koga Y, Zhu E, et al. 2011. Timing specific requirement of microRNA function is essential for embryonic and postnatal hippocampal development. *PLoS One* 6: e26000
- Li ST, Matsushita M, Moriwaki A, Saheki Y, Lu YF, et al. 2004. HIV-1 Tat inhibits long-term potentiation and attenuates spatial learning [corrected]. *Ann Neurol* 55: 362-371
- Li W, Huang Y, Reid R, Steiner J, Malpica-Llanos T, et al. 2008. NMDA receptor activation by HIV-Tat protein is clade dependent. *J Neurosci* 28: 12190-12198
- Liao D, Lin H, Law PY, Loh HH. 2005. Mu-opioid receptors modulate the stability of dendritic spines. *Proc Natl Acad Sci U S A* 102: 1725-1730
- Ling GS, Paul D, Simantov R, Pasternak GW. 1989. Differential development of acute tolerance to analgesia, respiratory depression, gastrointestinal transit and hormone release in a morphine infusion model. *Life Sci* 45: 1627-1636
- Liu LW, Lu J, Wang XH, Fu SK, Li Q, Lin FQ. 2013. Neuronal apoptosis in morphine addiction and its molecular mechanism. *Int J Clin Exp Med* 6: 540-545
- Liu NQ, Lossinsky AS, Popik W, Li X, Gujuluva C, et al. 2002. Human immunodeficiency virus type 1 enters brain microvascular endothelia by macropinocytosis dependent on lipid rafts and the mitogen-activated protein kinase signaling pathway. *J Virol* 76: 6689-6700
- Loacker S, Sayyah M, Wittmann W, Herzog H, Schwarzer C. 2007. Endogenous dynorphin in epileptogenesis and epilepsy: anticonvulsant net effect via kappa opioid receptors. *Brain* 130: 1017-1028
- Lojek E, Bornstein RA. 2005. The stability of neurocognitive patterns in HIV infected men: classification considerations. *J Clin Exp Neuropsychol* 27: 665-682

- Long LL, Song YM, Xu L, Yi F, Long HY, et al. 2014. Aberrant neuronal synaptic connectivity in CA1 area of the hippocampus from pilocarpine-induced epileptic rats observed by fluorogold. *Int J Clin Exp Med* 7: 2687-2695
- Lovett-Barron M, Kaifosh P, Kheirbek MA, Danielson N, Zaremba JD, et al. 2014. Dendritic inhibition in the hippocampus supports fear learning. *Science* 343: 857-863
- Lovett-Barron M, Losonczy A. 2014. Behavioral consequences of GABAergic neuronal diversity. *Curr Opin Neurobiol* 26: 27-33
- Lue W-M, Su M-T, Lin W-B, Tao P-L. 1999. The role of nitric oxide in the development of morphine tolerance in rat hippocampal slices. *European Journal of Pharmacology* 383: 129-135
- Lutz PE, Kieffer BL. 2013. Opioid receptors: distinct roles in mood disorders. *Trends Neurosci* 36: 195-206
- Mahadevan A, Satishchandra P, Prachet KK, Sidappa NB, Ranga U, et al. 2006. Optic nerve axonal pathology is related to abnormal visual evoked responses in AIDS. *Acta Neuropathol* 112: 461-469
- Maimone D, Annunziata P, Cioni C, Leonardi A, Guazzi GC. 2009. Intrathecal synthesis of anti-myelin basic protein IgG in HIV-1+ patients. *Acta Neurologica Scandinavica* 90: 285-292
- Maki PM, Cohen MH, Weber K, Little DM, Fornelli D, et al. 2009. Impairments in memory and hippocampal function in HIV-positive vs HIV-negative women: a preliminary study. *Neurology* 72: 1661-1668
- Mamik MK, Ghorpade A. 2012. Src homology-2 domain-containing protein tyrosine phosphatase (SHP) 2 and p38 regulate the expression of chemokine CXCL8 in human astrocytes. *PLoS One* 7: e45596
- Mamik MK, Ghorpade A. 2014. Chemokine CXCL8 promotes HIV-1 replication in human monocyte-derived macrophages and primary microglia via nuclear factor-kappaB pathway. *PLoS One* 9: e92145
- Marks WD, Paris JJ, Schier CJ, Denton MD, Fitting S, et al. 2016. HIV-1 Tat causes cognitive deficits and selective loss of parvalbumin, somatostatin, and neuronal nitric oxide synthase expressing hippocampal CA1 interneuron subpopulations. *J Neurovirol* 22: 747-762
- Martin R, Bajo-Graneras R, Moratalla R, Perea G, Araque A. 2015. Circuit-specific signaling in astrocyte-neuron networks in basal ganglia pathways. *Science* 349: 730-734

- Marx PA, Alcabes PG, Drucker E. 2001. Serial human passage of simian immunodeficiency virus by unsterile injections and the emergence of epidemic human immunodeficiency virus in Africa. *Philos Trans R Soc Lond B Biol Sci* 356: 911-920
- Masanetz S, Lehmann MH. 2011. HIV-1 Nef increases astrocyte sensitivity towards exogenous hydrogen peroxide. *Virology* 8: 35
- Masliah E, Ge N, Achim CL, Hansen LA, Wiley CA. 1992. Selective neuronal vulnerability in HIV encephalitis. *J Neuropathol Exp Neurol* 51: 585-593
- Masliah E, Heaton RK, Marcotte TD, Ellis RJ, Wiley CA, et al. 1997. Dendritic injury is a pathological substrate for human immunodeficiency virus-related cognitive disorders. HNRC Group. The HIV Neurobehavioral Research Center. *Ann Neurol* 42: 963-972
- Masliah E, DeTeresa RM, Mallory ME, Hansen LA. 2000. Changes in pathological findings at autopsy in AIDS cases for the last 15 years. *Aids* 14: 69-74
- Masvekar RR, El-Hage N, Hauser KF, Knapp PE. 2015. GSK3beta-activation is a point of convergence for HIV-1 and opiate-mediated interactive neurotoxicity. *Mol Cell Neurosci* 65: 11-20
- Mattson MP, Haughey NJ, Nath A. 2005. Cell death in HIV dementia. *Cell Death Differ* 12 Suppl 1: 893-904
- McArthur JC. 2004. HIV dementia: an evolving disease. *J Neuroimmunol* 157: 3-10
- McArthur JC, Steiner J, Sacktor N, Nath A. 2010. Human immunodeficiency virus-associated neurocognitive disorders: Mind the gap. *Ann Neurol* 67: 699-714
- McBain CJ, Fisahn A. 2001. Interneurons unbound. *Nat Rev Neurosci* 2: 11-23
- McLane VD, Cao L, Willis CL. 2014. Morphine increases hippocampal viral load and suppresses frontal lobe CCL5 expression in the LP-BM5 AIDS model. *J Neuroimmunol* 269: 44-51
- McQuiston AR, Saggau P. 2003. Mu-opioid receptors facilitate the propagation of excitatory activity in rat hippocampal area CA1 by disinhibition of all anatomical layers. *J Neurophysiol* 90: 1936-1948
- McQuiston AR. 2007. Effects of mu-opioid receptor modulation on GABAB receptor synaptic function in hippocampal CA1. *J Neurophysiol* 97: 2301-2311

- McQuiston AR. 2008. Layer selective presynaptic modulation of excitatory inputs to hippocampal cornu Ammon 1 by mu-opioid receptor activation. *Neuroscience* 151: 209-221
- McQuiston AR. 2014. Acetylcholine release and inhibitory interneuron activity in hippocampal CA1. *Front Synaptic Neurosci* 6: 20
- Megías M, Emri Z, Freund TF, Gulyás AI. 2001. Total number and distribution of inhibitory and excitatory synapses on hippocampal CA1 pyramidal cells. *Neuroscience* 102: 527-540
- Mehla R, Bivalkar-Mehla S, Nagarkatti M, Chauhan A. 2012. Programming of neurotoxic cofactor CXCL-10 in HIV-1-associated dementia: abrogation of CXCL-10-induced neuro-glial toxicity in vitro by PKC activator. *J Neuroinflammation* 9: 239
- Mehta A, Prabhakar M, Kumar P, Deshmukh R, Sharma PL. 2013. Excitotoxicity: bridge to various triggers in neurodegenerative disorders. *Eur J Pharmacol* 698: 6-18
- Meltzer MS, Skillman DR, Gomas PJ, Kalter DC, Gendelman HE. 1990. Role of mononuclear phagocytes in the pathogenesis of human immunodeficiency virus infection. *Annu Rev Immunol* 8: 169-194
- Meulendyke KA, Ubaida-Mohien C, Drewes JL, Liao Z, Gama L, et al. 2014. Elevated brain monoamine oxidase activity in SIV- and HIV-associated neurological disease. *J Infect Dis* 210: 904-912
- Meyer VJ, Rubin LH, Martin E, Weber KM, Cohen MH, et al. 2013. HIV and recent illicit drug use interact to affect verbal memory in women. *J Acquir Immune Defic Syndr* 63: 67-76
- Midde NM, Gomez AM, Zhu J. 2012. HIV-1 Tat protein decreases dopamine transporter cell surface expression and vesicular monoamine transporter-2 function in rat striatal synaptosomes. *J Neuroimmune Pharmacol* 7: 629-639
- Milstein AD, Bloss EB, Apostolides PF, Vaidya SP, Dilly GA, et al. 2015. Inhibitory Gating of Input Comparison in the CA1 Microcircuit. *Neuron* 87: 1274-1289
- Moga D, Hof PR, Vissavajhala P, Moran TM, Morrison JH. 2002. Parvalbumin-containing interneurons in rat hippocampus have an AMPA receptor profile suggestive of vulnerability to excitotoxicity. *Journal of Chemical Neuroanatomy* 23: 249-253
- Moore DJ, Masliah E, Rippeth JD, Gonzalez R, Carey CL, et al. 2006. Cortical and subcortical neurodegeneration is associated with HIV neurocognitive impairment. *AIDS* 20: 879-887
- Morris BJ. 1989. Neuronal localisation of neuropeptide Y gene expression in rat brain. *J Comp Neurol* 290: 358-368

- Mouton PR. 2002. *Principals and practices of unbiased stereology: an introduction for bioscientists*. Baltimore: The Johns Hopkins University.
- Mukerjee R, Chang JR, Del Valle L, Bagashev A, Gayed MM, et al. 2011. Deregulation of microRNAs by HIV-1 Vpr protein leads to the development of neurocognitive disorders. *J Biol Chem* 286: 34976-34985
- Muller-Oehring EM, Schulte T, Rosenbloom MJ, Pfefferbaum A, Sullivan EV. 2010. Callosal degradation in HIV-1 infection predicts hierarchical perception: a DTI study. *Neuropsychologia* 48: 1133-1143
- Muller C, Remy S. 2014. Dendritic inhibition mediated by O-LM and bistratified interneurons in the hippocampus. *Front Synaptic Neurosci* 6: 23
- Mwanza JC, Nyamabo LK, Tylleskar T, Plant GT. 2004. Neuro-ophthalmological disorders in HIV infected subjects with neurological manifestations. *Br J Ophthalmol* 88: 1455-1459
- Nath A, Psooy K, Martin C, Knudsen B, Magnuson DS, et al. 1996. Identification of a human immunodeficiency virus type 1 Tat epitope that is neuroexcitatory and neurotoxic. *J Virol* 70: 1475-1480
- Nath A, Conant K, Chen P, Scott C, Major EO. 1999. Transient exposure to HIV-1 Tat protein results in cytokine production in macrophages and astrocytes. A hit and run phenomenon. *J Biol Chem* 274: 17098-17102
- Nath A, Steiner J. 2014. Synaptodendritic injury with HIV-Tat protein: What is the therapeutic target? *Exp Neurol* 251: 112-114
- Nath A. 2015. Eradication of human immunodeficiency virus from brain reservoirs. *J Neurovirol* 21: 227-234
- Newmark RE, Schon K, Ross RS, Stern CE. 2013. Contributions of the hippocampal subfields and entorhinal cortex to disambiguation during working memory. *Hippocampus* 23: 467-475
- NIDA. 2017. Drug Facts: Drug Use and Viral Infections (HIV, Hepatitis). <https://www.drugabuse.gov/publications/drugfacts/drug-use-viral-infections-hiv-hepatitis>. Oct 17
- Noguchi J, Matsuzaki M, Ellis-Davies GC, Kasai H. 2005. Spine-neck geometry determines NMDA receptor-dependent Ca²⁺ signaling in dendrites. *Neuron* 46: 609-622

- Norman JP, Perry SW, Kasischke KA, Volsky DJ, Gelbard HA. 2007. HIV-1 trans activator of transcription protein elicits mitochondrial hyperpolarization and respiratory deficit, with dysregulation of complex IV and nicotinamide adenine dinucleotide homeostasis in cortical neurons. *J Immunol* 178: 869-876
- Ochs SM, Dorostkar MM, Aramuni G, Schon C, Filser S, et al. 2015. Loss of neuronal GSK3beta reduces dendritic spine stability and attenuates excitatory synaptic transmission via beta-catenin. *Mol Psychiatry* 20: 482-489
- Oka H, Yoshida K. 1985. Septohippocampal connections to field CA1 of the rat identified with field potential analysis and retrograde labeling by horseradish peroxidase. *Neurosci Lett* 58: 19-24
- Okuyama T, Kitamura T, Roy DS, Itohara S, Tonegawa S. 2016. Ventral CA1 neurons store social memory. *Science* 353: 1536-1541
- Oliva AA, Jiang MH, Lam T, Smith KL, Swann JW. 2000. Novel hippocampal interneuronal subtypes identified using transgenic mice that express green fluorescent protein in GABAergic interneurons. *Journal of Neuroscience* 20: 3354-3368
- Oliva AA, Jr., Lam TT, Swann JW. 2002. Distally directed dendrotoxicity induced by kainic Acid in hippocampal interneurons of green fluorescent protein-expressing transgenic mice. *J Neurosci* 22: 8052-8062
- Orban-Kis K, Szabadi T, Szilagyi T. 2015. The loss of Ivy cells and the hippocampal input modulatory O-LM cells contribute to the emergence of hyperexcitability in the hippocampus. *Rom J Morphol Embryol* 56: 155-161
- Paillart JC, Skripkin E, Ehresmann B, Ehresmann C, Marquet R. 2002. In vitro evidence for a long range pseudoknot in the 5'-untranslated and matrix coding regions of HIV-1 genomic RNA. *J Biol Chem* 277: 5995-6004
- Pang X, Panee J, Liu X, Berry MJ, Chang SL, Chang L. 2013. Regional variations of antioxidant capacity and oxidative stress responses in HIV-1 transgenic rats with and without methamphetamine administration. *J Neuroimmune Pharmacol* 8: 691-704
- Pantano S, Tyagi M, Giacca M, Carloni P. 2002. Amino Acid Modification in the HIV-1 Tat Basic Domain: Insights from Molecular Dynamics and in vivo Functional Studies. *Journal of Molecular Biology* 318: 1331-1339
- Pantano S, Tyagi M, Giacca M, Carloni P. 2004. Molecular dynamics simulations on HIV-1 Tat. *Eur Biophys J* 33: 344-351

- Patel S, Leibrand CR, Palasuberniam P, Couraud PO, Weksler B, et al. 2017. Effects of HIV-1 Tat and Methamphetamine on Blood-Brain Barrier Integrity and Function In Vitro. *Antimicrob Agents Chemother*
- Patton HK, Chu WJ, Hetherington HP, den Hollander J, Stewart KE, et al. 2001. Alkaline pH changes in the cerebellum of asymptomatic HIV-infected individuals. *NMR Biomed* 14: 12-18
- Pelkey KA, Chittajallu R, Craig MT, Tricoire L, Wester JC, McBain CJ. 2017. Hippocampal GABAergic Inhibitory Interneurons. *Physiol Rev* 97: 1619-1747
- Peluso R, Haase A, Stowring L, Edwards M, Ventura P. 1985. A Trojan Horse mechanism for the spread of visna virus in monocytes. *Virology* 147: 231-236
- Peng Z, Zhang N, Wei W, Huang CS, Cetina Y, et al. 2013. A reorganized GABAergic circuit in a model of epilepsy: evidence from optogenetic labeling and stimulation of somatostatin interneurons. *J Neurosci* 33: 14392-14405
- Persidsky Y, Gendelman HE. 2003. Mononuclear phagocyte immunity and the neuropathogenesis of HIV-1 infection. *J Leukoc Biol* 74: 691-701
- Petito CK, Chen HX, Mastro AR, Torres-Munoz J, Roberts B, Wood C. 1999. HIV infection of choroid plexus in AIDS and asymptomatic HIV-infected patients suggests that the choroid plexus may be a reservoir of productive infection. *Journal of Neurovirology* 5: 670-677
- Pfefferbaum A, Rosenbloom MJ, Rohlfing T, Kemper CA, Deresinski S, Sullivan EV. 2009. Frontostriatal fiber bundle compromise in HIV infection without dementia. *AIDS* 23: 1977-1985
- Pfefferbaum A, Rogosa DA, Rosenbloom MJ, Chu W, Sasso SA, et al. 2014. Accelerated aging of selective brain structures in human immunodeficiency virus infection: a controlled, longitudinal magnetic resonance imaging study. *Neurobiol Aging* 35: 1755-1768
- Pfeiffer M, Koch T, Schroder H, Laugsch M, Holtt V, Schulz S. 2002. Heterodimerization of somatostatin and opioid receptors cross-modulates phosphorylation, internalization, and desensitization. *J Biol Chem* 277: 19762-19772
- Philippon V, Vellutini C, Gambarelli D, Harkiss G, Arbuthnott G, et al. 1994. The basic domain of the lentiviral Tat protein is responsible for damages in mouse brain: involvement of cytokines. *Virology* 205: 519-529

- Pikkarainen M, Rnkk S, Savander V, Insausti R, Pitknen A. 1999. Projections from the lateral, basal, and accessory basal nuclei of the amygdala to the hippocampal formation in rat. *The Journal of Comparative Neurology* 403: 229-260
- Plager MD, Vogt BA. 1988. Mu- and delta-opioid receptor binding peaks and kappa-homogeneity in the molecular layers of rat hippocampal formation. *Brain Res* 460: 150-154
- Plummer DJ, Bartsch DU, Azen SP, Max S, Sadun AA, Freeman WR. 2001. Retinal nerve fiber layer evaluation in human immunodeficiency virus-positive patients. *Am J Ophthalmol* 131: 216-222
- Pomara N, Crandall DT, Choi SJ, Johnson G, Lim KO. 2001. White matter abnormalities in HIV-1 infection: a diffusion tensor imaging study. *Psychiatry Res* 106: 15-24
- Porter JT, Cauli B, Staiger JF, Lambolez B, Rossier J, Audinat E. 1998. Properties of bipolar VIPergic interneurons and their excitation by pyramidal neurons in the rat neocortex. *European Journal of Neuroscience* 10: 3617-3628
- Portugal GS, Al-Hasani R, Fakira AK, Gonzalez-Romero JL, Melyan Z, et al. 2014. Hippocampal long-term potentiation is disrupted during expression and extinction but is restored after reinstatement of morphine place preference. *J Neurosci* 34: 527-538
- Rácz B, Halasy K. 2002. Kappa opioid receptor is expressed by somatostatin- and neuropeptide Y-containing interneurons in the rat hippocampus. *Brain Research* 931: 50-55
- Rameau GA, Tukey DS, Garcin-Hosfield ED, Titcombe RF, Misra C, et al. 2007. Biphasic coupling of neuronal nitric oxide synthase phosphorylation to the NMDA receptor regulates AMPA receptor trafficking and neuronal cell death. *J Neurosci* 27: 3445-3455
- Ranson WR. 1932. *The Anatomy of the Nervous System from the Standpoint of Development and Function*. pp. 265-282. Philadelphia: W.B. Saunders Company.
- Rao VR, Ruiz AP, Prasad VR. 2014. Viral and cellular factors underlying neuropathogenesis in HIV associated neurocognitive disorders (HAND). *AIDS Res Ther* 11: 13
- Raybuck JD, Hargus NJ, Thayer SA. 2017. A GluN2B-Selective NMDAR Antagonist Reverses Synapse Loss and Cognitive Impairment Produced by the HIV-1 Protein Tat. *J Neurosci* 37: 7837-7847
- Rayne F, Debaisieux S, Yezid H, Lin YL, Mettling C, et al. 2010. Phosphatidylinositol-(4,5)-bisphosphate enables efficient secretion of HIV-1 Tat by infected T-cells. *EMBO J* 29: 1348-1362

- Razavi Y, Alamdary SZ, Katebi SN, Khodaghohi F, Haghparast A. 2014. Morphine-induced apoptosis in the ventral tegmental area and hippocampus after the development but not extinction of reward-related behaviors in rats. *Cell Mol Neurobiol* 34: 235-245
- Rees CL, Wheeler DW, Hamilton DJ, White CM, Komendantov AO, Ascoli GA. 2016. Graph Theoretic and Motif Analyses of the Hippocampal Neuron Type Potential Connectome. *eNeuro* 3
- Rees CL, Moradi K, Ascoli GA. 2017. Weighing the Evidence in Peters' Rule: Does Neuronal Morphology Predict Connectivity? *Trends Neurosci* 40: 63-71
- Reeves JD, Doms RW. 2002. Human immunodeficiency virus type 2. *J Gen Virol* 83: 1253-1265
- Roberts ES, Chana G, Nguyen TB, Perera G, Landau S, et al. 2013. The spatial relationship between neurons and astrocytes in HIV-associated dementia. *J Neurovirol* 19: 123-130
- Robinson-Papp J, Elliott K, Simpson DM, Morgello S, Manhattan HIVBB. 2012. Problematic prescription opioid use in an HIV-infected cohort: the importance of universal toxicology testing. *J Acquir Immune Defic Syndr* 61: 187-193
- Rochefort NL, Konnerth A. 2012. Dendritic spines: from structure to in vivo function. *EMBO Rep* 13: 699-708
- Rock RB, Gekker G, Hu S, Sheng WS, Cheeran M, et al. 2004. Role of microglia in central nervous system infections. *Clin Microbiol Rev* 17: 942-964, table of contents
- Saboory E, Derchansky M, Ismaili M, Jahromi SS, Brull R, et al. 2007. Mechanisms of morphine enhancement of spontaneous seizure activity. *Anesth Analg* 105: 1729-1735, table of contents
- Sacktor N, McDermott MP, Marder K, Schifitto G, Selnes OA, et al. 2002. HIV-associated cognitive impairment before and after the advent of combination therapy. *J Neurovirol* 8: 136-142
- Sadegh M, Fathollahi Y. 2014. Repetitive systemic morphine alters activity-dependent plasticity of Schaffer-collateral-CA1 pyramidal cell synapses: involvement of adenosine A1 receptors and adenosine deaminase. *J Neurosci Res* 92: 1395-1408
- Sadun AA, Pepose JS, Madigan MC, Laycock KA, Tenhula WN, Freeman WR. 1995. AIDS-related optic neuropathy: a histological, virological and ultrastructural study. *Graefes Arch Clin Exp Ophthalmol* 233: 387-398

- Samikkannu T, Agudelo M, Gandhi N, Reddy PV, Saiyed ZM, et al. 2011. Human immunodeficiency virus type 1 clade B and C gp120 differentially induce neurotoxin arachidonic acid in human astrocytes: implications for neuroAIDS. *J Neurovirol* 17: 230-238
- Sanchez-Alavez M, Criado J, Gomez-Chavarin M, Jimenez-Anguiano A, Navarro L, et al. 2000. HIV- and FIV-derived gp120 alter spatial memory, LTP, and sleep in rats. *Neurobiol Dis* 7: 384-394
- Sanchez-Blazquez P, Rodriguez-Munoz M, Garzon J. 2010. Mu-opioid receptors transiently activate the Akt-nNOS pathway to produce sustained potentiation of PKC-mediated NMDAR-CaMKII signaling. *PLoS One* 5: e11278
- Savio T, Levi G. 1993. Neurotoxicity of HIV coat protein gp120, NMDA receptors, and protein kinase C: a study with rat cerebellar granule cell cultures. *J Neurosci Res* 34: 265-272
- Schier CJ, Marks WD, Paris JJ, Barbour AJ, McLane VD, et al. 2017. Selective vulnerability of striatal D2 versus D1 dopamine receptor-expressing medium spiny neurons in HIV-1 Tat transgenic male mice. *J Neurosci*
- Schwartz M, Baruch K. 2014. The resolution of neuroinflammation in neurodegeneration: leukocyte recruitment via the choroid plexus. *EMBO J* 33: 7-22
- Seress L, Abraham H, Lin H, Totterdell S. 2002. Nitric oxide-containing pyramidal neurons of the subiculum innervate the CA1 area. *Exp Brain Res* 147: 38-44
- Shah S, Nonnemacher MR, Pirrone V, Wigdahl B. 2010. Innate and adaptive factors regulating human immunodeficiency virus type 1 genomic activation. *J Neuroimmune Pharmacol* 5: 278-293
- Sharp PM, Bailes E, Chaudhuri RR, Rodenburg CM, Santiago MO, Hahn BH. 2001. The origins of acquired immune deficiency syndrome viruses: where and when? *Philos Trans R Soc Lond B Biol Sci* 356: 867-876
- Sharp PM, Hahn BH. 2011. Origins of HIV and the AIDS pandemic. *Cold Spring Harb Perspect Med* 1: a006841
- Shin AH, Thayer SA. 2013. Human immunodeficiency virus-1 protein Tat induces excitotoxic loss of presynaptic terminals in hippocampal cultures. *Mol Cell Neurosci* 54: 22-29
- Sik A, Penttonen M, Buzsaki G. 1997. Interneurons in the hippocampal dentate gyrus: an in vivo intracellular study. *Eur J Neurosci* 9: 573-588

- Silverberg MJ, Ray GT, Saunders K, Rutter CM, Campbell CI, et al. 2012. Prescription long-term opioid use in HIV-infected patients. *Clin J Pain* 28: 39-46
- Smialowska M, Domin H, Zieba B, Kozniowska E, Michalik R, et al. 2009. Neuroprotective effects of neuropeptide Y-Y2 and Y5 receptor agonists in vitro and in vivo. *Neuropeptides* 43: 235-249
- Snider WD, Simpson DM, Nielsen S, Gold JW, Metroka CE, Posner JB. 1983. Neurological complications of acquired immune deficiency syndrome: analysis of 50 patients. *Ann Neurol* 14: 403-418
- Sobhian B, Laguette N, Yatim A, Nakamura M, Levy Y, et al. 2010. HIV-1 Tat assembles a multifunctional transcription elongation complex and stably associates with the 7SK snRNP. *Mol Cell* 38: 439-451
- Somogyi J, Szabo A, Somogyi P, Lamsa K. 2012. Molecular analysis of ivy cells of the hippocampal CA1 stratum radiatum using spectral identification of immunofluorophores. *Front Neural Circuits* 6: 35
- Soontornniyomkij V, Moore DJ, Gouaux B, Soontornniyomkij B, Tatro ET, et al. 2012. Cerebral beta-amyloid deposition predicts HIV-associated neurocognitive disorders in APOE epsilon4 carriers. *AIDS* 26: 2327-2335
- Soulas C, Donahue RE, Dunbar CE, Persons DA, Alvarez X, Williams KC. 2009. Genetically modified CD34+ hematopoietic stem cells contribute to turnover of brain perivascular macrophages in long-term repopulated primates. *Am J Pathol* 174: 1808-1817
- Stark C. 2007. Functional Role of the Hippocampus In *The Hippocampus Book*, ed. P Andersen, R Morris, D Amaral, T Bliss, J O'Keefe, pp. 549-580. New York: Oxford University Press
- Stein C, Schafer M, Machelska H. 2003. Attacking pain at its source: new perspectives on opioids. *Nat Med* 9: 1003-1008
- Stein C. 2016. Opioid Receptors. *Annu Rev Med* 67: 433-451
- Steinert JR, Chernova T, Forsythe ID. 2010. Nitric oxide signaling in brain function, dysfunction, and dementia. *Neuroscientist* 16: 435-452
- Stumm RK, Zhou C, Schulz S, Hollt V. 2004. Neuronal types expressing mu- and delta-opioid receptor mRNA in the rat hippocampal formation. *J Comp Neurol* 469: 107-118
- Sun Y, Nguyen AQ, Nguyen JP, Le L, Saur D, et al. 2014. Cell-type-specific circuit connectivity of hippocampal CA1 revealed through Cre-dependent rabies tracing. *Cell Rep* 7: 269-280

- Supcun B, Ghadiri MK, Zeraati M, Stummer W, Speckmann EJ, Gorji A. 2012. The effects of tetanic stimulation on plasticity of remote synapses in the hippocampus-perirhinal cortex-amygdala network. *Synapse* 66: 965-974
- Svoboda KR, Adams CE, Lupica CR. 1999. Opioid Receptor Subtype Expression Defines Morphologically Distinct Classes of Hippocampal Interneurons. *The Journal of Neuroscience* 19: 85-95
- Tan JW, Duan TT, Zhou QX, Ding ZY, Jing L, et al. 2015. Impaired contextual fear extinction and hippocampal synaptic plasticity in adult rats induced by prenatal morphine exposure. *Addict Biol* 20: 652-662
- Tate DF, Sampat M, Harezlak J, Fiecas M, Hogan J, et al. 2011. Regional areas and widths of the midsagittal corpus callosum among HIV-infected patients on stable antiretroviral therapies. *J Neurovirol* 17: 368-379
- Taylor BS, Sobieszczyk ME, McCutchan FE, Hammer SM. 2008. The challenge of HIV-1 subtype diversity. *N Engl J Med* 358: 1590-1602
- Theodore S, Cass WA, Dwoskin LP, Maragos WF. 2012. HIV-1 protein Tat inhibits vesicular monoamine transporter-2 activity in rat striatum. *Synapse* 66: 755-757
- Thomas CA, Dobkin J, Weinberger OK. 1994. TAT-mediated transcellular activation of HIV-1 long terminal repeat directed gene expression by HIV-1-infected peripheral blood mononuclear cells. *J Immunol* 153: 3831-3839
- Thompson PM, Dutton RA, Hayashi KM, Toga AW, Lopez OL, et al. 2005. Thinning of the cerebral cortex visualized in HIV/AIDS reflects CD4+ T lymphocyte decline. *Proc Natl Acad Sci U S A* 102: 15647-15652
- Thompson PM, Dutton RA, Hayashi KM, Lu A, Lee SE, et al. 2006. 3D mapping of ventricular and corpus callosum abnormalities in HIV/AIDS. *Neuroimage* 31: 12-23
- Ton H, Xiong H. 2013. Astrocyte Dysfunctions and HIV-1 Neurotoxicity. *J AIDS Clin Res* 4: 255
- Torres L, Noel RJ, Jr. 2014. Astrocytic expression of HIV-1 viral protein R in the hippocampus causes chromatolysis, synaptic loss and memory impairment. *J Neuroinflammation* 11: 53
- Toth K, Borhegyi Z, Freund T. 1993. Postsynaptic targets of GABAergic hippocampal neurons in the medial septum-diagonal band of Broca complex. *The Journal of Neuroscience* 13: 3712-3724

- Toth K, Eross L, Vajda J, Halasz P, Freund TF, Magloczky Z. 2010. Loss and reorganization of calretinin-containing interneurons in the epileptic human hippocampus. *Brain* 133: 2763-2777
- Toth K, Magloczky Z. 2014. The vulnerability of calretinin-containing hippocampal interneurons to temporal lobe epilepsy. *Front Neuroanat* 8: 100
- Tozzi V, Balestra P, Serraino D, Bellagamba R, Corpolongo A, et al. 2005. Neurocognitive impairment and survival in a cohort of HIV-infected patients treated with HAART. *AIDS Res Hum Retroviruses* 21: 706-713
- Tran SV, Guiloff RJ, Scaravilli F. 1995. AIDS-associated vacuolar myelopathy. A morphometric study. *Brain* 118: 1247-1261
- Traudt CM, Tkac I, Ennis KM, Sutton LM, Mammel DM, Rao R. 2012. Postnatal morphine administration alters hippocampal development in rats. *J Neurosci Res* 90: 307-314
- Tremblay ME, Marker DF, Puccini JM, Muly EC, Lu SM, Gelbard HA. 2013. Ultrastructure of microglia-synapse interactions in the HIV-1 Tat-injected murine central nervous system. *Commun Integr Biol* 6: e27670
- Tricoire L, Pelkey KA, Daw MI, Sousa VH, Miyoshi G, et al. 2010. Common origins of hippocampal Ivy and nitric oxide synthase expressing neurogliaform cells. *J Neurosci* 30: 2165-2176
- Tricoire L, Vitalis T. 2012. Neuronal nitric oxide synthase expressing neurons: a journey from birth to neuronal circuits. *Front Neural Circuits* 6: 82
- Tyan L, Chamberland S, Magnin E, Camire O, Francavilla R, et al. 2014. Dendritic inhibition provided by interneuron-specific cells controls the firing rate and timing of the hippocampal feedback inhibitory circuitry. *J Neurosci* 34: 4534-4547
- Valentino RJ, Bostock E, Dingledine R. 1982. Opioid pharmacology in the rat hippocampal slice. *Life Sci* 31: 2339-2342
- Valentino RJ, Dingledine R. 1982. Pharmacological characterization of opioid effects in the rat hippocampal slice. *Journal of Pharmacology and Experimental Therapeutics* 223: 502-509
- van der Graaf M, Diepersloot RJ. 1986. Transmission of human immunodeficiency virus (HIV/HTLV-III/LAV): a review. *Infection* 14: 203-211

- Vander Jagt TA, Connor JA, Shuttleworth CW. 2008. Localized loss of Ca²⁺ homeostasis in neuronal dendrites is a downstream consequence of metabolic compromise during extended NMDA exposures. *J Neurosci* 28: 5029-5039
- Vartak-Sharma N, Gelman BB, Joshi C, Borgamann K, Ghorpade A. 2014. Astrocyte elevated gene-1 is a novel modulator of HIV-1-associated neuroinflammation via regulation of nuclear factor-kappaB signaling and excitatory amino acid transporter-2 repression. *J Biol Chem* 289: 19599-19612
- Vasko MR, Domino EF. 1978. Tolerance development to the biphasic effects of morphine on locomotor activity and brain acetylcholine in the rat. *Journal of Pharmacology and Experimental Therapeutics* 207: 848-858
- Vinck M, Bos JJ, Van Mourik-Donga LA, Oplaat KT, Klein GA, et al. 2015. Cell-Type and State-Dependent Synchronization among Rodent Somatosensory, Visual, Perirhinal Cortex, and Hippocampus CA1. *Front Syst Neurosci* 9: 187
- Vizcaychipi MP, Watts HR, O'Dea KP, Lloyd DG, Penn JW, et al. 2014. The therapeutic potential of atorvastatin in a mouse model of postoperative cognitive decline. *Ann Surg* 259: 1235-1244
- Walker BD, Burton DR. 2008. Toward an AIDS vaccine. *Science* 320: 760-764
- Walsh JG, Reinke SN, Mamik MK, McKenzie BA, Maingat F, et al. 2014. Rapid inflammasome activation in microglia contributes to brain disease in HIV/AIDS. *Retrovirology* 11: 35
- Wang WW, Hu SQ, Li C, Zhou C, Qi SH, Zhang GY. 2010. Transduced PDZ1 domain of PSD-95 decreases Src phosphorylation and increases nNOS (Ser847) phosphorylation contributing to neuroprotection after cerebral ischemia. *Brain Res* 1328: 162-170
- Weiss R. 1993. How does HIV cause AIDS? *Science* 260: 1273-1279
- Weitzdoerfer R, Hoeger H, Engidawork E, Engelmann M, Singewald N, et al. 2004. Neuronal nitric oxide synthase knock-out mice show impaired cognitive performance. *Nitric Oxide* 10: 130-140
- Wen D, Zang G, Sun D, Yu F, Mei D, et al. 2014. Cholecystokinin-octapeptide restored morphine-induced hippocampal long-term potentiation impairment in rats. *Neurosci Lett* 559: 76-81
- Wersinger SR, Ginns EI, O'Carroll AM, Lolait SJ, Young WS, 3rd. 2002. Vasopressin V1b receptor knockout reduces aggressive behavior in male mice. *Mol Psychiatry* 7: 975-984
- Wheeler DW, White CM, Rees CL, Komendantov AO, Hamilton DJ, Ascoli GA. 2015. Hippocampome.org: a knowledge base of neuron types in the rodent hippocampus. *Elife* 4

- WHO. 2016. Progress report 2016: Prevent HIV, Test and Treat All. ed. Wh Organization.
<http://www.who.int/hiv/en/>
- WHO. 2017. HIV/AIDS <http://www.who.int/mediacentre/factsheets/fs360/en/>. Oct 17
- Williams TJ, Milner TA. 2011. Delta opioid receptors colocalize with corticotropin releasing factor in hippocampal interneurons. *Neuroscience* 179: 9-22
- Wilson TW, Fox HS, Robertson KR, Sandkovsky U, O'Neill J, et al. 2013. Abnormal MEG oscillatory activity during visual processing in the prefrontal cortices and frontal eye-fields of the aging HIV brain. *PLoS One* 8: e66241
- Wimpey TL, Opheim KE, Chavkin C. 1989. Effects of chronic morphine administration on the mu and delta opioid responses in the CA1 region of the rat hippocampus. *Journal of Pharmacology and Experimental Therapeutics* 251: 405-411
- Witwer KW. 2014. HIV-1 Tat- and Vpr-responsive microRNAs of neuronal cells. *J Biol Chem* 289: 3104
- Wohlschlaeger J, Wenger E, Mehraein P, Weis S. 2009. White matter changes in HIV-1 infected brains: a combined gross anatomical and ultrastructural morphometric investigation of the corpus callosum. *Clin Neurol Neurosurg* 111: 422-429
- Worobey M, Gemmel M, Teuwen DE, Haselkorn T, Kunstman K, et al. 2008. Direct evidence of extensive diversity of HIV-1 in Kinshasa by 1960. *Nature* 455: 661-664
- Wu P, Ding ZB, Meng SQ, Shen HW, Sun SC, et al. 2014a. Differential role of Rac in the basolateral amygdala and cornu ammonis 1 in the reconsolidation of auditory and contextual Pavlovian fear memory in rats. *Psychopharmacology (Berl)* 231: 2909-2919
- Wu S, Yue Y, Tian H, Tao L, Wang Y, et al. 2014b. Tramiprosate protects neurons against ischemic stroke by disrupting the interaction between PSD95 and nNOS. *Neuropharmacology* 83: 107-117
- Xapelli S, Agasse F, Ferreira R, Silva A, Malva J. 2006. Neuropeptide Y as an Endogenous Antiepileptic, Neuroprotective and Pro-Neurogenic Peptide. *Recent Patents on CNS Drug Discovery* 1: 315-324
- Xu C, Fitting S. 2016. Inhibition of GABAergic Neurotransmission by HIV-1 Tat and Opioid Treatment in the Striatum Involves mu-Opioid Receptors. *Front Neurosci* 10: 497
- Xu Q, Li WY, Guan Y. 2013. Mu-opioidergic modulation differs in deep and superficial wide-dynamic range dorsal horn neurons in mice. *Neurosci Lett* 549: 157-162

- Xu R, Feng X, Xie X, Zhang J, Wu D, Xu L. 2012. HIV-1 Tat protein increases the permeability of brain endothelial cells by both inhibiting occludin expression and cleaving occludin via matrix metalloproteinase-9. *Brain Res* 1436: 13-19
- Xuan A, Wang GB, Shi DP, Xu JL, Li YL. 2013. Initial study of magnetic resonance diffusion tensor imaging in brain white matter of early AIDS patients. *Chin Med J (Engl)* 126: 2720-2724
- Yamada J, Jinno S. 2015. Subclass-specific formation of perineuronal nets around parvalbumin-expressing GABAergic neurons in Ammon's horn of the mouse hippocampus. *J Comp Neurol* 523: 790-804
- Ye L, Huang Y, Zhao L, Li Y, Sun L, et al. 2013. IL-1beta and TNF-alpha induce neurotoxicity through glutamate production: a potential role for neuronal glutaminase. *J Neurochem* 125: 897-908
- Yu XM, Askalan R, Keil GJ, 2nd, Salter MW. 1997. NMDA channel regulation by channel-associated protein tyrosine kinase Src. *Science* 275: 674-678
- Yuferov V, Ho A, Morgello S, Yang Y, Ott J, Kreek MJ. 2013. Expression of ephrin receptors and ligands in postmortem brains of HIV-infected subjects with and without cognitive impairment. *J Neuroimmune Pharmacol* 8: 333-344
- Zanelli S, Naylor M, Kapur J. 2009. Nitric oxide alters GABAergic synaptic transmission in cultured hippocampal neurons. *Brain Res* 1297: 23-31
- Zhang J, Tamilarasu N, Hwang S, Garber ME, Huq I, et al. 2000. HIV-1 TAR RNA enhances the interaction between Tat and cyclin T1. *J Biol Chem* 275: 34314-34319
- Zhang Y, Wang M, Li H, Zhang H, Shi Y, et al. 2012. Accumulation of nuclear and mitochondrial DNA damage in the frontal cortex cells of patients with HIV-associated neurocognitive disorders. *Brain Res* 1458: 1-11
- Zhao P, Huang Y, Zuo Z. 2006. Opioid preconditioning induces opioid receptor-dependent delayed neuroprotection against ischemia in rats. *J Neuropathol Exp Neurol* 65: 945-952
- Zheng F, Seeger T, Nixdorf-Bergweiler BE, Alzheimer C. 2011. Layer-specific processing of excitatory signals in CA1 interneurons depends on postsynaptic M(2) muscarinic receptors. *Neurosci Lett* 494: 217-221

- Zhou L, Ng T, Yuksel A, Wang B, Dwyer DE, Saksena NK. 2008. Short communication: absence of HIV infection in the choroid plexus of two patients who died rapidly with HIV-associated dementia. *AIDS Res Hum Retroviruses* 24: 839-843
- Zhou L, Saksena NK. 2013. HIV Associated Neurocognitive Disorders. *Infect Dis Rep* 5: e8
- Zhou M, Luo P, Lu Y, Li CJ, Wang DS, et al. 2015. Imbalance of HCN1 and HCN2 expression in hippocampal CA1 area impairs spatial learning and memory in rats with chronic morphine exposure. *Prog Neuropsychopharmacol Biol Psychiatry* 56: 207-214
- Zhou Y, Liu J, Xiong H. 2016. HIV-1 Glycoprotein 120 Enhancement of N-Methyl-D-Aspartate NMDA Receptor-Mediated Excitatory Postsynaptic Currents: Implications for HIV-1-Associated Neural Injury. *J Neuroimmune Pharmacol*
- Zhu F, Yan CX, Zhao Y, Zhao Y, Li PP, Li SB. 2011. Effects of pre-training morphine on spatial memory acquisition and retrieval in mice. *Physiol Behav* 104: 754-760
- Zhu T, Korber BT, Nahmias AJ, Hooper E, Sharp PM, Ho DD. 1998. An African HIV-1 sequence from 1959 and implications for the origin of the epidemic. *Nature* 391: 594-597
- Zou S, Fuss B, Fitting S, Hahn YK, Hauser KF, Knapp PE. 2015. Oligodendrocytes Are Targets of HIV-1 Tat: NMDA and AMPA Receptor-Mediated Effects on Survival and Development. *J Neurosci* 35: 11384-11398
- Zucchini S, Pittaluga A, Brocca-Cofano E, Summa M, Fabris M, et al. 2013. Increased excitability in tat-transgenic mice: role of tat in HIV-related neurological disorders. *Neurobiol Dis* 55: 110-119

Vita

William D Marks (Will) is from Buffalo, NY. He received a Bachelor of Science from the Franciscan University of Steubenville, where he majored in Biology and minored in Psychology, in 2009. He then returned home and went on to receive a Master of Arts in Biology at The SUNY College at Buffalo, also known as Buffalo State College, in 2012. While at Buffalo State, he worked under Martha Skerrett on the biophysical properties of gap junction channels that form rectifying electrical synapses in the arthropod central nervous system. He then moved on to VCU where he completed his doctoral studies on the effects of HIV-1 Tat and morphine on the structure and function of the hippocampus with his advisor Dr. Kurt Hauser. Will has accepted a postdoctoral appointment at UT Southwestern Medical Center in Dallas TX, in the lab of Dr. Takashi Kitamura. He will be studying the functional neurocircuitry of interactions between the hippocampus and entorhinal cortex underlying the perception of time in spatial processing, and he plans to remain in academia following his postdoctoral training, returning to the field of neurovirology to apply intensive functional circuitry techniques to questions in the field

Will has published four papers to date, three of which are first author, in the Journal of Neuroscience, the Journal of Neurovirology, and the Journal of Neurophysiology. Additionally, Will has received multiple honors for his work, including the Outstanding Masters Thesis Award (2013) by the SUNY College at Buffalo Graduate School, the Outstanding Predoctoral Research Award (2015) from the International Society for Neurovirology, and the BioLegend Young Investigator travel award (2017), by BioLegend and the American Society for Neurochemistry.